Unimolecular and water reactions of oxygenated and unsaturated Criegee intermediates under atmospheric conditions

— Electronic Supporting Information —

L. Vereecken, A. Novelli, A. Kiendler-Scharr, A. Wahner

Contents

A. Literature SCI rate coefficients

1. Selected literature data for unimolecular reactions

Table 1: Selected literature data based on recent experimental work and high-level (often post-CCSD(T)) theoretical work for unimolecular reactions. Barrier height E_b in kcal mol^{-1}, rate coefficient k(T) near 298 K in s^{-1}. Only the energetically most favorable reaction path is considered here (1,3-ring closure for CH$_2$OO and *anti*-CH$_3$CHOO, 1,5-ring closure for *Z*-(CH=CH$_2$)(CH$_3$)COO), 1,4-H-migration for all other). See Vereecken and Francisco,[1] Vereecken et al.,[2] or section A.4 for a more extensive list of data.

CI	E_b	k(298 K)	T / K	Methodology[a]	Reference
CH$_2$OO		0.19±0.07	297	E: C$_2$H$_4$ ozonolysis; titration CI with SO$_2$	Berndt et al. 2015[3]
	18.9	0.25	297	T: CHEAT1 modified ; RRKM	Berndt et al. 2015[3]
	19.0	0.3	298	T: W3X-L//CCSD(T)-F12 ; CVTST	Long et al. 2016[4]
	19.1	0.3	298	T: HEAT-345(Q) ; SCTST	Nguyen et al. 2015[5]
		< 11.6	293	E: RI$_2$ photolysis ; cavity ring down	Chhantyal-Pun et al. 2016[6]
		8.8±13	298	E: C$_2$H$_4$ ozonolysis; Relative to CI + SO$_2$	Newland et al. 2015[7]
	19.0	0.3	298	T: CCSD(T)/aVTZ//M06-2X + CF	Vereecken et al., 2017[8][b]
	19.6	0.036[b]	298	T+E: CCSD(T)//M06-2X + adj. to exp	Stone et al., 2018[9]
	20.5			T: DLPNO-CCSD(T)	Peltola et al. 2020[10]
syn-CH$_3$CHOO	17.1	166	298	T: HEAT modified ; RRKM	Fang et al. 2016[11]
	17.0	328	298	T: W3X-L//CCSD(T)-F12 ; CVTST	Long et al. 2016[4]
		122	298	T+E: mHEAT + RRKM + exp. k(E)	Fang et al. 2016[12]
		288±275	298	E: C$_4$H$_8$ ozonolysis; Relative to CI + SO$_2$	Newland et al. 2015[7]
		76±25	298	E: C$_4$H$_8$ ozonolysis	Fenske et al. 2000[13]
		20±10	≤293[c]	E: C$_4$H$_8$ ozonolysis ; OH LIF	Novelli et al. 2014[14]
		> 3	297	E: C$_4$H$_8$ ozonolysis; titration CI with SO$_2$	Berndt et al. 2015[3]
	16.8	136	298	T: CCSD(T)/aVTZ//M06-2X + CF	Vereecken et al., 2017[8][b]
anti-CH$_3$CHOO	15.6	55.4	298	T: W3X-L//CCSD(T)-F12 ; CVTST	Long et al. 2016[4]
		> 3	297	E: C$_4$H$_8$ ozonolysis; titration CI with SO$_2$	Berndt et al. 2015[3]
	15.7	53	298	T: CCSD(T)/aVTZ//M06-2X + CF	Vereecken et al., 2017[8][b]
syn-C$_2$H$_5$CHOO	16.5	279	298	T: CCSD(T)-F12/CBS//B2PLYPD3 ; RRKM	Fang et al. 2016[15]
	16.5	205	298	T: CCSD(T)/aVTZ//M06-2X + CF	Vereecken et al., 2017[8][b]
(CH$_3$)$_2$COO	16.2	369	298	T: HEAT modified ; RRKM	Fang et al. 2016[11]
		276	298	T+E: mHEAT + RRKM + exp. k(E)	Fang et al. 2017[16]
		305±70	293	E: RI$_2$ photolysis ; cavity ring down	Chhantyal-Pun et al. 2017[6]
		1000±200[d]	298	E: TME ozonolysis; Relative to CI + SO$_2$	Newland et al. 2015[7]
		269±82	283	E: TME ozonolysis; UV absorption	Smith et al. 2016[17]
		361±49	298	E: TME ozonolysis; UV absorption	Smith et al. 2016[17]
		628±60	310	E: TME ozonolysis; UV absorption	Smith et al. 2016[17]
		916±56	323	E: TME ozonolysis; UV absorption	Smith et al. 2016[17]
	15.9	400	298	T: QCISD(T)/CBS//B3LYP; SCTST	Smith et al. 2016[17]
		643±87	293	E: TME oznolysis; H$_2$SO$_4$ CI-APi-TOF	Berndt et al. 2014[18]
	16.1	478	298	T: CCSD(T)/aVTZ//M06-2X + CF	Vereecken et al., 2017[8][b]
	16.4	420	298	T: W3X-L//CCSD(T)-F12a/DZ-F12	Long et al. 2018[19]
	15.5	1070	298	T: CCSD(T)-F12a//M06-2X ; TST	Deng et al. 2018[20]
E-(CH$_3$)(CH=CH$_2$)COO	18.0	33	298	T: ANL0-B2F	Barber et al. 2018[21]
		70±15	298	E: Photolysis + UV-absorption	Lin et al., 2020[22]
Z- (CH=CH$_2$) (CH$_3$)COO	12.0	2140	298	T: ANL0-B2F	Barber et al. 2018[21]
Z-C$_3$H$_6$CHO-CHOO	9.7	1700	298	T: CCSD(T)-F12a ; MS-CVT/SVT	Long et al. 2019[23]
Z-C$_5$H$_8$CHO-CHOO	8.0	790	298	T: CCSD(T)-F12a ; MS-CVT/SVT	Long et al. 2019[23]
E-C$_3$H$_6$CHO-CHOO	14.3	190	298	T: CCSD(T)-F12a ; MS-CVT/SVT	Long et al. 2019[23]
E-C$_3$H$_6$CHO-CHOO	13.4	78	298	T: CCSD(T)-F12a ; MS-CVT/SVT	Long et al. 2019[23]
Z-(C$_7$H$_{10}$)	16.3	631	298	T: CCSD(T)-F12a//M06-2X ; TST	Deng et al. 2018[20]
E-(C$_7$H$_{10}$)	15.0	68	298	T: CCSD(T)-F12a//M06-2X ; TST	Deng et al. 2018[20]

[a] Concise description of experimental (E:) and theoretical (T:) methodologies. See references for more details.

[b] High-pressure limit

[c] These measurements may have been affected by expansion cooling in the probe nozzle.

[d] Relative rate converted using $k($ (CH$_3$)$_2$COO + SO$_2$ $) = 1.6×10^{-10}$ cm^3 molecules^{-1} s^{-1}

Table 2: Intramolecular secondary ozonide (SOZ) formation in substituted carbonyl oxides, listing barrier heights E_b (kcal mol^{-1}), rate coefficient k (s^{-1}) at 298 K.

Carbonyl oxide	E_b	k(298K)	Reference
Z-n-OCHC$_4$H$_8$CHOO	5.1		Chuong et al. 2004[24]
Z -n-OCHCH$_2$CHOO	15.7		Kuwata et al. 2011[25]
β-caryophyllene CI-1a	12.3	5.3	Nguyen et al. 2009[26]
β-caryophyllene CI-1b	10.6	486	Nguyen et al. 2009[26]
β-caryophyllene CI-2a	8.1	1100	Nguyen et al. 2009[26]
β-caryophyllene CI-2b	13.3	7.4	Nguyen et al. 2009[26]
α-phellandrene CI1a	13.6 [a]		Mackenzie-Rae et al. 2016[27]
α-phellandrene CI1b	6.5 [a]		Mackenzie-Rae et al. 2016[27]
α-phellandrene CI2a	4.2 [a]		Mackenzie-Rae et al. 2016[27]
α-phellandrene CI2b	5.8 [a]		Mackenzie-Rae et al. 2016[27]
α-phellandrene CI3a	14.4 [a]		Mackenzie-Rae et al. 2016[27]
α-phellandrene CI3b	9.3 [a]		Mackenzie-Rae et al. 2016[27]
α-phellandrene CI4a	6.7 [a]		Mackenzie-Rae et al. 2016[27]
α-phellandrene CI4b	7.5 [a]		Mackenzie-Rae et al. 2016[27]
Z-pinonaldehyde-K-oxide	13.5	8.7	Vereecken et al., 2017[8]
Z-pinonaldehyde-A-oxide	16.0	2.8×10^{-2}	Vereecken et al., 2017[8]
E-n-OCHC$_3$H$_6$CHOO	14.1	0.9	Long et al., 2019[23]
Z-n-OCHC$_3$H$_6$CHOO	2.5	7.1×10^9	Long et al., 2019[23]
E-n-OCHC$_4$H$_8$CHOO	5.1	2.4×10^7	Long et al., 2019[23]
Z-n-OCHC$_4$H$_8$CHOO	2.1	3.2×10^8	Long et al., 2019[23]
Z-(CH$_2$CH$_2$COOH)CHOO	11.4	8.9×10^2	This work
Z-(CH$_2$CH$_2$CH$_2$COOH)CHOO	7.4	8.2×10^4	This work

[a] $\Delta G^{\neq}$(298K) from a single-conformer analysis

2. Rate coefficients for the reaction of SCI with H_2O

Table 3: Barrier heights (kcal mol^{-1}) and rate coefficients (cm^3 molecule^{-1} s^{-1}) available in the literature on the CI + H_2O reaction. Relative position of R_1 and R_2 as in section S.

R_1	R_2	E_b [a]	k(298K)	Ref.
H	H		$< 4 \times 10^{-15}$ (Exp)	Welz et al. 2012[28]
			$10^{-12} - 10^{-15}$ (Exp)	Leather et al. 2012[29]
			$(2.5 \pm 1) \times 10^{-17}$ (Exp)	Ouyang et al. 2013[30]
			$< 9 \times 10^{-17}$ (Exp)	Stone et al. 2014[31]
			$(3.2 \pm 1.2) \times 10^{-16}$ (Exp)	Berndt et al. 2015[3]
			$(1.3 \pm 0.4) \times 10^{-15}$ (Exp)	Newland et al. 2015[7]
		2.0	$1.66\text{-}5.60 \times 10^{-15}$	Anglada et al. 2011[32]
		1.9	5.9×10^{-17}	Anglada et al. 2002[33]
		4.3	5.8×10^{-18}	Ryzhkov and Ariya 2004[34]
		2.8	3.69×10^{-16}	Lin et al. 2016[35]
		2.2	3.05×10^{-15}	Anglada and Solé 2016[36]
		2.8	2.32×10^{-18}	Chen et al. 2016[37]
		3.5	2.4×10^{-16}	Long et al. 2016[4]
		3.1	4.4×10^{-16}	Caravan et al. 2020[38]
			3.6×10^{-16}	Yin and Takahashi, 2018[39]
CH_3	H		$< 4 \times 10^{-15}$ (Exp)	Taatjes et al. 2013[40]
			$< 2 \times 10^{-16}$ (Exp)	Sheps et al. 2014[41]
		5.3	$2.39\text{-}3.23 \times 10^{-18}$	Anglada et al. 2011[32]
		7.0	7.23×10^{-21}	Kuwata et al. 2010[42]
		5.8	4.2×10^{-20}	Anglada et al. 2002[33]
		1.2	7.33×10^{-21}	Ryzhkov and Ariya 2004[34]
		7.0	1.98×10^{-19}	Lin et al. 2016[35]
		6.0	2.89×10^{-18}	Anglada and Solé 2016[36]
		7.5	1.9×10^{-19}	Long et al. 2016[4]
			1.5×10^{-19}	Yin and Takahashi, 2018[39]
$CH_2\text{-}C_8H_{13}O$	H	10.5 [c]		Jiang et al. 2013[43] [c]
H	CH_3		$(1.0 \pm 0.4) \times 10^{-14}$ (Exp)	Taatjes et al. 2013[40]
			$(2.4 \pm 0.4) \times 10^{-14}$ (Exp)	Sheps et al. 2014[41]
			$(2.3 \pm 2.1) \times 10^{-14}$ (Exp)	Newland et al. 2015[7]
		-1.2	$1.68\text{-}2.03 \times 10^{-13}$	Anglada et al. 2011[32]
		0.6	2.87×10^{-16}	Kuwata et al. 2010[42]
		-0.7	2.5×10^{-15}	Anglada et al. 2002[33]
		-5.3	4.0×10^{-16}	Ryzhkov and Ariya 2004[34]
		0.3	3.4×10^{-14}	Lin et al. 2016[35]
		-1.2	1.35×10^{-13}	Anglada and Solé 2016[36]
		1.2	5.2×10^{-15}	Long et al. 2016[4]
			1.4×10^{-14}	Yin and Takahashi, 2018[39]
CH_3	CH_3		$< 1.5 \times 10^{-16}$ (Exp)	Huang et al. 2015[44]
			$(2.1 \pm 0.6) \times 10^{-15}$ (Exp)	Newland et al. 2015[7]
		3.6	3.87×10^{-17}	Anglada et al. 2011[32]
		4.0	7.5×10^{-19}	Anglada et al. 2002[33]
		4.0	1.4×10^{-19}	Ryzhkov and Ariya 2004[34]
		3.6	2.41×10^{-17}	Anglada and Solé 2016[36]
			2.3×10^{-18}	Yin and Takahashi, 2018[39]
		5.9	1.1×0^{-17}	Long et al. 2018[19]
CH_3	$CH_2\text{-}CH_2\text{-}C_6H_9O$	9.2		Jiang et al. 2013[43] [c]
CH_3	$\text{-cyc-}C_6H_8\text{-}CH_3$	8.5		Jiang et al. 2013[43] [c]
E-nopinone oxide (bicyclic)		2.07		Lin et al. 2014[45]
H	s-trans-$CH=CH_2$		5.1×10^{-17}	Yin and Takahashi, 2018[39]
H	s-cis-$CH=CH_2$		1.8×10^{-16}	Yin and Takahashi, 2018[39]
CH_3	s-trans-$CH=CH_2$	8.2	(1.4 s^{-1}) [b]	Aplincourt and Anglada 2003[46]
		6.8	2.93×10^{-19}	Anglada et al. 2011[32]
		9.8	1.62×10^{-21}	Kuwata et al. 2010[42]
		6.8	3.35×10^{-19}	Anglada and Solé 2016[36]
			$\leq 4.0 \times 10^{-17}$ (exp)	Caravan et al., 2020[38]
		8.9	1.1×10^{-19}	Caravan et al. 2020[38]

CH_3	*s-cis*-$CH=CH_2$	6.8	(8.8 s^{-1}) [b]	Aplincourt and Anglada 2003[46]
		5.2	1.97×10^{-18}	Anglada et al. 2011[32]
		7.6	3.43×10^{-20}	Kuwata et al. 2010[42]
		5.2	2.91×10^{-18}	Anglada and Solé 2016[36]
s-trans-$CH=CH_2$	CH_3	6.1	(49 s^{-1}) [b]	Aplincourt and Anglada 2003[46]
		4.7	1.39×10^{-18}	Anglada et al. 2011[32]
		4.3	1.87×10^{-17}	Anglada and Solé 2016[36]
		6.2	8×10^{-19}	Caravan et al. 2020[38]
s-cis-$CH=CH_2$	CH_3	7.5	(15 s^{-1}) [b]	Aplincourt and Anglada 2003[46]
		5.8	8.31×10^{-18}	Anglada et al. 2011[32]
		5.8	3.65×10^{-18}	Anglada and Solé 2016[36]
H	*s-trans*-$C(CH_3)=CH_2$	3.9	(3.8×10^{3} s^{-1}) [b]	Aplincourt and Anglada 2003[46]
		1.9	1.89×10^{-15}	Anglada et al. 2011[32]
		1.9	2.91×10^{-15}	Anglada and Solé 2016[36]
H	*s-cis*-$C(CH_3)=CH_2$	2.1	(4.6×10^{4} s^{-1}) [b]	Aplincourt and Anglada 2003[46]
		0.2	1.36×10^{-14}	Anglada et al. 2011[32]
		0.2	1.67×10^{-14}	Anglada and Solé 2016[36]
H	$C(CH_3)=CH_2$		1.2×10^{-15} (exp) [d]	Newland et al. 2016[7]
			$\sim 3 \times 10^{-17}$ (exp) [e]	Lin et al. 2021[47]
H	$C\equiv CH$		1.3×10^{-17}	Yin and Takahashi, 2018[39]
s-trans-$CH=CH_2$	H		5.0×10^{-20}	Yin and Takahashi, 2018[39]
s-cis-$CH=CH_2$	H		5.2×10^{-21}	Yin and Takahashi, 2018[39]
s-trans-$C(CH_3)=CH_2$	H	2.4	(5.8×10^{4} s^{-1}) [b]	Aplincourt and Anglada 2003[46]
		4.7	4.86×10^{-18}	Anglada et al. 2011[32]
		4.7	6.87×10^{-18}	Anglada and Solé 2016[36]
s-cis-$C(CH_3)=CH_2$	H	3.9	(1.6×10^{4} s^{-1}) [b]	Aplincourt and Anglada 2003[46]
		6.8	5.58×10^{-19}	Anglada et al. 2011[32]
		6.8	2.25×10^{-19}	Anglada and Solé 2016[36]
$C\equiv CH$	H		6.7×10^{-21}	Yin and Takahashi, 2018[39]
F	F	-8.0	4.6×10^{-9}	Anglada et al. 2011[32]
H	n-$C_{12}H_{23}$		$10^{-3} \times k_{acid}$ (Exp)	Tobias and Ziemann 2001[48]
cyc-OCH_2CH_2O-COO		-7.1	7.06×10^{-11}	Anglada et al. 2011[32]
cyc-$CH=CH$-COO		-4.0	1.23×10^{-11}	Anglada et al. 2011[32]

[a] Energy barrier relative to the separated reactants CI + H_2O. The reaction proceeds through a strong pre-reactive complex CI--H_2O which is not considered here.

[b] Value in brackets is the unimolecular reaction of the CI--H_2O complex to the hydroxy-hydroperoxide.

[c] Limonene, single-conformer analysis only

[d] Bulk rate coefficient assigned to *E*-$(C(CH_3)=CH_2)CHOO$ as it is the only (non-CH_2OO) isoprene-derived CI that is predicted to have a high rate coefficient with H_2O.

[e] Rate coefficient was not determined, but the total loss to water and water dimer was observed to be a factor 4.5 to 7 below that predicted using the rate coefficients by Vereecken et al.[8]

3. Rate coefficients for the reaction of SCI with $(H_2O)_2$

Table 4: Barrier heights (kcal mol^{-1}) and rate coefficients (cm^3 molecule^{-1} s^{-1}) available in the literature on the CI + $(H_2O)_2$ reaction. Relative position of R_1 and R_2 as in section S.

R_1	R_2	E_b $(H_2O)_2$[a]	k(298K) $(H_2O)_2$	Ref
H	H		$(6.5 \pm 0.5) \times 10^{-12}$ (Exp)	Chao et al. 2015[49]
			$(4.0 \pm 1.2) \times 10^{-12}$ (Exp)	Lewis et al. 2015[50]
			$(7.4 \pm 0.6) \times 10^{-12}$ (Exp)	Smith et al. 2015[51]
			$131\times$ k(H_2O)	Ryzhkov and Ariya 2006[52]
		-8.9	2.1×10^{-12}	Ryzhkov and Ariya 2004[34]
		-6.6	5.4×10^{-12}	Lin et al. 2016[35]
		-8.5	1.7×10^{-10}	Anglada and Solé 2016[36]
		-10.0	2.7×10^{-11}	Chen et al. 2016[37]
			2.3×10^{-12}	Yin and Takahashi, 2018[39]
CH$_3$	H	-5.9	1.2×10^{-16}	Ryzhkov and Ariya 2004[34]
		-3.2	2.6×10^{-14}	Lin et al. 2016[35]
		-5.9	4.8×10^{-13}	Anglada and Solé 2016[36]
			3.3×10^{-15}	Yin and Takahashi, 2018[39]
H	CH$_3$	-10.1	2.0×10^{-12}	Ryzhkov and Ariya 2004[34]
		-7.5	1.6×10^{-11}	Lin et al. 2016[35]
		-9.9	5.9×10^{-10}	Anglada and Solé 2016[36]
			4.4×10^{-12}	Yin and Takahashi, 2018[39]
CH$_3$	CH$_3$	-4.3	5.8×10^{-17}	Ryzhkov and Ariya 2004[34]
		-6.1	3.7×10^{-13}	Anglada and Solé 2016[36]
			3.4×10^{-16}	Yin and Takahashi, 2018[39]
H	*s-trans*-CH=CH$_2$		3.3×10^{-15}	Yin and Takahashi, 2018[39]
H	*s-cis*-CH=CH$_2$		3.3×10^{-14}	Yin and Takahashi, 2018[39]
CH$_3$	*s-trans*-CH=CH$_2$	-1.5	9.2×10^{-16}	Anglada and Solé 2016[36]
			$\leq 3.0 \times 10^{-14}$ (exp)	Caravan et al., 2020[38]
CH$_3$	*s-cis*-CH=CH$_2$	-4.0	1.3×10^{-14}	Anglada and Solé 2016[36]
			$\leq 3.0 \times 10^{-14}$ (exp)	Caravan et al., 2020[38]
s-trans-CH=CH$_2$	*H*		4.1×10^{-20}	Yin and Takahashi, 2018[39]
s-cis-CH=CH$_2$	*H*		1.2×10^{-16}	Yin and Takahashi, 2018[39]
s-trans-CH=CH$_2$	CH$_3$	-4.3	4.7×10^{-14}	Anglada and Solé 2016[36]
s-cis-CH=CH$_2$	CH$_3$	-2.4	5.4×10^{-15}	Anglada and Solé 2016[36]
H	*s-trans*-C(CH$_3$)=CH$_2$	-6.2	3.3×10^{-12}	Anglada and Solé 2016[36]
H	*s-cis*-C(CH$_3$)=CH$_2$	-8.0	2.2×10^{-11}	Anglada and Solé 2016[36]
	C(CH$_3$)=CH$_2$		$\sim 6 \times 10^{-14}$ (exp) [b]	Lin et al. 2021[47]
H	C≡CH		2.5×10^{-15}	Yin and Takahashi, 2018[39]
s-trans-C(CH$_3$)=CH$_2$	H	-4.9	1.1×10^{-15}	Anglada and Solé 2016[36]
s-cis-C(CH$_3$)=CH$_2$	H	-2.0	2.4×10^{-15}	Anglada and Solé 2016[36]
C≡CH	H		4.0×10^{-17}	Yin and Takahashi, 2018[39]

[a] Energy barrier relative to the separated reactants CI + $(H_2O)_2$. The reaction proceeds through a strong pre-reactive complex CI--$(H_2O)_2$ which is not included here.

[b] Rate coefficient was not determined, but the total loss to water and water dimer was observed to be a factor 4.5 to 7 below that predicted using the rate coefficients by Vereecken et al.[8]

4. Additional rate coefficient and energetic data on CI unimolecular reactions

There is significantly more experimental and theoretical data available on unimolecular reactions of CI than listed under section A.1. There is, however, significant variation across the literature data, owing to experimental uncertainties and difficulties, or the applications of lower levels of theory, which is why we have selected a subset of the data that we feel is among the best available. Still, it is useful to give an overview of all the available literature for reference purposes; the collected data is given in Table 5, in a format similar to an earlier review by Vereecken and Francisco[1] and Vereecken et al.[8] The study on α-phellandrene ozonolysis by MacKenzie-Rae et al.[27] is not included in this overview. These authors reported ΔH(298K) and ΔG(298K) barrier heights, which include thermal correction based on a single conformer, i.e. not accounting for internal rotation, making the values less reliable. In all cases, it is recommended to consult (and reference) the original publication when using values from this table. Data from Vereecken et al.[8] are also excluded, due to the large number of values.

Table 5: Barrier heights for unimolecular processes for stabilized Criegee Intermediates, and their rate coefficients when available. R_1 and R_2 orientation in the CI as indicated in sectionS. For most cases, the alkyl substituent is a methyl group; otherwise, the number of carbons in the substituent is indicated, for di-substituted CI this is the (R1,R2) carbon number; the prefix "c" indicates a cyclic substituent.

R_1	R_2	Process	Barrier (kcal mol^{-1})	k(298K) (s^{-1})	Reference
H	H	O-loss	47.0		Cremer et al., 1993[53]
			32.4		Anglada et al., 1996[54]
			51.2		Nguyen et al., 2007[55]
			49.2		Lehman et al., 2013[56]
			≤ 54[a]		Lehman et al., 2013[56]
			≤ 47[a]		Lehman et al., 2013[56]
			16.5 (anion)		Karton et al. 2013[57]
			54.2		Nguyen et al., 2015[58]
			47.0		Dawes et al., 2015[59]
			49.0 ± 0.3		Li et al., 2015[60]
		ester channel	17.7		Gutbrod et al., 1996[61]
			24.0		Anglada et al., 1996[54]
			19.9		Aplincourt and Ruiz-López, 2000[62]
			20.7		Kroll et al., 2001[63]
			20.6		Selçuki and Aviyente, 2001[64]
			19.8	0.024	Zhang and Zhang, 2002[65,66]
			23.8		Bach et al., 1992[67]
				0.19±0.07[a]	Berndt et al., 2015[3]
			18.9	0.03-0.58[f]	Berndt et al., 2015[3]
			18.2	0.3	Olzmann et al., 1997[68]
			<19.7[g]		Kalinowski et al., 2014[69]
			19.2		Cremer et al., 1993[53]
			18.9		Chen et al., 2002[70]
			19.0		Li et al., 2014[71]
			22.8		Cremer et al., 1988[72]
				≤ 11.6±8.0[a]	Chhantyal-Pun et al., 2015[73]
			19.6		Fang and Fu, 2002[74]
			19.0		Nguyen et al. 2014[75]
			19.1		Nguyen et al. 2015[5]
			18.7		Nguyen et al., 2015[58]
			19.4		Nguyen et al., 2015[58]
				-8.58±13[a]	Newland et al., 2015[7]
			19.4	0.34 [i]	Chen et al., 2016[37]
			19.0	0.31 [i]	Long et al., 2016[4]
			20.0	0.42	Yin and Takahashi, 2017[76]
		1,3-H-shift	30.8		Gutbrod et al., 1996[61]
			32.0	1.2×10^{-12}	Zhang and Zhang, 2002[65,66]
			30.8		Olzmann et al., 1997[68]
			32.5		Chen et al., 2002[70]

			31.8		Nguyen et al., 2015[5]
			30.7	8.2×10^(-9 i)	Chen et al. 2016[37]
			31.6		Long et al. 2016[4]
			33.0		Yin and Takahashi, 2017[76]
		syn-anti isom	25.7		Anglada et al., 1996[54]
			25.3		Hull, 1978[77]
			32.1		Cremer, 1979[78]
		direct-HCOOH	52.3		Chen et al. 2016[37]
			(16.1)[j]		Nguyen et al. 2015[58]
			51.17		Yin and Takahashi, 2017[76]
Alkyl	H	O-loss ester channel	34.1		Anglada et al., 1996[54]
			23.8		Gutbrod et al. 1997[79]
			28.4		Anglada et al., 1996[54]
			24.0		Selçuki and Aviyente, 2001[64]
			24.1		Kuwata et al., 2010[42]
			23.6		Kuwata et al., 2011[25]
			21.3 (C2)[c]		Kuwata et al., 2011[25]
			24.0 (C14)		Nguyen et al., 2009[80]
			23.3		Nguyen et al., 2009[80]
			23.7		Long et al. 2016[4]
			23.6		Yin and Takahashi, 2017[76]
			22.9 (C2)		Yin and Takahashi, 2017[76]
			24.4		Kuwata et al., 2018[81]
			22.9 (C6)		Deng et al. 2018[20]
		hydroperoxide	14.8		Gutbrod et al. 1997[79]
			21.2		Anglada et al., 1996[54]
			19.1 (C5)		Chuong et al., 2004[24]
			16.7		Kroll et al., 2001[63]
			17.9	24	Kuwata et al., 2010[42]
			12.7 (C2)[c]		Kuwata et al., 2011[25]
			16.9		Kuwata et al., 2003[82]
				76 [a]	Fenske et al., 2000[13]
			18.7 (C14)	1.6	Nguyen et al., 2009[80]
			15.7		Nguyen et al., 2009[80]
			19.6		Zhang and Zhang, 2005[83]
			17.1	166	Fang et al., 2016[11]
			≤16.0 eff.[a]		Liu et al., 2014[84]
			17.9		Liu et al., 2014[85]
			17.4 (C2)		Liu et al., 2014[85]
			16.3		Liu et al., 2015[86]
				20±10.0[a]	Novelli et al. 2014[14]
				288±275[a]	Newland et al., 2015[7]
			16.4 (C6O)		Leonardo et al., 2011[87]
			15.5 (C4O)		Leonardo et al., 2011[87]
				3[a]	Berndt et al., 2012[88]
				2.5[a]	Horie et al., 1997[89]
				2.9[a]	Horie et al., 1999[90]
				<250[a]	Taatjes et al., 2013[40]
			16.5		Kidwell et al. 2016[91]
			17.01	328 [i]	Long et al. 2016[4]
			17.2	124	Nguyen et al., 2016[92]
				122 [1]	Fang et al., 2016[12]
			16.7	182	Yin and Takahashi, 2017[76]
			16.3 (C2)	552	Yin and Takahashi, 2017[76]
			17.1 (CD3)	3	Green et al., 2017[93]
			16.1	300	Kuwata et al., 2018[81]
			16.3	241	Burd et al., 2018[94]
			16.3 (C6)	631	Deng et al. 2018[20]
			16.6 (C5O)	1700	Long et al. 2019[23]
			16.1 (C6O)	790	Long et al. 2019[23]
		syn-anti isom	30.5		Anglada et al., 1996[54]
			33.7		Kuwata et al. 2005[95]
			38.0		Kuwata et al., 2010[42]
			33.7		Kuwata et al., 2011[25]

			32.6		Nguyen et al., 2009[80]
			38.1		Nguyen et al., 2015[58]
			25.1		Hull, 1978[77]
			35.6		Cremer, 1979[78]
			41.9		Yin and Takahashi, 2017[76]
			40.6 (C2)		Yin and Takahashi, 2017[76]
			37.4 (C6O)		Long et al. 2019[23]
		Alkyl rotation	2.1		Bowman et al., 2015[96]
			2.5		Yin and Takahashi, 2017[76]
H	Alkyl	O-loss	31.6		Anglada et al., 1996[54]
		ester channel	20.6		Anglada et al., 1996[54]
			13.3 (C5)		Chuong et al., 2004[24]
			16.9		Kroll et al., 2001[63]
			17.1		Selçuki and Aviyente, 2001[64]
			15.4	67.3	Kuwata et al., 2010[42]
			16.6		Kuwata et al., 2011[25]
			15.0 (C2O)[c]		Kuwata et al., 2011[25]
			16.0 (C14)	5.3	Nguyen et al., 2009[80]
			15.5		Nguyen et al., 2009[80]
			27.6 (C9)		Zhang and Zhang, 2005[83]
			15.63	55.4 [i]	Long et al, 2016[4]
			15.4	72.5	Yin and Takahashi, 2017[76]
			15.3 (C2)	105	Yin and Takahashi, 2017[76]
			15.0 (C6)	68	Deng et al. 2018[20]
			14.0 (C5O)	190	Long et al. 2019[23]
			14.7 (C6O)	78	Long et al. 2019[23]
		acyl + OH	30.1		Kuwata et al., 2010[42]
		(1,3-H-shift)	29.2		Kuwata et al., 2011[25]
			29.8		Kuwata et al., 2011[25]
			27.6 (C14)		Nguyen et al., 2009[80]
			32.5		Zhang and Zhang, 2005[83]
			29.0		Long et al, 2016[4]
			28.5		Yin and Takahashi, 2017[76]
			28.3 (C2)		Yin and Takahashi, 2017[76]
		syn-anti isom	28.3		Anglada et al., 1996[54]
			30.1		Kuwata et al. 2005[95]
			34.5		Kuwata et al., 2010[42]
			30.1		Kuwata et al., 2011[25]
			28.9		Nguyen et al., 2009[80]
			38.4		Yin and Takahashi, 2017[76]
			37.4 (C2)		Yin and Takahashi, 2017[76]
			35.4 (C5O)		Long et al. 2019[23]
		Alkyl rotation	1.2		Bowman et al., 2015[96]
			1.0		Yin and Takahashi, 2017[76]
Alkyl	Alkyl	ester channel	18.7		Gutbrod et al., 1996[61]
			21.7		Kroll et al., 2001[63]
			21.6		Selçuki and Aviyente, 2001[64]
			21.7		Olzmann et al., 1997[68]
			22.6 (C13,C1)		Nguyen et al., 2009[80]
			21.1 (C1,C13)		Nguyen et al., 2009[80]
			28.2 (cC8,C1)		Zhang and Zhang, 2005[83]
			21.0		Leonardo et al., 2011[87]
			20.8	3.3×10^{-3}	Smith et al., 2016[17]
			20.8 (CD3)	3.0×10^{-3}	Smith et al., 2016[17]
			20.8		Yin and Takahashi, 2017[76]
			21.5		Kuwata et al., 2018[81]
			21.1		Long et al. 2018[19]
		hydroperoxide	13.6		Gutbrod et al., 1996[61]
			16.0 [a]	6.4±9 [a,b]	Kroll et al., 2001[63]
			14.8		Olzmann et al., 1997[68]
			16.2	362	Fang et al., 2016[11]
			18.6 (C14,C1)	0.57	Nguyen et al., 2009[80]
			16.6 (C1,C14)	42	Nguyen et al., 2009[80]
			10.3 (C1,C8)	25.9	Sun et al., 2011[97]

9

			18.6 (cC8,C1)		Zhang and Zhang, 2005[83]
			17.1		Liu et al., 2014[85]
			≤16.0		Liu et al., 2014[98]
			E_A=5.9±1.2[a]	361±49[a]	Smith et al., 2016[17]
			15.9 (E_A=8-9)	400	Smith et al., 2016[17]
				3.0±0.4[a]	Newland et al., 2015[7]
				<65±65[a]	Berndt et al., 2012[88]
			(CD3)	<100	Smith et al., 2016[17]
			16.6 (CD3)	10.6	Smith et al., 2016[17]
			15.7 (C1,C3O)		Leonardo et al., 2011[87]
			19.6 (C1,C6)		Leonardo et al., 2011[87]
			16.0		Leonardo et al., 2011[87]
			15.8		Li et al., 2016[99]
				305±70[a]	Chhantyal-Pun et al., 2017[6]
				276[1]	Fang et al., 2017[16]
			16.0	572	Yin and Takahashi, 2017[76]
			15.5	794	Kuwata et al., 2018[81]
			15.5	913	Burd et al. 2018[94]
			16.2	340	Drozd et al. 2017[100]
			15.5	1070	Deng et al. 2018[20]
			16.4	420	Long et al. 2018[19]
		alkyl rotation	1.2 (C1, C2)		Kuwata et al., 2005[95]
			2.4 (C2, C1)		Kuwata et al., 2005[95]
3-membered ring		ester channel	9.4 (cC3)		Anglada and Bofill, 1997[101]
		syn-anti isom	20.7		Anglada and Bofill, 1997[101]
6-membered ring		ester channel	17.1 (bicyclic)	1	Nguyen et al., 2009[102]
			20.9 (bicyclic)		Nguyen et al., 2009[102]
			19.7 (bicyclic)		Zhang and Zhang, 2005[83]
			17.0 (bicyclic)	1	Wang and Wang 2017[103]
			16.9 (bicyclic)	1	Wang and Wang 2017[103]
		hydroperoxide	15.4 (bicyclic)	50	Nguyen et al., 2009[102]
			16.4 (bicyclic)		Zhang and Zhang, 2005[83]
			14.5 (bicyclic)	2700	Wang and Wang 2017[103]
			23.8 (bicyclic)		Wang and Wang 2017[103]
		syn-anti isom	30.0 (bicyclic)		Nguyen et al., 2009[102]
		ring opening	23.6 (bicyclic)		Nguyen et al., 2009[102]
9-membered ring		ester channel	23.3 (bicyclic)		Nguyen et al., 2009[80]
			24.7 (bicyclic)		Nguyen et al., 2009[80]
		hydroperoxide	20.3 (bicyclic)		Nguyen et al., 2009[80]
H	s-cis-CH=CH2	ester channel	14.3	311	Yin and Takahashi, 2017[76]
		acyl + OH (1,3-H-shift)	31.4		Yin and Takahashi, 2017[76]
		syn-anti isom	38.1		Yin and Takahashi, 2017[76]
		vinyl rotation	6.4		Yin and Takahashi, 2017[76]
		1,4-ring closure	42.1		Yin and Takahashi, 2017[76]
H	s-trans-CH=CH2	ester channel	16.6		Yin and Takahashi, 2017[76]
		acyl + OH (1,3-H-shift)	30.4		Yin and Takahashi, 2017[76]
		syn-anti isom	39.7		Yin and Takahashi, 2017[76]
		vinyl rotation	8.7		Yin and Takahashi, 2017[76]
CH3	s-cis-CH=CH2	ester channel	24.0		Gutbrod et al. 1997[79]
			19.2		Kuwata et al., 2005[95]
			19.5	0.018	Zhang and Zhang, 2002[65,66]
		hydroperoxide	15.5		Gutbrod et al. 1997[79]
			16.9	146	Kuwata et al., 2010[42]
			17.4		Kuwata et al., 2005[95]
			18.4	0.11	Zhang and Zhang, 2002[65,66]
		syn-anti isom	21.8		Kuwata et al., 2005[95]
		vinyl rotation	5.9 (C1, C2H3)		Kuwata et al., 2005[95]
CH3	s-trans-CH=CH2	ester channel	23.0		Gutbrod et al. 1997[79]
			22.2		Kuwata et al., 2005[95]
			22.1	3.2×10^{-4}	Zhang and Zhang, 2002[65,66]
		hydroperoxide	16.0		Gutbrod et al. 1997[79]
			18.3	14.7	Kuwata et al., 2010[42]

			18.0		Kuwata et al., 2005[95]
			18.8	0.066	Zhang and Zhang, 2002[65,66]
		syn-anti isom	26.0		Kuwata et al., 2005[95]
		vinyl rotation	7.6 (C1, C2H3)		Kuwata et al., 2005[95]
s-cis-CH=CH$_2$	H	ester channel	25.7		Yin and Takahashi, 2017[76]
		syn-anti isom	41.2		Yin and Takahashi, 2017[76]
		vinyl rotation	9.4		Yin and Takahashi, 2017[76]
		ring closure	12.1	9312	Yin and Takahashi, 2017[76]
s-trans-CH=CH$_2$	H	ester channel	19.5		Yin and Takahashi, 2017[76]
		hydroperoxide vinyl (1,4-Hshift)	23.3		Yin and Takahashi, 2017[76]
		syn-anti isom	40.4		Yin and Takahashi, 2017[76]
		vinyl rotation	9.2		Yin and Takahashi, 2017[76]
s-cis-CH=CH$_2$	CH$_3$	ester channel	22.0		Kuwata et al., 2005[95]
			22.2		Zhang and Zhang, 2002[65]
		syn-anti isom	20.6		Kuwata et al., 2005[95]
		vinyl rotation	8.0		Kuwata et al., 2005[95]
		ring closure	11.0		Kuwata et al., 2005[95]
s-trans-CH=CH$_2$	CH$_3$	ester channel	16.8		Kuwata et al., 2005[95]
			17.5	0.62	Zhang and Zhang, 2002[65,66]
		hydroperoxide vinyl (1,4-Hshift)	18.8		Kuwata et al., 2005[95]
			21.9	6.9×10^{-4}	Zhang and Zhang, 200[66,83]
		syn-anti isom	23.1		Kuwata et al., 2005[95]
		vinyl rotation	8.0		Kuwata et al., 2005[95]
H	s-cis-C(CH$_3$)=CH$_2$	ester channel	24.1		Gutbrod et al. 1997[79]
			14.5		Zhang and Zhang, 2002[65]
			13.9		Kuwata and Valin, 2008[104]
		1,3-H-shift	31.6		Gutbrod et al. 1997[79]
			31.6		Zhang and Zhang, 2002[65]
			32.6		Kuwata and Valin, 2008[104]
		syn-anti isom	18.2		Kuwata and Valin, 2008[104]
H	s-trans-C(CH$_3$)=CH$_2$	ester channel	20.3		Gutbrod et al. 1997[79]
			16.7	3.6	Zhang and Zhang, 2002[65,66]
			16.4		Kuwata and Valin, 2008[104]
		1,3-H-shift	31.1		Gutbrod et al. 1997[79]
			31.2	1.4×10^{-10}	Zhang and Zhang, 2002[65,66]
			31.2		Kuwata and Valin, 2008[104]
		syn-anti isom	21.3		Kuwata and Valin, 2008[104]
s-cis-C(CH$_3$)=CH$_2$	H	ester channel	25.5		Zhang and Zhang, 2002[65]
			25.3		Kuwata and Valin, 2008[104]
		1,5-ring closure	11.9		Kuwata and Valin, 2008[104]
		syn-anti isom	20.4		Kuwata and Valin, 2008[104]
s-trans-C(CH$_3$)=CH$_2$	H	ester channel	16.9	2.2	Zhang and Zhang, 2002[65,66]
			16.3		Kuwata and Valin, 2008[104]
		1,5-H-shift	36.2	2.2×10^{-11}	Zhang and Zhang, 2002[65,66]
			35.9		Kuwata and Valin, 2008[104]
		syn-anti isom	18.6		Kuwata and Valin, 2008[104]
CHO	H	1,4+1,2-ring closure	19.2 [k]		Cremer et al., 2001[105]
		1,4-ring closure	23.6 [k]		Cremer et al., 2001[105]
		1,5-ring closure	36.6 [k]		Cremer et al., 2001[105]
		1,4-H-shift	20.6 [k]		Cremer et al., 2001[105]
		ester channel	16.9 [k]		Cremer et al., 2001[105]
		O(^{1}D) loss	53.0 [k]		Cremer et al., 2001[105]
		O(3P) loss	52.0 [k]		Cremer et al., 2001[105]
		syn-anti isom	17.3 [k]		Cremer et al., 2001[105]
H	CHO	ester channel	21.8 [k]		Cremer et al., 2001[105]
		O(^{1}D) loss	55.5 [k]		Cremer et al., 2001[105]
		O(^{3}P) loss	54.5 [k]		Cremer et al., 2001[105]
		syn-anti isom	20.0 [k]		Cremer et al., 2001[105]
s-syn-OH	H	1,4-H-migration	barrierless[d]		Selçuki and Aviyente, 2000[106]
			barrierless[d]		Lei et al., 2020[107]
s-anti-OH	H	ester channel	18.8		Selçuki and Aviyente, 2000[106]
s-anti-OCH$_3$	H	ester channel	18.1		Selçuki and Aviyente, 2001[64]
s-syn-OCH$_3$	H	ester channel	12.5		Selçuki and Aviyente, 2001[64]

H	s-syn-OH	ester channel	8.0	Selçuki and Aviyente, 2000[106]
H	s-anti-OH	ester channel	7.9	Selçuki and Aviyente, 2000[106]
H	s-anti-OCH$_3$	ester channel	7.50	Selçuki and Aviyente, 2001[64]
H	s-syn-OCH$_3$	ester channel	7.93	Selçuki and Aviyente, 2001[64]
H	Cl	syn-anti isom	1.1	Ljubić and Sabljić, 2002[108]
H	F	O-loss	27.2	Ljubić and Sabljić, 2005[109]
		ester channel	11.3	Ljubić and Sabljić, 2005[109]
			7.9	Cremer et al., 1988[72]
		1,3-H-shift	22.6	Ljubić and Sabljić, 2005[109]
		syn-anti isom	1.7	Ljubić and Sabljić, 2002[108]
Cl	H	syn-anti isom	2.8	Ljubić and Sabljić, 2002[108]
F	H	ester channel	20.0	Ljubić and Sabljić, 2005[109]
			17.1	Cremer et al., 1988[72]
		syn-anti isom	3.4	Ljubić and Sabljić, 2002[108]
H	CN	ester channel	20.9	Selçuki and Aviyente, 2001[64]
CN	H	ester channel	22.6	Selçuki and Aviyente, 2001[64]
CN	CN	ester channel	22.8	Selçuki and Aviyente, 2001[64]
[not applicable]	=O	ester channel	barrierless	Keßel et al., 2017[110]
=C=O	[not applicable]	cycl. + frag.[h]	< 1 kcal mol^{-1}	Keßel et al., 2017[110]
C≡CH	H	ester channel	22.3	Yin and Takahashi, 2017[76]
		syn-anti isom	41.0	Yin and Takahashi, 2017[76]
H	C≡CH	ester channel	17.3	Yin and Takahashi, 2017[76]
		acyl + OH (1,3-H-shift)	29.9	Yin and Takahashi, 2017[76]
		syn-anti isom	40.4	Yin and Takahashi, 2017[76]

[a] experimental data

[b] at 100 Torr

[c] alkyl substituent is -CH$_2$-CHO

[d] rearranges to performic acid, HC(O)OOH

[e] 1,5-H-shift of methyl hydrogen.

[f] Range includes fall-off and variation of barrier height.

[g] Reported value is without ZPE corrections, which decrease the barrier height

[h] cyclizes to a transient 4-membered ring, which decomposes spontaneously to CO_2 + CO

[i] T-dependent data available

[j] Methodologically flawed result; see Harding and Klippenstein,[82] Chen et al.,[83] and Vereecken et al.[8] for further information.

[k] ΔH(298K)

[l] Value obtained by combining experimentally observed energy-specific k(E), with RRKM rate coefficient calculations.

B. Internal rotation of substituents

For internal rotation around the single bond in the conjugated π-systems of β-unsaturated CI, we find energy barriers of up to 9 kcal mol^{-1} (see Table 6), of a similar value as those reported in the literature earlier.[8,46,95,104,111,112] The rates of internal rotation are typically significantly faster by several orders of magnitude than the chemical isomerisations considered in this work, indicating that the *s-cis* and *s-trans* isomers will be in near-equilibrium and should be considered as a single pool of reactants rather than separable species. Some fast reaction classes, such as 1,5-ring closure of allyl-1,6-H-migration, can have comparable rate coefficients and may be affected by the rate of internal rotation. However, as these reactions have no relevant competing reactions, we do not investigate this aspect in more detail.

Table 6: Barrier heights (kcal mol^{-1}) and rate coefficients (s^{-1}) for *s-cis* ↔ *s-trans* internal rotation in β-unsaturated CI, i.e. rotation along the central single bond in conjugated systems. The isomerisation reaction is listed for rotation from the more stable conformer towards the less stable orientation; the reverse rotation has a lower barrier and higher reaction rates.

carbonyl oxide	E_b	k(298K)
E-(CH$_2$CH$_3$)(CH=CH$_2$)COO	7.6	3.1×10^7
Z-(CH=CH$_2$)(CH$_2$CH$_3$)COO	8.2	8.2×10^6
E-(iC$_3$H$_7$)(CH=CH$_2$)COO	5.2	5.0×10^8
Z-(CH=CH$_2$)(iC$_3$H$_7$)COO	7.9	1.4×10^7
Z-(*E*-CH=CHCH$_3$)(CH$_3$)COO	9.3	1.5×10^6
Z-(*Z*-CH=CHCH$_3$)(CH$_3$)COO	4.3	3.8×10^9
Z-(C(=CH$_2$)CH$_2$OH)CHOO	7.4	2.9×10^8
Z-(*Z*-CH=CHCH$_2$OH)CHOO	6.1	1.4×10^8

C. Stereoisomerisation

The E/Z-stereoisomerisation in carbonyl oxides occurs either by rotation of the outer oxygen around the (partial) double bond, or by an in-plane transition by straightening of the COO bond. We have examined the barrier height for stereoisomerization for a few oxygenated compounds to investigate the impact of the substituent and any possible H-bonding. Similar to other studies (see Table 5 and Vereecken et al.[8]), however, we find very high energy barriers for these processes (Table 7), confirming once more that E/Z-stereoisomerisation is a negligibly slow process in Criegee intermediates. The rate coefficients were not calculated but are expected to be $k(298K) \leq 10^{-10}$ s^{-1}, by analogy with Vereecken et al.[8]

Table 7: Stereo-isomerisation in carbonyl oxides by in-plane transition or by internal rotation (out-of-plane) of the outer oxygen, listing barrier heights E_b (kcal mol^{-1}), rate coefficient k (s^{-1}) at 298 K, and parameters for a Kooij equation fit $k(T)=A \times (T/K)^n \times \exp(-E_a/T)$ for the temperature range 200-450 K.

Carbonyl oxide	E_b	k(298K)	A / s^{-1}	n	E_a / K	Remarks
OH-bearing substituent						
E-(CH$_3$)(CH$_2$OH)COO	34.1					
Z-(CH$_2$OH)(CH$_3$)COO	37.4					
E-(CH$_2$CH$_2$CH$_2$CH$_2$OH)CHOO	(35.2)					M06-2X/aug-cc-pVTZ energy barrier
Ether substituents						
E-(CH$_3$)(CH$_2$OCH$_3$)COO	36.6					
Z-(CH$_2$OCH$_3$)(CH$_3$)COO	38.4					

The two stereoisomers of an asymmetric carbonyl oxide can have strongly different reactivity, not only in reaction rate but also in dominant and accessible reaction classes. The energetically highest-lying isomer often reacts faster by releasing some of its higher potential energy in the transition state, leading to lower effective barrier heights. Relative energies of the stereoisomers are shown in Table 8, supplementing the list in Vereecken et al.[8] The relative energy depends on many factors, such as electroactivity of the substituent, conjugation, and H-bonding. For many of the compounds listed in Table 8 there is a large difference in energy between the various conformers for a given isomer, with a strong preference to avoid steric hindrance, and to form strong H-bonds. Vereecken et al. analyzed the relative energy of the isomers using a group additivity paradigm; we refrain from doing the same here as the data set is too sparse relative to the number of substituents considered.

Table 8: Energy (kcal mol^{-1}) of carbonyl oxide stereoisomers relative to lowest-energy isomer.

Carbonyl oxide	Z isomer	E isomer
OH-bearing substituent		
$(CH_2OH)CHOO$	0.00	6.62
$(CH_2OH)(CH_3)COO$	0.00	3.32
$(C(CH_3)_2OH)CHOO$	0.00	6.05
$(CH_2CH_2OH)CHOO$	0.00	4.93
$(CH_2CH_2CH_2OH)CHOO$	0.00	5.76
$(CH_2CH_2CH_2OH)(CH_3)COO$	0.00	3.46
$(CH_2CH_2CH_2CH_2OH)CHOO$	0.00	2.01
alkoxy-bearing substituent		
$(OCH_3)CHOO$	3.94	0.00
$(OCH_3)(CH_3)COO$	0.22	0.00
$(CH_2OCH_3)(CH_3)COO$	0.00	1.80
OOH-bearing substituent		
$(OOH)CHOO$	0.00	15.08
$(OOH)(CH_3)COO$	0.00	11.53
$(CH_2OOH)CHOO$	0.00	5.49
$(CH_2OOH)(CH_3)COO$	0.00	1.64
$(CH_2CH_2OOH)CHOO$	0.00	6.63
$(CH_2CH_2CH_2OOH)CHOO$	0.00	3.21
Carboxylic acid substituent		
$(CH_2COOH)CHOO$	0.00	7.87
$(CH_2CH_2COOH)CHOO$	0.00	4.82
$(CH_2CH_2CH_2COOH)CHOO$	0.00	2.98
OOOH substituent		
$(OOOH)CHOO$	0.00	1.07
$(OOOH)(CH_3)COO$	3.71	0.00
ONO$_2$-bearing substituent		
$(ONO_2)CHOO$	0.00	1.84
$(CH_2ONO_2)(CH_3)COO$	0.00	2.35
Cyclic substituent (similar to 3-carene)		
$(CH_2\text{-}cycC_3H_5)CHOO$	0.00	3.59
$(CH_2\text{-}cycC_3H_5)(CH_3)COO$	0.00	0.12
unsaturated substituents		
$(CH_2CH_3)(CH{=}CH_2)COO$	2.25	0.00
$(CH{=}CH_2)(iC_3H_7)COO$	0.00	0.11

D. 1,3-H-migration in E-R$_2$CHOO (*anti*-RCHOO)
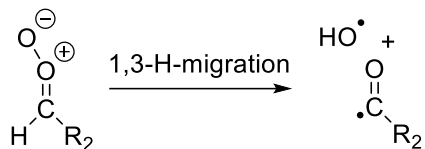
1,3-H-migration of a *syn*-H-atom, followed by OH elimination to form an acyl radical, is typically a slow reaction (see Table 5 and Vereecken et al.[8]). For most of the compounds studied in this work (Table 9), we similarly find high energy barriers and low reaction rates. The barriers for anti-substituents –OOH, –OOOH, and –ONO$_2$, however, are surprisingly low, with reaction rates exceeding 10 s^{-1}. For these compounds, however, we find that the 1,3-ring closure is faster by orders of magnitude, and we again conclude that 1,3-H-migration reactions are not important in any CI.

Table 9: 1,3-H-migration in E-RCHOO carbonyl oxides, listing barrier heights E_b (kcal mol^{-1}), rate coefficient k (s^{-1}) at 298 K, and parameters for a Kooij equation fit $k(T)=A\times(T/K)^n\times\exp(-E_a/T)$ for the temperature range 200-450 K.

Carbonyl oxide	E_b	k(298K)	A / s^{-1}	n	E_a / K	Remarks
Cyclic substituent (similar to 3-carene)						
E-(CH$_2$-cycC$_3$H$_5$)CHOO	28.4	2.0×10^{-6}	7.23E-133	47.55	-6050	
OH-bearing substituent						
E-(CH$_2$OH)CHOO	27.5	9.1×10^{-6}	7.35E-128	45.78	-6074	
E-(CH$_2$CH$_2$OH)CHOO	28.7	1.7×10^{-6}	2.72E-134	47.99	-6238	
E-(CH$_2$CH$_2$CH$_2$OH)CHOO	29.5	5.6×10^{-6}	1.07E-128	46.17	-5835	
E-(CH$_2$CH$_2$CH$_2$CH$_2$OH)CHOO	30.2	7.0×10^{-7}	9.69E-132	47.73	-4655	
E-(C(CH$_3$)$_2$OH)CHOO	28.5	1.3×10^{-6}	1.76E-134	48.00	-6249	
OOH-bearing substituent						
E-(OOH)CHOO	17.8	2.6×10^{1}	3.32E-71	27.10	-3326	OH + CO$_2$ + OH products
E-(CH$_2$OOH)CHOO	27.7	3.7×10^{-6}	7.47E-132	47.02	-6444	
E-(CH$_2$CH$_2$OOH)CHOO	29.2	5.5×10^{-6}	1.96E-127	45.75	-5685	
Carboxylic acid substituent						
E-(CH$_2$C(=O)OH)CHOO	29.6	9.7×10^{-7}	9.06E-138	49.18	-6429	
E-(CH$_2$CH$_2$C(=O)OH)CHOO	28.4	3.1×10^{-6}	8.56E-132	47.17	-6080	
ONO$_2$-bearing substituent						
E-(ONO$_2$)CHOO	18.4	3.9×10^{1}	2.95E-73	27.94	-3430	
OOOH-substituent						
E-(OOOH)CHOO	18.7	1.3×10^{1}	6.45E-75	28.43	-3412	HOOOCOOH carbene product [a]

[a] The carbene is expected to further decompose in a stepwise or concerted reaction, possibly to HO$_2$ + $^\bullet$OCOOH or directly to HO$_2$ + CO$_2$ + OH.

E. Alkyl-1,4-H-migration forming vinyl hydroperoxides (VHP)
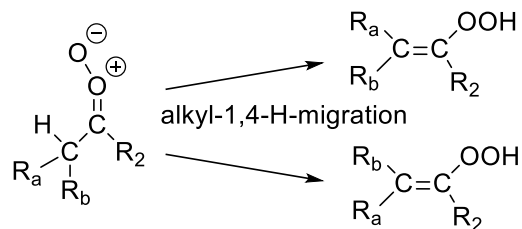
The rate coefficient predictions across the relevant range of substituents are listed in Table 10. For CI where the vinyl hydroperoxide product after 1,4-H-migration has two stereoisomers, we list the total VHP formation. Vereecken et al.[8] examined the yield of Z- versus E-VHP product and found that the formation of Z-VHP is always a minor channel contributing < 5 % at 298K. The results indicate that, as for stereoisomerism, the rate coefficients are influenced by both the R_1 and R_2 substituents. We find rate coefficients in the range of 10^0 to 10^3 s^{-1}, in line with earlier predictions for this reaction class.[8] The rate coefficients show strong non-Arrhenius behavior due to extensive tunneling, which increases the rate coefficient by one to two orders of magnitude at room temperature, and is the main driver for reaction at lower temperatures.

Table 10: Alkyl-1,4-H-migration in carbonyl oxides, listing barrier heights E_b (kcal mol^{-1}), rate coefficient k (s^{-1}) at 298 K, and parameters for a Kooij equation fit $k(T)=A \times (T/K)^n \times \exp(-E_a/T)$ for the temperature range 200-450 K.

Carbonyl oxide	E_b	k(298K)	A / s^{-1}	n	E_a / K	Remarks
Cyclic substituent (similar to 3-carene)						
E-(CH$_3$)(CH$_2$-cycC$_3$H$_5$)COO	16.1	3.4×10^2	1.32E-59	23.52	-2213	
Z-(CH$_2$-cycC$_3$H$_5$)(CH$_3$)COO	15.0	1.5×10^3	1.47E-52	21.14	-1867	
Z-(CH$_2$-cycC$_3$H$_5$)CHOO	16.1	2.9×10^2	5.11E-59	23.24	-2240	
OH-bearing substituent						
Z-(CH$_2$OH)CHOO	18.2	3.9×10^1	5.39E-71	27.27	-3022	
Z-(CH$_2$CH$_2$OH)CHOO	17.9	3.6×10^1	2.25E-69	26.78	-2704	
Z-(CH$_2$CH$_2$CH$_2$OH)CHOO	19.1	2.0×10^1	5.15E-77	29.69	-2840	
Z-(CH$_2$CH$_2$CH$_2$CH$_2$OH)CHOO	17.5	1.4×10^2	4.94E-57	22.74	-1500	
E-(CH$_3$)(CH$_2$OH)COO	16.4	2.9×10^2	8.11E-61	23.92	-2308	
Z-(CH$_2$OH)(CH$_3$)COO	18.2	2.0×10^1	9.76E-74	28.23	-3070	
Z-(CH$_2$CH$_2$CH$_2$OH)(CH$_3$)COO	20.3	2.7×10^0	1.91E-86	32.96	-3166	
E-(CH$_3$)(CH$_2$CH$_2$CH$_2$OH)COO	17.2	5.7×10^2	1.25E-55	22.25	-1801	
Ether substituents						
E-(CH$_3$)(CH$_2$OCH$_3$)COO	16.6	1.1×10^2	2.26E-63	24.68	-2483	
Z-(CH$_2$OCH$_3$)(CH$_3$)COO	17.0	2.8×10^2	4.45E-66	25.81	-2713	
OOH-bearing substituent						
Z-(CH$_2$OOH)CHOO	16.4	2.6×10^2	8.64E-63	24.51	-2629	
Z-(CH$_2$CH$_2$OOH)CHOO	19.7	1.9×10^1	2.16E-76	29.63	-2506	
Z-(CH$_2$CH$_2$CH$_2$OOH)CHOO	19.6	1.6×10^1	1.56E-83	32.10	-3155	
E-(CH$_3$)(OOH)COO	15.9	4.3×10^2	1.35E-56	22.55	-1862	
E-(CH$_3$)(CH$_2$OOH)COO	16.2	8.3×10^1	8.73E-63	24.41	-2462	
Z-(CH$_2$OOH)(CH$_3$)COO	15.5	6.6×10^2	2.72E-57	22.69	-2240	
Aldehyde substituent						
(CH=O)$_2$COO	18.9	4.3×10^0	6.15E-78	29.11	-3997	
ONO$_2$-bearing substituent						
E-(CH$_3$)(ONO$_2$)COO	14.9	2.3×10^3	7.77E-51	20.63	-1675	
E-(CH$_3$)(CH$_2$ONO$_2$)COO	15.6	4.8×10^2	1.44E-58	23.12	-2282	
Z-(CH$_2$ONO$_2$)(CH$_3$)COO	14.8	2.2×10^3	4.01E-56	22.41	-2271	
Alkoxy substituents						
E-(CH$_3$)(OCH$_3$)COO	16.9	6.9×10^1	1.16E-63	24.88	-2212	
OOOH-substituent						
E-(CH$_3$)(OOOH)COO	15.4	7.4×10^2	1.75E-55	22.21	-1843	
Carboxylic acid substituent						
Z-(CH$_2$C(=O)OH)CHOO	15.1	2.4×10^3	1.97E-52	21.35	-1550	
Z-(CH$_2$CH$_2$C(=O)OH)CHOO	17.7	3.7×10^1	3.12E-68	26.35	-2671	
Z-(CH$_2$CH$_2$CH$_2$C(=O)OH)CHOO	14.8	6.3×10^2	1.46E-58	22.98	-2595	
E-(CH$_3$)(CH$_2$C(=O)OH)COO	16.7	3.1×10^2	1.60E-62	24.56	-2422	
Unsaturated substituents						
E-(CH$_2$CH$_3$)(CH=CH$_2$)COO	17.9	3.0×10^1	1.36E-68	26.38	-2809	
E-(iC$_3$H$_7$)(CH=CH$_2$)COO	18.1	1.1×10^1	4.09E-72	27.42	-3149	
E-(iC$_3$H$_7$)(CH$_2$CH=CH$_2$)COO	18.0	7.6×10^0	9.11E-72	27.32	-2980	
E-(CH$_3$)(CH$_2$CH=CH$_2$)COO	16.4	4.3×10^2	2.92E-61	24.07	-2479	
Multifunctionalized CI						
Z-(CH(OOH)CH$_2$OH)(CH$_3$)COO	18.4	1.2×10^1	1.80E-73	28.38	-2476	

F. Vinyl-1,4- and acyl-1,4-H-migration forming cumulene hydroperoxides
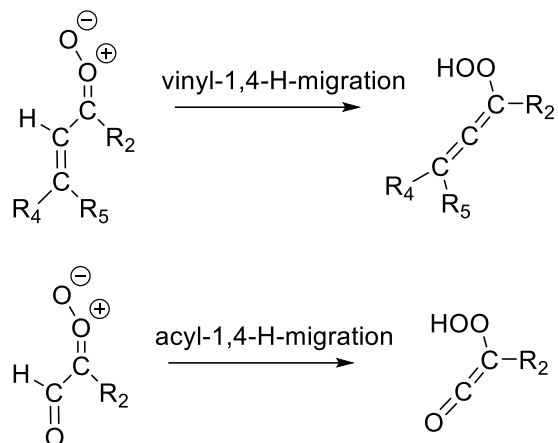
The rate coefficient predictions across the relevant range of substituents are listed in Table 11. In most cases we find high barriers, in agreement with earlier work by Kuwata et al.[95] and Vereecken et al.,[8] and low rate coefficients despite strong rate enhancement by tunneling. For two compounds we see barriers below 20 kcal mol^{-1} and reaction rates at 298 K up to 30 s^{-1}. However, for Z-(Z-CH=CHCH$_3$)(CH$_3$)COO, the 1,5-ring closure reaction is faster by many orders of magnitudes, while for (CH=O)$_2$COO the 1,3-ring closure is faster by 1 order or magnitude. Based on this, we again conclude that these two reaction classes are non-competitive.

Table 11: Vinyl- and acyl-1,4-H-migration in carbonyl oxides, listing barrier heights E_b (kcal mol^{-1}), rate coefficient k (s^{-1}) at 298 K, and parameters for a Kooij equation fit $k(T)=A\times(T/K)^n\times\exp(-E_a/T)$ for the temperature range 200-450 K.

Carbonyl oxide	E_b	k(298K)	A / s^{-1}	n	E_a / K	Remarks
Unsaturated substituents						
Z-(CH=CH$_2$)(CH$_2$CH$_3$)COO	21.3	1.0×10^{-1}	7.82E-90	33.57	-3477	
Z-(CH=CH$_2$)(iC$_3$H$_7$)COO	20.9	2.9×10^{-1}	3.65E-88	33.00	-3607	
Z-(E-CH=CHCH$_3$)(CH$_3$)COO	21.3	7.2×10^{-2}	4.26E-88	33.11	-2969	
Z-(Z-CH=CHCH$_3$)(CH$_3$)COO	17.6	2.9×10^{1}	1.04E-68	26.60	-2490	
Aldehyde substituent						
(CH=O)$_2$COO	18.9	4.3×10^{0}	6.15E-78	29.11	-3997	

G. Allyl-1,4- and allyl-1,6-H-migration forming β-unsaturated VHP
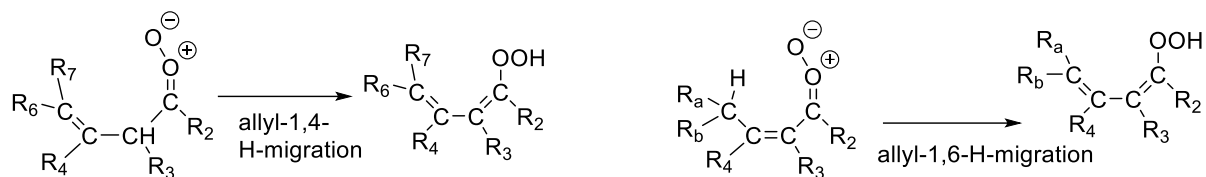
Table 12 and Table 13 list barrier height and rate coefficients for allyl-H-migration. As found in earlier work,[8] we see that these reactions are very fast, especially for 1,6-H-migrations where the ring strain in the transition state is minimal. The double bond enhances the reaction significantly compared to traditional alkyl 1,4-H-migrations. Table 13 shows two hydroxy-substituted compounds where we find that, compared[8] to having an H-atom or alkyl substituent, the –OH substituent increases the rate of reaction by a factor 2 to 200 by lowering the C–H bond strength of the migrating H-atoms as well as by H-bonding with the carbonyl oxide moiety.

Table 12: Allyl-1,4-H-migration in γ-unsaturated carbonyl oxides forming conjugated vinyl hydroperoxides, listing barrier heights E_b (kcal mol^{-1}), rate coefficient k (s^{-1}) at 298 K, and parameters for a Kooij equation fit $k(T)=A\times(T/K)^n\times\exp(-E_a/T)$ for the temperature range 200-450 K.

Carbonyl oxide	E_b	k(298K)	A / s^{-1}	n	E_a / K	Remarks
Z-(CH$_2$CH=CH$_2$)(iC$_3$H$_7$)COO	13.1	7.1×10^3	1.27E-44	18.35	-1605	
Z-(CH$_2$CH=CH$_2$)(CH$_3$)COO	13.5	7.0×10^3	2.97E-45	18.69	-1459	

Table 13: Allyl-1,6-H-migration in β-unsaturated carbonyl oxides forming conjugated vinyl hydroperoxides, listing barrier heights E_b (kcal mol^{-1}), rate coefficient k (s^{-1}) at 298 K, and parameters for a Kooij equation fit $k(T)=A\times(T/K)^n\times\exp(-E_a/T)$ for the temperature range 200-450 K.

Carbonyl oxide	E_b	k(298K)	A / s^{-1}	n	E_a / K	Remarks
Z-(Z-CH=CHCH$_3$)(CH$_3$)COO	6.5	2.5×10^8	4.80E-05	5.44	512	
Z-(Z-CH=CHCH$_2$OH)CHOO	8.9	8.7×10^6	6.78E-08	6.37	1141	
Z-(Z-CH=CHCH$_2$CH$_2$OH)CHOO	6.9	1.3×10^8	3.57E-03	4.63	611	

H. Vinyl-, allyl-, and β-oxo-1,5-H-migration
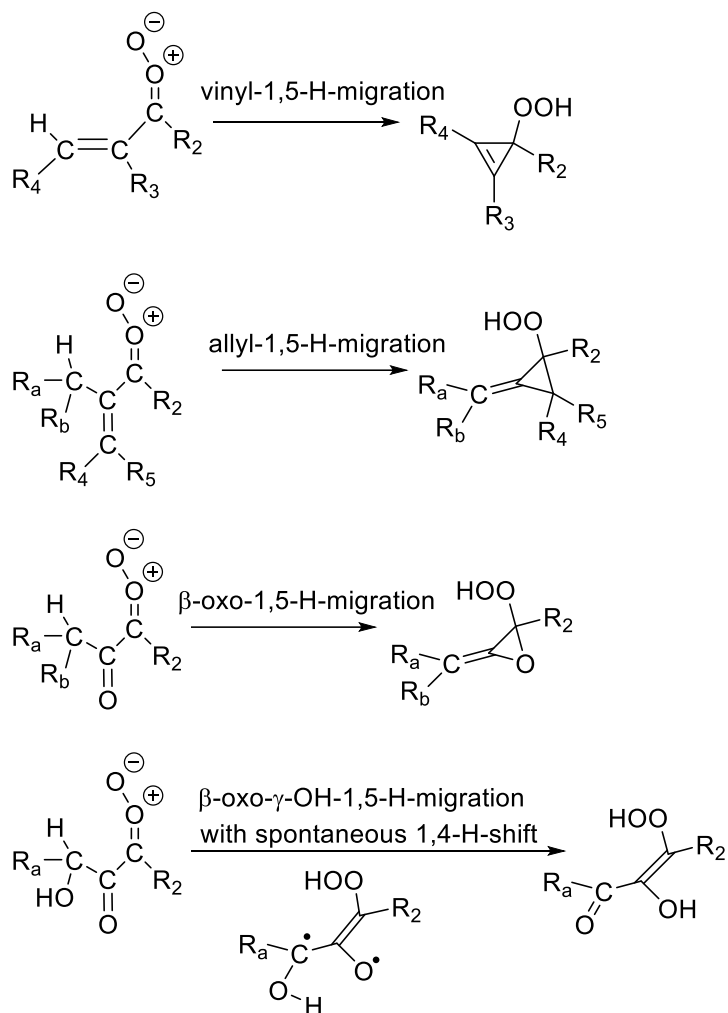
1,5-H-migrations in β-unsaturated CI are not favorable, as the reaction leads to a transient high-energy singlet biradical intermediate that then recombines barrierlessly to a strained ring, or undergoes other isomerisations to form a closed-shell product such as an H-migration of a neighboring OH group (see scheme above). The rate coefficients calculated in this work are listed in Table 14; as also found in Vereecken et al.[8] the rate coefficients are low, k(298 K) < 10^{-2} s^{-1}, and these reaction classes are not competitive.

Table 14: 1,5-H-migrations in β-unsaturated carbonyl oxides, listing barrier heights E_b (kcal mol^{-1}), rate coefficient k (s^{-1}) at 298 K, and parameters for a Kooij equation fit $k(T)=A\times(T/K)^n\times\exp(-E_a/T)$ for the temperature range 200-450 K.

Carbonyl oxide	E_b	k(298K)	A / s^{-1}	n	E_a / K	Reaction type
Z-(C(=O)CH$_2$OH)CHOO	22.0	8.5×10^{-3}	3.05E-96	35.34	-4128	β-oxo-γ-OH-1,5-H-shift
Z-(C(=CH$_2$)CH$_2$OH)CHOO	37.0	1.5×10^{-11}	3.66E-186	64.90	-9654	Allyl-1,5-H-migration

I. Hydroperoxide-1,5-H-migration
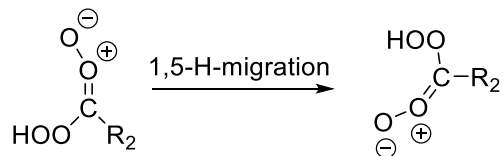
CI with an α-OOH substituent can undergo a 1,5-H-migration, leading to a product identical to the reactant; this reaction is perhaps best described as an isomorphic tautomerization. As listed in Table 15, the H-migration is essentially barrierless, with the small potential energy barrier disappearing after ZPE corrections. The reaction is aided by the strong H-bond between the hydroperoxide moiety and the carbonyl oxide group, where the dominant conformer of *syn*-OOH-CI is always that with the H-bonded 6-membered ring. This very fast rearrangement has no impact on the chemical fate of the CI, other than scrambling of isotope-specific isomers, though theoretical calculations must account for the doubling of the accessible quantum states in rate and entropy calculations. Given the low impact of this reaction class beyond entropic effects we did not investigate it in more detail.

Table 15: 1,5-H-migration in hydroperoxide carbonyl oxides. Listed is the barrier height for tautomerization (kcal mol^{-1})

Carbonyl oxide	E_b
Z-(OOH)CHOO	-0.94
Z-(OOH)(CH$_3$)COO	-0.86

J. Hydrotrioxide-1,6-H-migration forming peracid + $^1O_2$
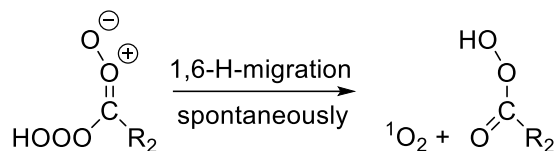
Carbonyl oxides with an α-OOOH substituent are formed in the ozonolysis of α-unsaturated hydrotrioxides. While no studies are available on such compounds, vinyl-hydrotrioxides (C=COOOH), are considered in chemical models implementing the reaction of OH radicals with vinylperoxides, C=COO$^•$ + $^•$OH, as implied by the recent work of Fittschen et al.[113–119] Theoretical work by our group[116] has shown that stabilization of the hydrotrioxide is a strong function of the size of the RO_2, with ROOOH compounds with 4 or more non-H-atoms in the R-group expected to be mostly thermally stabilized. As the chemistry and impact of hydrotrioxides remains very uncertain, it is worthwhile to examine the impact of the substituent on ozonolysis and CI chemistry. We find that the 1,6-H-migration to the carbonyl moiety is barrierless (Table 16), after which the product spontaneously eliminates a singlet O_2 molecule. Though $^1O_2$ has a high enthalpy of formation, the overall reaction remains highly exothermic by over 50 kcal mol^{-1}. Given these characteristics, it seems likely that the hydrotrioxide substituent already reacts during the decomposition of the primary ozonide which, combined with the impact of H-bonding on this decomposition, will affect the ozonolysis of vinyl-hydrotrioxides. The peracid product could also be chemically activated, decomposing promptly. Elimination of singlet $^1O_2$ likely requires multi-reference methodologies to characterize accurately; we have not done so at this time as the rate limiting initial stage comprises an H-migration which is likely sufficiently well described at our level of theory.

Table 16: 1,6-H-migration in hydrotrioxide carbonyl oxides. Listed is the barrier height E_b and the product energy E_{prod} (kcal mol^{-1})

Carbonyl oxide	E_b	E_{prod}
Z-(OOOH)CHOO	Barrierless	-51.6
Z-(OOOH)(CH$_3$)COO	Barrierless	-51.1

K. 1,3-Ring closure forming dioxirane
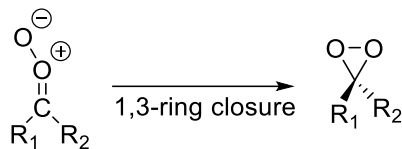
1,3-ring closure is one of the few unimolecular CI reaction classes that are available to all CI. In most cases it is not the dominant channel, especially for compounds that have H-migration reactions or other ring closure reactions accessible. Table 17 shows the list of reactions characterized in the current study, and indeed for many compounds the reaction rate is too slow to compete with other unimolecular or bimolecular (water) reactions. Notable exceptions are the CI with a *syn*-H-atom substituent, or with α-hetero-atom substituents such as –OH, –OR, –OOH, –OOOH, –C(=O)R, or –ONO$_2$, where both *syn*- and *anti*-substitution can greatly enhance the 1,3-ring closure and can lead to rate coefficient at 298 K exceeding 10^2 s^{-1}, up to 10^9 s^{-1}. The expected fate of the hot dioxiranes formed is ring opening and decomposition. In this work, we do not investigate this subsequent chemistry nor the observable end products. Vereecken et al.[8] also studied this reaction class in terms of group additivity ; as the data points are sparse compared to the combinatorial number of substitution patterns covered in this work we refrain from continuing this analysis at this time.

Table 17: 1,3-ring closure in carbonyl oxides, listing barrier heights E_b (kcal mol^{-1}), rate coefficient k (s^{-1}) at 298 K, and parameters for a Kooij equation fit $k(T)=A\times(T/K)^n\times\exp(-E_a/T)$ for the temperature range 200-450 K.

Carbonyl oxide	E_b	k(298K)	A / s^{-1}	n	E_a / K	Remarks
Cyclic substituent (simlar to 3-carene)						
E-(CH$_3$)(CH$_2$-cycC$_3$H$_5$)COO	20.8	2.8×10^{-3}	4.26E+08	1.50	10210	
Z-(CH$_2$-cycC$_3$H$_5$)(CH$_3$)COO	20.1	1.9×10^{-2}	5.76E+09	1.19	9899	
E-(CH$_2$-cycC$_3$H$_5$)CHOO	15.4	4.8×10^1	3.03E+09	1.23	7441	
Z-(CH$_2$-cycC$_3$H$_5$)CHOO	22.8	3.7×10^{-4}	5.65E+05	2.51	10560	
OH-bearing substituent						
E-(CH$_2$OH)CHOO	14.6	1.3×10^2	1.32E+09	1.28	6985	
Z-(CH$_2$OH)CHOO	19.6	2.3×10^{-2}	3.04E+09	0.97	9271	
E-(CH$_2$CH$_2$OH)CHOO	12.7	3.9×10^2	1.04E+06	1.87	5530	
Z-(CH$_2$CH$_2$OH)CHOO	22.3	3.6×10^{-4}	1.91E+05	2.49	10225	
E-(CH$_2$CH$_2$CH$_2$OH)CHOO	12.9	3.2×10^3	7.25E+14	-0.98	6124	
Z-(CH$_2$CH$_2$CH$_2$OH)CHOO	21.7	6.3×10^{-4}	1.74E+08	1.43	10277	
Z-(CH$_2$CH$_2$CH$_2$OH)(CH$_3$)COO	19.6	1.2×10^{-2}	2.09E+09	1.04	9484	
E-(CH$_3$)(CH$_2$CH$_2$CH$_2$OH)COO	16.7	9.8×10^{-1}	1.33E+15	-1.30	8178	
E-(CH$_2$CH$_2$CH$_2$CH$_2$OH)CHOO	13.9	3.6×10^2	1.33E+21	-2.93	7766	
Z-(CH$_2$CH$_2$CH$_2$CH$_2$OH)CHOO	23.5	1.1×10^{-4}	2.65E+08	1.70	11393	
E-(CH$_3$)(CH$_2$OH)COO	20.0	2.3×10^{-2}	1.14E+11	0.63	9793	
Z-(CH$_2$OH)(CH$_3$)COO	17.3	8.2×10^{-1}	3.70E+10	0.69	8487	
Z-(C(CH$_3$)$_2$OH)CHOO	20.0	2.1×10^{-2}	1.94E+06	2.24	9280	
E-(C(CH$_3$)$_2$OH)CHOO	15.0	4.7×10^1	4.87E+09	1.08	7331	
Z-(C(CH$_3$)$_2$OH)(CH$_3$)COO	18.0	4.5×10^{-1}	1.67E+10	0.96	8883	
Z-(C(=O)CH$_2$OH)CHOO	17.2	1.6×10^0	6.59E+03	3.05	7660	
Ether substituents						
E-(CH$_3$)(CH$_2$OCH$_3$)COO	20.0	5.7×10^{-3}	6.45E+07	1.61	9638	
Z-(CH$_2$OCH$_3$)(CH$_3$)COO	19.6	1.0×10^{-1}	1.18E+11	0.80	9635	
OOH-bearing substituent						
Z-(OOH)CHOO	14.0	6.7×10^1	1.86E+09	0.91	6646	
Z-(OOH)(CH$_3$)COO	11.9	3.7×10^3	5.97E+10	0.49	5772	
Z-(CH$_2$OOH)CHOO	16.4	1.1×10^{-2}	3.28E+06	2.15	9471	

Z-(CH$_2$OOH)(CH$_3$)COO	19.5	2.8×10^{-2}	2.26E+09	1.20	9522
Z-(CH$_2$CH$_2$OOH)CHOO	22.2	3.9×10^{-4}	7.41E+06	1.99	10438
Z-(CH$_2$CH$_2$CH$_2$OOH)CHOO	21.9	4.4×10^{-4}	3.18E+03	3.11	9991
E-(OOH)CHOO	5.7	1.7×10^{8}	9.34E+08	1.21	2564
E-(CH$_2$OOH)CHOO	15.0	9.7×10^{1}	3.26E+09	1.08	6998
E-(CH$_2$CH$_2$OOH)CHOO	12.4	3.7×10^{3}	2.38E+16	-1.66	5969
E-(CH$_3$)(OOH)CHOO	9.7	4.2×10^{5}	4.82E+12	0.02	4871
E-(CH$_3$)(CH$_2$OOH)COO	20.1	5.3×10^{-3}	4.54E+08	1.23	9597
OOOH-substituent					
E-(OOOH)CHOO	5.8	2.6×10^{8}	6.07E+11	0.32	2842
E-(CH$_3$)(OOOH)COO	9.7	3.8×10^{5}	1.10E+13	-0.10	4947
Aldehyde substituent					
(CH=O)$_2$COO	14.9	4.2×10^{1}	2.40E+06	2.08	6796
ONO$_2$-bearing substituent					
E-(ONO$_2$)CHOO	6.3	2.8×10^{8}	6.54E+12	0.08	3130
E-(CH$_3$)(ONO$_2$)COO	10.8	6.7×10^{4}	2.84E+12	0.09	5388
E-(CH$_3$)(CH$_2$ONO$_2$)COO	19.7	1.3×10^{-2}	3.69E+07	1.76	9463
Z-(ONO$_2$)CHOO	10.4	1.4×10^{5}	1.44E+07	1.93	4650
Z-(CH$_2$ONO$_2$)(CH$_3$)COO	18.4	2.1×10^{-1}	1.64E+07	1.99	8789
Alkoxy substitutents					
Z-(OCH$_3$)CHOO	12.0	2.7×10^{3}	4.74E+09	0.81	5658
Z-(OCH$_3$)(CH$_3$)COO	9.5	1.1×10^{5}	5.65E+10	0.42	4637
Z-(OCH$_3$)(OH)COO	4.1	2.1×10^{9}	2.27E+12	0.01	2092
E-(OCH$_3$)CHOO	7.1	7.1×10^{7}	2.57E+12	0.25	3559
E-(CH$_3$)(OCH$_3$)COO	11.3	4.7×10^{4}	5.31E+11	0.47	5646
(OCH$_3$)$_2$COO	7.1	1.7×10^{7}	2.99E+12	0.01	3616
Epoxide substituent					
Z-(cyc-CH$_2$OCH-)CHOO	21.9	5.6×10^{-4}	3.53E+05	2.45	10199
Ester substituents					
Z-(C(=O)OCH$_3$)CHOO	16.7	1.7×10^{0}	2.61E+04	2.71	7477
Carboxylic acid substituents					
Z-(C(=O)OH)CHOO	22.3	9.0×10^{-4}	1.60E+05	2.73	10301
Z-(CH$_2$C(=O)OH)CHOO	25.1	6.1×10^{-6}	1.02E+01	4.21	11412
Z-(CH$_2$CH$_2$C(=O)OH)CHOO	22.7	2.9×10^{-4}	5.59E+04	2.86	10552
Z-(CH$_2$CH$_2$CH$_2$C(=O)OH)CHOO	19.6	1.1×10^{-3}	9.83E-12	7.61	7398
E-(CH$_2$C(=O)OH)CHOO	15.3	4.2×10^{1}	1.31E+07	1.97	7123
E-(CH$_3$)(CH$_2$C(=O)OH)COO	21.9	1.9×10^{-3}	4.04E10	0.93	10716
E-(CH$_2$CH$_2$C(=O)OH)CHOO	15.0	4.8×10^{1}	2.48E+08	1.53	7205
Unsaturated substituents					
E-(CH$_2$CH$_3$)(CH=CH$_2$)COO	19.8	2.6×10^{-2}	3.16E+11	0.55	9913
Z-(CH=CH$_2$)(CH$_2$CH$_3$)COO	17.5	5.8×10^{-1}	1.65E+09	1.11	8368
E-(iC$_3$H$_7$)(CH=CH$_2$)COO	17.3	4.4×10^{-1}	6.01E+09	0.87	8431
Z-(CH=CH$_2$)(iC$_3$H$_7$)COO	16.7	1.9×10^{0}	2.27E+09	1.09	8077
Z-(E-CH=CHCH$_3$)(CH$_3$)COO	18.0	4.3×10^{-1}	1.26E+09	1.28	8677
Z-(Z-CH=CHCH$_3$)(CH$_3$)COO	18.3	2.2×10^{-1}	2.70E+09	1.18	8933
Z-(CH$_2$CH=CH$_2$)(iC$_3$H$_7$)COO	19.0	4.8×10^{-2}	1.43E+05	2.68	8992
Z-(CH$_2$CH=CH$_2$)(CH$_3$)COO	19.7	1.5×10^{-2}	2.40E+05	2.61	9369
E-(iC$_3$H$_7$)(CH$_2$CH=CH$_2$)COO	19.7	1.8×10^{-2}	1.59E+10	0.87	9677
E-(CH$_3$)(CH$_2$CH=CH$_2$)COO	20.7	6.0×10^{-3}	8.01E+08	1.42	10053
Multifunctionalized CI					
Z-(CH(OOH)CH$_2$OH)(CH$_3$)COO	19.4	5.1×10^{-2}	6.11E+09	1.19	9630
Z-(C(=CH$_2$)CH$_2$OH)CHOO	19.5	4.7×10^{-2}	8.86E+05	2.44	9132
Z-(C(=CH$_2$)CH$_2$CH$_2$OH)CHOO	20.4	6.1×10^{-2}	6.35E+09	1.45	10014

L. 1,5-Ring closure forming cyclic peroxides
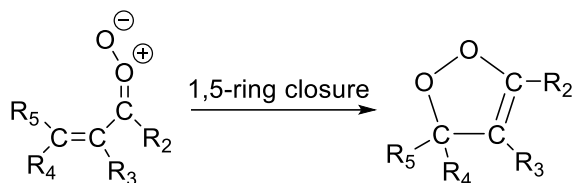
Syn-β-unsaturated CI can undergo a 1,5-ring closure reaction, where similar to the work by Kuwata et al.[95,104], Vereecken et al.[8] and Barber et al.[21] we find low reaction barriers and high rate coefficients exceeding 10^2 s^{-1} at 298 K (see Table 18). For nearly all s*yn*-β-unsaturated CI, this reaction is the dominant loss process unless an allyl-1,6-H-migration is accessible. This reaction is therefore particularly important in the ozonolysis of conjugated π-systems, such as isoprene, myrcene, α-terpinene, ocimene, and other terpenoids. The dioxole product of this reaction, i.e. a cyclic peroxide with a 5-membered ring, is expected[21,95,104] to break the O–O bond, where the resulting singlet diradical will re-arrange to either a carbonyl-epoxide or a dicarbonyl. Recent work by Vansco et al.[120] observed reaction products that are readily formed through this dioxole formation and subsequent decomposition, supporting the theoretical studies.

Table 18: 1,5-Ring closure in β-unsaturated carbonyl oxides, listing barrier heights E_b (kcal mol^{-1}), rate coefficient k (s^{-1}) at 298 K, and parameters for a Kooij equation fit $k(T)=A\times(T/K)^n\times\exp(-E_a/T)$ for the temperature range 200-450 K.

Carbonyl oxide	E_b	k(298K)	A / s^{-1}	n	E_a / K	Remarks
Z-(CH=CH$_2$)(CH$_2$CH$_3$)COO	11.9	1.2×10^4	9.77E+10	0.50	5584	
Z-(CH=CH$_2$)(iC$_3$H$_7$)COO	11.9	1.1×10^4	1.68E+11	0.44	5668	
Z-(E-CH=CHCH$_3$)(CH$_3$)COO	10.8	4.2×10^4	3.96E+11	0.30	5287	
Z-(Z-CH=CHCH$_3$)(CH$_3$)COO	9.4	2.7×10^5	6.95E+10	0.45	4469	
Z-(C(=CH$_2$)CH$_2$OH)CHOO	15.2	1.6×10^2	1.52E+11	0.79	7510	
Z-(C(=CH$_2$)CH$_2$CH$_2$OH)CHOO	15.0	8.5×10^2	6.78E+14	-0.21	7806	
Z-(Z-CH=CHCH$_2$OH)CHOO	8.8	9.2×10^5	5.12E+17	-1.92	4792	
Z-(Z-CH=CHCH$_2$CH$_2$OH)CHOO	10.1	1.6×10^5	2.20E+13	-0.50	4735	

M. Intramolecular secondary ozonide (SOZ) formation
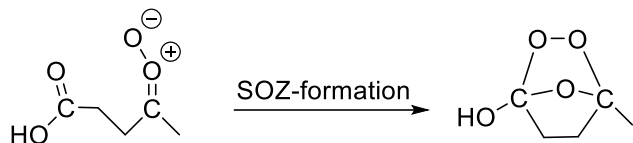
Intramolecular cycloaddition of the carbonyl oxide moiety on a carbonyl group leads to bicyclic secondary ozonides. We have characterized for the first time a number of transition states where this process occurs with the carbonyl part of a carboxylic acid group. As for carbonyl-based SOZ formation (Table 2), the process is strongly affected by ring strain, and the entropic hindrance by the loss of degrees of freedom for internal rotation. Based on the scarce literature data (Table 2), Vereecken and Francisco[1] suggested that SOZ would probably only be important if the intervening number of carbon atoms would be 6 or more, i.e. $O=CC_{n\geq4}C=O^+O^-$ compounds. Recently, Long et al.[23] showed that the process can still be competitive with only 5 intervening carbons, i.e. $O=CC_3C=O^+O^-$ compounds. In this work, we show that acid-substituted CI can also undergo SOZ formation, and that the reaction can be competitive even with only 4 intervening carbons, i.e. $O=C(OH)C_2C=O^+O^-$ compounds. For the 2 CI listed in Table 19, the thermal SOZ formation is similar in rate or faster than the alternative unimolecular reactions such as 1,4-H-migration, or ring closure by 1,2-insertion into the acidic OH group. As such, this reaction can be a dominant pathway if the ring strain is not too large. In bimolecular SCI + acid reactions, SOZ formation was identified as one of the fastest reaction channels with the lowest energy barrier, but the 1,4-insertion pathway was found to be barrierless and faster.[121] Hence, acid-based intramolecular SOZ formation might be competitive only as long as the transition state ring size geometrically prevents the 1,4-insertion mechanism from occurring.

Due to the entropic hindrance of the bicyclization, chemically excited CI often do not yield SOZ,[1,80,122] as the higher internal energy makes the difference in barrier height between the processes less important than for thermal SCI, and other processes are often entropically more favorable. It is thus not clear *a priori* how much SOZ is formed from ozonolyis of alkenes. After ozonolysis of a cycloalkene, where all CI are formed with high internal energy, combining the carbonyl oxide and carbonyl groups formed in the ozonolysis to form a SOZ often leads to low yields, except for larger molecules like sesquiterpenes where the effect of chemical activation is reduced by dissipation of the excess energy over a large set of degrees of freedom, i.e. where most CI are thermalized to SCI. For ozonolysis of a non-cycloalkene with pre-existing carbonyl or acids substituents the probability of SOZ formation is higher as the fragmentation of the primary ozonide leads to a higher yield of stabilized (or less energized) CI, favoring the lowest-barrier process even if entropically less permissive.

Table 19: Secondary ozonide formation in acid-substituted carbonyl oxides, listing barrier heights E_b (kcal mol^{-1}), rate coefficient k (s^{-1}) at 298 K, and parameters for a Kooij equation fit $k(T)=A\times(T/K)^n\times\exp(-E_a/T)$ for the temperature range 200-450 K.

Carbonyl oxide	E_b	k(298K)	A / s^{-1}	n	E_a / K	Remarks
Z-(CH$_2$CH$_2$C(=O)OH)CHOO	11.4	8.9×10^2	5.32E+15	-1.70	5877	
Z-(CH$_2$CH$_2$CH$_2$C(=O)OH)CHOO	7.4	8.2×10^4	6.15E+15	-2.28	3596	

N. 1,2-insertion in –OH forming cyclic ethers
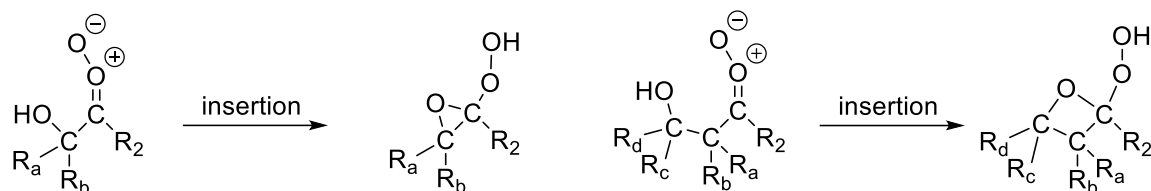
The bimolecular reactions of SCI with alcohols has been studied both experimentally and theoretically,[48,123–129] but are found to be relatively slow under atmospheric conditions. In this work, we study for the first time the intramolecular insertion of carbonyl oxides in a hydroxy substituent (Table 20). The products of these reactions are cyclo-ethers (called epoxides for 3-membered rings) with an α-hydroperoxide substituent. The reactions are competitive, with a barrier height that is decreasing for larger product ring sizes, such that the reaction remains important even for fairly remote hydroxy substituents (though obviously the less favorable reaction entropy for longer distances will reduce the reaction rate). The reactions are exothermic, which may lead to prompt product decomposition of the weak hydroperoxide bond (D_e(O–OH) ~ 40 kcal mol^{-1}). Interestingly, for a long enough substituent chain length, the insertion reaction can occur with hydroxylated substituents in both *syn-* and *anti-*position (see Table 20). As discussed elsewhere, these insertion reactions can also be catalyzed by water molecules.

Table 20: 1,2-Insertion reaction in an –OH group with hydroperoxide-cycloether formation, listing barrier heights E_b and product energy E_{prod} (kcal mol^{-1}), rate coefficient k (s^{-1}) at 298 K, and parameters for a Kooij equation fit $k(T)=A\times(T/K)^n\times\exp(-E_a/T)$ for the temperature range 200-450 K. The ring closure can occur at any ring span.

Carbonyl oxide	E_b	E_{prod}	k(298K)	A / s^{-1}	n	E_a / K	Remarks
2-OH-substitution, forming 3-membered ring (epoxide)							
Z-(CH$_2$OH)CHOO	14.3	-12.8	1.9×10^2	7.87E-05	5.28	4575	
Z-(CH$_2$OH)(CH$_3$)COO	13.0	-10.1	7.7×10^2	1.38E+11	0.31	6186	
Z-(C(CH$_3$)$_2$OH)CHOO	13.7	-9.9	8.1×10^2	6.22E+00	3.90	5172	
Z-(C(CH$_3$)$_2$OH)(CH$_3$)COO	13.4	-6.4	6.9×10^2	8.58E+10	0.56	6499	
3-OH-substitution, forming 4-membered ring							
Z-(CH$_2$CH$_2$OH)CHOO	15.1	-18.0	7.0×10^0	4.49E+13	-0.91	7251	
E-(CH$_2$CH$_2$OH)CHOO	18.6	-22.9	6.8×10^{-3}	2.11E+15	-1.70	9108	
Z-(CH(OOH)CH$_2$OH)(CH$_3$)COO	12.0	-16.1	4.7×10^3	1.05E+04	2.47	4432	
Z-(C(=O)CH$_2$OH)CHOO	11.4	-21.5	8.7×10^3	5.65E+06	1.67	4764	
Z-(C(=CH$_2$)CH$_2$OH)CHOO	20.4	-12.4	3.7×10^{-3}	3.38E+09	0.86	9672	
4-OH-substitution, forming 5-membered ring							
Z-(CH$_2$CH$_2$CH$_2$OH)CHOO	6.9	-32.3	1.0×10^7	4.30E+18	-2.41	3882	
E-(CH$_2$CH$_2$CH$_2$OH)CHOO	2.8	-38.1	4.4×10^9	9.79E+24	-5.09	1894	
Z-(CH$_2$CH$_2$CH$_2$OH)(CH$_3$)COO	6.7	-29.7	1.5×10^7	1.01E+15	-1.13	3441	
E-(CH$_3$)(CH$_2$CH$_2$CH$_2$OH)COO	6.3	-33.1	1.1×10^7	2.54E+24	-4.84	3685	
Z-(C(=CH$_2$)CH$_2$CH$_2$OH)CHOO	10.4	-30.8	6.3×10^4	1.28E+18	-2.05	5657	
Z-(Z-CH=CHCH$_2$OH)CHOO	7.4	-34.3	5.7×10^6	1.39E+21	-3.26	4339	
5-OH-substitution, forming 6-membered ring							
Z-(CH$_2$CH$_2$CH$_2$CH$_2$OH)CHOO	7.1	-35.7	1.7×10^6	4.47E+30	-7.02	4842	
E-(CH$_2$CH$_2$CH$_2$CH$_2$OH)CHOO	5.6	-37.7	5.0×10^7	8.32E+36	-8.94	4879	
Z-(Z-CH=CHCH$_2$CH$_2$OH)CHOO	7.6	-35.6	1.4×10^6	1.67E+19	-3.06	3775	

O. 1,2-insertion in –OOH forming cyclic peroxides
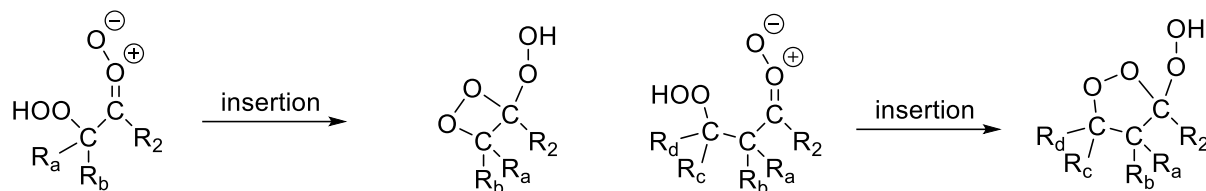
The bimolecular reactions of SCI with hydroperoxides has been studied both experimentally and theoretically,[130–133] but are found to be relatively slow under atmospheric conditions. In this work, we study for the first time the intramolecular insertion of carbonyl oxides in a hydroperoxide substituent (Table 21). The products of these reactions are cyclo-peroxides with an α-hydroperoxide substituent. The reactions are competitive, with a barrier height that is decreasing for larger product ring sizes, such that the reaction remains important even for fairly remote hydroperoxide substituents (though obviously the less favorable reaction entropy for longer distances will reduce the reaction rate). The reactions are exothermic, which may lead to prompt product decomposition of the weak peroxide or hydroperoxide bond (D_e(O–O) ~ 40 kcal mol^{-1}). Interestingly, for a long enough substituent chain length, the insertion reaction can occur with hydroperoxide substituents in both *syn-* and *anti-*position (see Table 21). As discussed elsewhere, these insertion reactions can also be catalyzed by water molecules.

Table 21: 1,2-Insertion reaction in an –OOH group with hydroperoxide-cycloperoxide formation, listing barrier heights E_b and product energy E_{prod} (kcal mol^{-1}), rate coefficient k (s^{-1}) at 298 K, and parameters for a Kooij equation fit $k(T)=A\times(T/K)^n\times\exp(-E_a/T)$ for the temperature range 200-450 K. The ring closure can occur at any ring span.

Carbonyl oxide	E_b	E_{prod}	k(298K)	A / s^{-1}	n	E_a / K	Remarks
2-OOH-substitution, forming 4-membered ring							
Z-(CH$_2$OOH)CHOO	12.5	-22.0	7.2×10^2	6.99E+09	0.42	5505	
Z-(CH$_2$OOH)(CH$_3$)COO	9.94	-20.9	9.8×10^4	2.45E+03	2.59	3300	
Z-(CH(OOH)CH$_2$OH)(CH$_3$)COO	10.3	-20.4	8.5×10^4	3.46E-10	6.99	2004	
E-(CH$_2$OOH)CHOO	19.0	-27.3	2.7×10^{-3}	4.32E+13	-1.15	9168	
E-(CH$_3$)(CH$_2$OOH)COO	22.1	-22.5	1.8×10^{-5}	6.06E+11	-0.43	10626	
3-OOH-substitution, forming 5-membered ring							
Z-(CH$_2$CH$_2$OOH)CHOO	7.0	-34.4	1.6×10^7	2.89E+17	-1.96	3708	
E-(CH$_2$CH$_2$OOH)CHOO	2.3	-44.2	8.9×10^9	4.19E+26	-5.74	1701	
4-OOH-substitution, forming 6-membered ring							
Z-(CH$_2$CH$_2$CH$_2$OOH)CHOO	11.3	-32.3	1.7×10^4	1.16E+21	-3.12	6253	
E-(CH$_2$CH$_2$CH$_2$OOH)CHOO	8.6	-39.6	3.7×10^5	2.87E+20	-3.09	4969	

P. 1,2-insertion in –C(=O)OH forming cyclic esters or CO$_2$+alkene
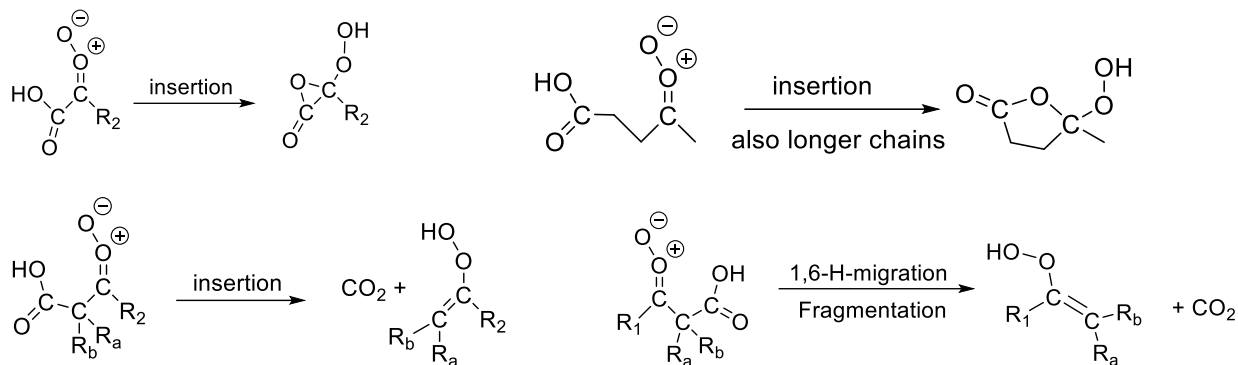
The bimolecular reactions of SCI with acids have been studied both experimentally and theoretically,[10,48,121,133–148] and are found to be very fast, with rate coefficients nearing the collision limit. In this work, we study for the first time the intramolecular insertion of carbonyl oxides in a carboxylic substituent (Table 22). The products of these reactions are lactones (cycloesters) with an α-hydroperoxide substituent, except for β-COOH substitution where the reaction forms CO$_2$ and an alkene (for both *syn-* and *anti-*substitution). The insertion reaction can occur with carboxylic substituents in both *syn-* and *anti-*position (see Table 22). Many of these reactions are competitive, with a barrier height that is most favorable for *syn*-β-COOH substitution due to the different reaction mechanism eliminating CO$_2$, a process that is not accessible for differently sized ring products. The barrier, however, is sufficiently low at any ring size such that the reaction remains important even for remote carboxylic acid substituents (though obviously the less favorable reaction entropy for longer distances will reduce the reaction rate). For the distances examined here, the reaction proceeds by 1,2-insertion, which is not the most favorable mechanism for combining CI with acidic functions.[121] If is expected that at even longer separations, 1,4-insertion reactions become possible, likely with even lower barrier heights as this mechanism allows for a barrierless process in bimolecular acid+SCI reactions. The reactions are exothermic, and may lead to chemical activation enabling prompt product decomposition of the weak hydroperoxide bond (D$_e$(O–OH) ~ 40 kcal mol^{-1}). As discussed elsewhere, these insertion reactions can also be catalyzed by water molecules.

Table 22: 1,2-Insertion reaction in the hydroxy moiety of an –C(=O)OH group with hydroperoxide-cycloester or CO$_2$ + alkene formation, listing barrier heights E_b (kcal mol^{-1}), rate coefficient k (s^{-1}) at 298 K, and parameters for a Kooij equation fit $k(T)=A \times (T/K)^n \times exp(-E_a/T)$ for the temperature range 200-450 K. The ring closure can occur at any ring span.

Carbonyl oxide	E_b	E_{prod}	k(298K)	A / s^{-1}	n	E_a / K	Remarks
1-COOH-substitution, forming 3-membered ring							
Z-(C(=O)OH)CHOO	9.6	-0.4	9.1×10^5	9.81E+10	0.79	4790	
2-COOH-substitution, forming CO$_2$ + alkene							
Z-(CH$_2$C(=O)OH)CHOO	3.1	-28.5	4.0×10^{10}	1.14E+11	0.54	1232	Product: CO$_2$ + CH$_2$=CHOOH [a]
E-(CH$_2$C(=O)OH)CHOO	14.0	-37.4	2.2×10^1	6.40E+12	-0.53	6970	Product: CO$_2$ + CH$_2$=CHOOH [b]
E-(CH$_3$)(CH$_2$C(=O)OH)COO	15.4	-27.6	2.0×10^0	3.59E+09	0.48	7162	Product: CO$_2$ + CH$_2$=C(CH$_3$)OOH [b]
3-COOH-substitution, forming 5-membered ring							
Z-(CH$_2$CH$_2$C(=O)OH)CHOO	12.3	-32.4	5.0×10^2	1.69E+16	-1.68	6435	
E-(CH$_2$CH$_2$C(=O)OH)CHOO	10.7	-39.5	6.9×10^3	4.64E+04	1.92	3835	
4-COOH-substitution, forming 6-membered ring							
Z-(CH$_2$CH$_2$CH$_2$C(=O)OH)CHOO	11.3	-29.8	1.2×10^3	4.71E+13	-1.19	5241	
E-(CH$_2$CH$_2$CH$_2$C(=O)OH)CHOO	7.7	-36.1	4.1×10^5	6.46E+20	-3.74	4080	

[a] IRC calculations show formation of CO$_2$ + alkene directly from the SCI, without cycloadduct formation. The transition state for CO$_2$ elimination from the potential cycloadduct is 13.8 kcal mol^{-1} above the energy of the SCI, indicating that a concerted mechanism is more favorable.

[b] Ring closure after H-migration (which would make it an insertion) is not possible due to ring strain, forcing the carboxylic group to break its internal H-bond and rotate the acidic H-atom away from the acidic carbonyl group; in this configuration neither of the acidic O-atoms can gain a suitable position to bond with the carbonyl oxide carbon atom.

Q. Impact of specific substitutions

1. Impact of cyclic substituents on unimolecular reaction rates

In our previous study,[8] we examined the impact of cyclic substituents on CI chemistry, where the carbonyl oxide moiety is either implanted on a cyclic structure (as in nopinone oxide formed from β-pinene), or has a β-cyclic substituent (as in pinonaldehyde oxide from α-pinene). Deriving a SAR for such compounds is highly complex, as the rate coefficient can depend strongly on the ring position, size and ring strain, substitution, and the presence of multiple rings containing alkyl-, ether-, peroxide-, ester-, or other connections. The computational requirements to develop a reliable SAR for these compounds would be comparable in effort as investigating the relevant compounds themselves.

In this study, we briefly examine the impact of cycles that are located somewhat further from the carbonyl moiety. The main reaction channels available, i.e. 1,3-ring closure, 1,4-H-migration, and 1,5-ring closure in unsaturated CI, are not expected to be affected significantly by cycles in the substituents that are further than 2 carbons from the reaction site, i.e. δ-position or further. The main uncertainty remains then with substituents where the γ-carbon is part of a cyclic structure; an example compound in the atmosphere with such functionality is Δ^3-carene, where the carbonyl oxide moiety is separated by a single –CH_2– group from a highly strained three-membered ring. In Table 23, we list the unimolecular reactions for CI similar to those obtained from Δ^3-carene; these reactions are also listed in the corresponding section in this work. Alongside these reactions we list theoretical predictions[8] for regular alkyl substituents that are unaffected by ring strain.

As is easily seen, the highly strained three-membered ring in γ-position does not overly impact the reaction, with rate coefficients at 298K that are within a factor 3 of the SAR predictions, i.e. well within the expected reliability of the SAR. Larger rings, with concomitantly lower ring strain, will have an even lower impact on the reaction rates. We then conclude that cyclic structures beyond the β-carbon have little to no influence on CI chemistry. For these compounds, the results confirm the strategy proposed by Vereecken et al.[8] to handle cyclic CI for which no direct data is available as non-cyclic species.

Table 23: Reactions of selected carbonyl oxides with a strained cyclic substituent, listing barrier heights E_b (kcal mol^{-1}), rate coefficient k (s^{-1}) at 298 K, and parameters for a Kooij equation fit $k(T)=A\times(T/K)^n\times\exp(-E_a/T)$ for the temperature range 200-450 K. Corresponding CI with linear alkyl substituents are listed as reference compounds; their data from Vereecken et al.[8] are repeated here for convenience.

Carbonyl oxide	Reaction	E_b	k(298K)	A / s^{-1}	n	E_a / K
E-(CH_2-cycC_3H_5)CHOO	1,3-H-migration	28.4	2.0×10^{-6}	7.23E-133	47.55	-6050
E-(CH_2CH_3)CHOO [8]		28.2	4.0×10^{-6}			
E-(CH_3)(CH_2-cycC_3H_5)COO	1,4-H-migration	16.1	3.4×10^{2}	1.32E-59	23.52	-2213
E-(CH_3)(CH_2CH_3)COO [8]		16.5	4.3×10^{2}			
Z-(CH_2-cycC_3H_5)(CH_3)COO		15.0	1.5×10^{3}	1.47E-52	21.14	-1867
Z-(CH_2CH_3)(CH_3)COO [8]		15.6	6.9×10^{2}			
Z-(CH_2-cycC_3H_5)CHOO		16.1	2.9×10^{2}	5.11E-59	23.24	-2240
Z-(CH_2CH_3)CHOO [8]		16.5	2.1×10^{2}			
E-(CH_3)(CH_2-cycC_3H_5)COO	1,3-ring closure	20.8	2.8×10^{-3}	4.26E+08	1.50	10210
E-(CH_3)(CH_2CH_3)COO [8]		20.9	8.8×10^{-3}			
Z-(CH_2-cycC_3H_5)(CH_3)COO		20.1	1.9×10^{-2}	5.76E+09	1.19	9899
Z-(CH_2CH_3)(CH_3)COO [8]		19.8	2.4×10^{-2}			
E-(CH_2-cycC_3H_5)CHOO		15.4	4.8×10^{1}	3.03E+09	1.23	7441
E-(CH_2CH_3)CHOO [8]		15.6	7.4×10^{1}			
Z-(CH_2-cycC_3H_5)CHOO		22.8	3.7×10^{-4}	5.65E+05	2.51	10560
Z-(CH_2CH_3)CHOO [8]		22.9	4.3×10^{-4}			

2. *Elimination of HCOO from RCHOO*

HCOO elimination from an RCHOO CI has a high barrier, even with stabilization of the substituent product radical. For completeness, we calculated one example, where the α-hydroxy substituent stabilizes one of the product radical sites. The barrier for this process exceeds 35 kcal/mol, making the reaction negligible. Even stronger stabilization of the product radicals, *e.g.* through allyl delocalization of the radical electron over a double bond, is not expected to reduce the barrier to the extent that the reaction can be competitive with other loss processes. This reaction class is not considered further.
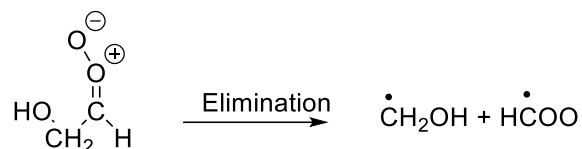
Table 24: HCOO elimination in oxygenated syn-RCHOO CI, listing barrier heights E_b (kcal mol^{-1}), rate coefficient k (s^{-1}) at 298 K, and parameters for a Kooij equation fit $k(T)=A\times(T/K)^n\times\exp(-E_a/T)$ for the temperature range 200-450 K.

Carbonyl oxide	E_b	k(298K)	A / s^{-1}	n	E_a / K	Remarks
Z-(CH₂OH)CHOO	36.1					

3. *H-migration from oxygenated groups to the carbonyl oxide moiety*
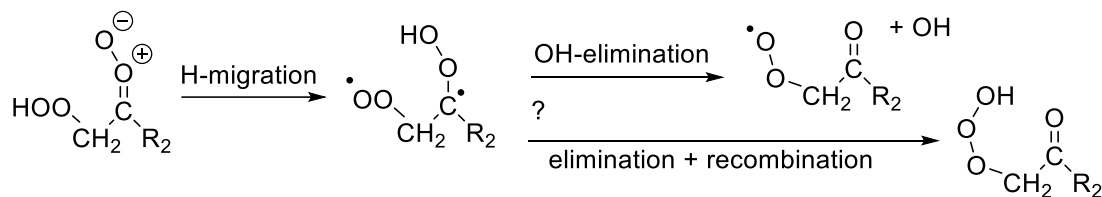
H-migration of an oxygenated H-atom leads formally to a diradical with an α-OOH alkyl radical and an oxygen-based radical (shown above for an –OOH substituent). α-OOH alkyl radicals are known to be unstable,[149,150] eliminating an OH radical without a barrier forming a carbonyl. With the oxygen-based radical in direct proximity of the departing OH group, a barrierless roaming radical-radical recombination reaction is the most favorable subsequent reaction, forming a carbonyl with a hydro-oxygenated group. We found transition states for this reaction class in several oxygenated CI and propose that such a reaction can occur for any H-migration span, and for most oxygenated groups with an H-atom examined here, i.e. –OH, –OOH, and –COOH. This reaction class is reminiscent of the concerted H-migration/ring closure reaction discussed in another sections, but contrary to those reactions the H-migration followed by a roaming OH-back-migration described here does not benefit energetically from a concerted H-shift and formation of a new C–O bond, thus leading to high barriers for reaction exceeding 20 kcal mol^{-1} for –OOH groups and expected to be even higher for the more strongly bonded –OH and –COOH groups. As such, this reaction class is not expected to be competitive in any CI, especially against the related 1,2-insertion reaction (see section N, O and P) which is always faster. The exact product speciation and yield are thus less important here, and no detailed analysis is provided at this time. One exception is the 1,5-H-migration in *syn-α*-OOH-substituted CI (see section I), which is barrierless and is essentially a non-reaction, forming the identical *syn-α*-OOH-substituted CI (barring *e.g.* isotopic labeling).

Table 25: H-migration of an O-bonded hydrogen atom in an oxygenated CI, listing barrier heights E_b (kcal mol^{-1}), rate coefficient k (s^{-1}) at 298 K, and parameters for a Kooij equation fit $k(T)=A\times(T/K)^n\times\exp(-E_a/T)$ for the temperature range 200-450 K.

Carbonyl oxide	E_b	E_{prod}	k(298K)	A / s^{-1}	n	E_a / K	Product
OOH-bearing substituent							
Z-(CH$_2$OOH)CHOO	24.2		1.8×10^{-6}	4.06E+12	-0.50	11744	HOOC$^\bullet$HCH$_2$OO$^\bullet$
Z-(CH$_2$OOH)(CH$_3$)COO	23.7		1.2×10^{-5}	3.21E+04	2.53	10763	HOOC$^\bullet$(CH$_3$)CH$_2$OO$^\bullet$

4. Impact of a syn-β-epoxide substituent

Epoxide moieties are known as reactive substituents that enable certain reaction classes that are typically not available to other compounds, by concerted opening of the strained three-membered ring. Unsaturated epoxides are expected to be formed in the OH-initiated oxidation of aromatic compounds, through several mechanisms that lead to the fragmentation of the 6-membered ring into an (epoxy)dicarbonylbutene and a C_2 fragment.[151] The β-epoxy-CI formed from these compounds has several unusual reaction pathways available, but the only energetically viable pathway is a traditional 1,4-migration forming an epoxy-vinylhydroperoxide (see scheme below). The barrier for this process is significantly higher (~21 kcal mol^{-1}) than for an alkyl-1,4-H-migration (as low as 15 kcal mol^{-1}). Consequently, the unimolecular decay of syn-β-epoxy CI is expected to be slow. The reaction of the cyc(-CH$_2$OCH-)CHOO epoxy-CI with H$_2$O molecules is also rather slow, k(298K) ~ 8.8×10^{-18} cm^3 molecule^{-1} s^{-1} (Table 27), similar to other alkyl syn-RCHOO CI.

The slow rate of unimolecular reactions and reaction with water this suggests that β-epoxy-CI are among the longer-lived CI characterized thus far. Their yield in the atmosphere is limited, given the rather small emission factors for aromatics, and the expected low ozonolysis rates of the oxygenated unsaturated species forming these CI. There are some potential reaction pathways such as 1,5-ring closure reactions with concerted ring opening, for which we were unable to find a transition state. Though we do not expect these channels to be competitive, we should concede that the chemistry of β-epoxy-CI, and their atmospheric impact, is far from fully characterized at this time.
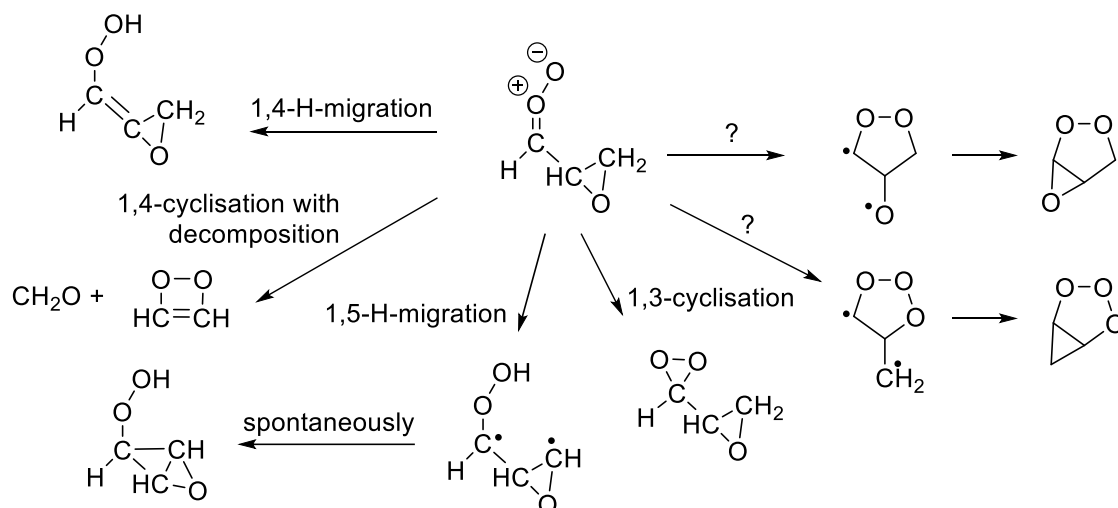
Table 26: Unimolecular reactions of an β-epoxy-CI, listing barrier heights E_b (kcal mol^{-1}), rate coefficient k (s^{-1}) at 298 K, and parameters for a Kooij equation fit $k(T)=A\times(T/K)^n\times\exp(-E_a/T)$ for the temperature range 200-450 K.

Carbonyl oxide	E_b	k(298K)	A / s^{-1}	n	E_a / K	Reaction type
Z-(cyc-CH$_2$OCH-)CHOO	20.8	1.1×10^{-1}	1.36E-89	33.20	-3947	1,4-H-migration (VHP channel)
	39.1	3.6×10^{-17}	2.06E+11	0.36	19656	1,5-H-migration
	22.0	5.6×10^{-4}	1.36E-89	33.20	-3947	1,3-cyclisation (dioxirane channel)
	32.9	3.6×10^{-12}	2.59E+06	2.11	15843	1,4-cyclisation
	Not found					1,5-cyclisation on C-atom
	Not found					1,5-cyclisation on O-atom

R. The reaction of CI with H_2O

Table 27: Rate constant predictions for the reaction of CI with H_2O monomers forming hydroxyl hydroperoxides, obtained after barrier height corrections in the theoretical data, listing barrier heights E_b (kcal mol^{-1}), rate coefficient k (cm^3 molecule^{-1} s^{-1}) at 298 K, and parameters for a Kooij equation fit $k(T)=A\times(T/K)^n\times\exp(-E_a/T)$ cm^3 molecule^{-1} s^{-1} for the temperature range 200-450 K.

Carbonyl oxide	E_b	k(298K)	A / s^{-1}	n	E_a / K	Remarks
Alkyl-substituents						
E-(C$_2$H$_5$)(iC$_3$H$_7$)COO	4.9	3.3×10^{-18}	8.90E-20	1.59	1631	
Z-(iC$_3$H$_7$)(C$_2$H$_5$)COO	3.6	2.0×10^{-17}	1.21E-18	1.08	1000	
Unsaturated compounds						
E-(C$_2$H$_5$)(CH=CH$_2$)COO	7.2	1.9×10^{-19}	3.33E-17	0.82	2932	
Z-(CH=CH$_2$)(C$_2$H$_5$)COO	5.1	2.4×10^{-19}	1.12E-23	2.99	1423	
E-(iC$_3$H$_7$)(CH=CH$_2$)COO	5.1	1.1×10^{-18}	6.69E-20	1.52	1734	
Z-(E-CH=CHCH$_3$)CHOO	8.2	4.3×10^{-20}	2.11E-20	1.98	3152	
Z-(Z-CH=CHCH$_3$)CHOO	9.6	4.9×10^{-21}	7.36E-19	1.50	4031	
Z-(E-CH=CHCH$_3$)(CH$_3$)COO	6.3	7.1×10^{-19}	6.92E-22	2.45	2090	
Z-(Z-CH=CHCH$_3$)(CH$_3$)COO	4.7	3.9×10^{-18}	2.65E-22	2.34	1117	
E-(iC$_3$H$_7$)(CH$_2$CH=CH$_2$)COO	3.3	1.7×10^{-18}	1.73E-20	1.65	751	
Z-(CH$_2$CH=CH$_2$)(iC$_3$H$_7$)COO	3.9	5.4×10^{-18}	1.85E-24	3.14	890	
E-(CH$_3$)(CH$_2$CH=CH$_2$)COO	4.4	7.4×10^{-18}	6.90E-21	2.11	1495	
Z-(CH$_2$CH=CH$_2$)(CH$_3$)COO	4.4	7.8×10^{-18}	3.44E-22	2.50	1246	
OH-bearing substituents						
Z-(CH$_2$OH)CHOO	4.8	5.2×10^{-18}	8.65E-19	1.30	1667	
Z-(CH$_2$OH)(CH$_3$)COO	4.3	2.1×10^{-17}	1.18E-21	2.33	1026	
Z-(iC$_3$H$_6$OH)CHOO	4.3	1.2×10^{-17}	1.24E-18	1.31	1553	
Z-(iC$_3$H$_6$OH)(CH$_3$)COO	4.1	9.4×10^{-18}	1.56E-21	2.12	1007	
Z-(CH$_2$CH$_2$OH)CHOO	2.2	5.2×10^{-17}	3.08E-14	-0.76	620	
Z-(CH$_2$CH$_2$CH$_2$OH)CHOO	1.6	2.4×10^{-16}	6.55E-10	-2.12	816	
Z-(CH$_2$CH$_2$CH$_2$CH$_2$OH)CHOO	1.0	1.1×10^{-16}	3.73E+00	-5.99	1196	
E-(CH$_2$OH)CHOO	-1.2	1.9×10^{-13}	6.35E-18	1.11	-1181	
E-(CH$_3$)(CH$_2$OH)COO	3.2	6.6×10^{-17}	3.74E-19	1.45	914	
E-(iC$_3$H$_6$OH)CHOO	-1.5	7.0×10^{-14}	7.57E-21	1.88	-1593	
E-(CH$_2$CH$_2$OH)CHOO	-2.2	6.4×10^{-13}	4.45E-29	4.46	-3513	
E-(CH$_2$CH$_2$CH$_2$OH)CHOO	-1.3	1.4×10^{-13}	8.32E-28	4.17	-2689	
E-(CH$_2$CH$_2$CH$_2$CH$_2$OH)CHOO	0.5	1.0×10^{-14}	1.19E-31	5.84	-1715	
Ether-substituents						
E-(CH$_3$)(CH$_2$OCH$_3$)COO	4.5	9.2×10^{-18}	2.12E-19	1.56	1533	
Z-(CH$_2$OCH$_3$)(CH$_3$)COO	4.9	1.2×10^{-17}	2.72E-18	1.35	1852	
OOH-bearing substiuents						
Z-(CH$_2$OOH)(CH$_3$)COO	3.5	3.9×10^{-18}	6.58E-34	6.30	-121	
Z-(CH$_2$OOH)CHOO	3.3	2.5×10^{-17}	1.81E-17	0.66	1016	
Z-(CH$_2$CH$_2$OOH)CHOO	3.0	3.1×10^{-17}	1.99E-12	-1.17	1308	
Z-(CH$_2$CH$_2$CH$_2$OOH)CHOO	5.2	1.4×10^{-18}	1.24E-12	-0.95	2474	
E-(CH$_2$OOH)CHOO	-1.8	4.3×10^{-13}	1.32E-26	3.88	-2693	
E-(CH$_3$)(CH$_2$OOH)COO	2.9	1.2×10^{-16}	2.43E-41	8.53	-2460	
E-(CH$_2$CH$_2$OOH)CHOO	-1.3	1.8×10^{-13}	1.78E-23	2.64	-2382	
ONO$_2$-bearing substituents						
Z-(CH$_2$ONO$_2$)(CH$_3$)COO	5.5	3.4×10^{-18}	1.40E-21	2.46	1848	
E-(CH$_3$)(CH$_2$ONO$_2$)COO	4.5	7.3×10^{-18}	3.64E-21	2.21	1478	
Alkoxy-substituents						
Z-(OCH$_3$)CHOO	2.1	4.3×10^{-16}	3.13E-19	1.43	272	
Z-(OCH$_3$)(CH$_3$)COO	0.8	2.4×10^{-15}	1.45E-19	1.43	-471	
Z-(OCH$_3$)(OH)COO	-2.2	4.2×10^{-13}	5.90E-21	2.01	-1970	
E-(OCH$_3$)CHOO	-2.5	3.0×10^{-12}	2.01E-19	1.68	-2078	
E-(CH$_3$)(OCH$_3$)COO	1.3	3.7×10^{-15}	6.80E-22	2.42	-512	
Carboxylic acid bearing substituents						
Z-(COOH)CHOO	3.8	5.8×10^{-17}	4.33E-18	1.27	1373	

Z-(CH$_2$COOH)CHOO	2.9	8.9×10^{-17}	1.07E-15	0.25	1164
Z-(CH$_2$CH$_2$COOH)CHOO	5.8	1.2×10^{-18}	4.87E-23	2.94	1976
E-(CH$_2$COOH)CHOO	0.5	5.2×10^{-15}	1.14E-19	1.66	-374
E-(CH$_2$CH$_2$COOH)CHOO	-2.2	8.9×10^{-14}	2.93E-28	4.36	-2541
Ester substituent					
Z-(C(=O)OCH$_3$)CHOO	0.5	1.7×10^{-15}	5.44E-20	1.58	-406
Epoxy-substituent					
Z-(cyc-CH$_2$OCH-)CHOO	4.5	8.8×10^{-18}	1.41E-19	1.61	1511
Aldehyde substituents					
(CHO)$_2$COO	1.6	4.4×10^{-16}	2.61E-20	1.73	36
Multifunctional species					
Z-(C(=O)CH$_2$OH)CHOO	-0.1	5.2×10^{-15}	2.37E-19	1.28	-806

Table 28: Rate constant predictions for the reaction of CI with H$_2$O monomers catalyzing the insertion reaction, obtained after barrier height corrections in the theoretical data, listing barrier heights E$_b$ (kcal mol^{-1}), rate coefficient k (cm^3 molecule^{-1} s^{-1}) at 298 K, and parameters for a Kooij equation fit $k(T)=A\times(T/K)^n\times\exp(-E_a/T)$ cm^3 molecule^{-1} s^{-1} for the temperature range 200-450 K.

Carbonyl oxide	E$_b$	k(298K)	A / s^{-1}	n	E$_a$ / K	Remarks
OH-bearing substituents						
Z-(CH$_2$OH)CHOO	3.9	6.1×10^{-17}	8.13E-32	5.48	-909	
Z-(CH$_2$OH)(CH$_3$)COO	3.0	7.5×10^{-16}	3.24E-44	9.72	-2968	
Z-(iC$_3$H$_6$OH)CHOO	5.2	7.4×10^{-18}	8.58E-34	6.34	-161	
Z-(iC$_3$H$_6$OH)(CH$_3$)COO	6.5	1.7×10^{-18}	7.17E-53	12.70	-2033	
Z-(CH$_2$CH$_2$OH)CHOO	2.5	5.4×10^{-17}	5.01E-14	-0.70	855	
Z-(CH$_2$CH$_2$CH$_2$OH)CHOO	-7.0	($>5\times10^{-11}$)				
Z-(CH$_2$CH$_2$CH$_2$CH$_2$OH)CHOO	-4.8	(4.0×10^{-11})				
E-(CH$_2$CH$_2$OH)CHOO	0.4	1.2×10^{-15}	3.46E-13	-1.18	-325	
E-(CH$_2$CH$_2$CH$_2$OH)CHOO	-11.7	($>5\times10^{-11}$)				
E-(CH$_2$CH$_2$CH$_2$CH$_2$OH)CHOO	-8.4	($>5\times10^{-11}$)				
OOH-bearing substituents						
Z-(CH$_2$OOH)(CH$_3$)COO	-0.2	1.7×10^{-14}	7.63E-25	3.08	-1865	
Z-(CH$_2$OOH)CHOO	1.0	1.4×10^{-15}	1.50E-17	0.59	-352	
Z-(CH$_2$CH$_2$OOH)CHOO	-6.4	($>5\times10^{-11}$)				
Z-(CH$_2$CH$_2$CH$_2$OOH)CHOO	-3.5	3.6×10^{-12}	3.11E-09	-2.12	-1582	
E-(CH$_2$OOH)CHOO	-0.9	9.3×10^{-15}	1.70E-15	-0.45	-1273	
E-(CH$_3$)(CH$_2$OOH)COO	1.5	2.1×10^{-16}	8.77E-27	3.33	-1475	
E-(CH$_2$CH$_2$OOH)CHOO	-10.1	($>5\times10^{-11}$)				
E-(CH$_2$CH$_2$CH$_2$OOH)CHOO	-7.3	($>5\times10^{-11}$)				
Carboxylic acid bearing substituents						
Z-(COOH)CHOO	1.1	2.7×10^{-14}	9.99E-33	6.22	-2078	
Z-(CH$_2$COOH)CHOO	1.1	2.9×10^{-14}	8.08E-32	5.86	-2087	
Z-(CH$_2$CH$_2$COOH)CHOO	-1.1	4.6×10^{-14}	7.98E-20	1.29	-1756	
Z-(CH$_2$CH$_2$CH$_2$COOH)CHOO	-4.2	6.0×10^{-13}	9.63E-18	0.10	-3122	
E-(CH$_2$COOH)CHOO	-2.6	1.0×10^{-12}	1.34E-24	3.00	-3055	
E-(CH$_2$CH$_2$COOH)CHOO	-5.9	($>5\times10^{-11}$)				
Multi-functional species						
Z-(C(=O)CH$_2$OH)CHOO	-0.6	1.7×10^{-14}	2.95E-17	0.63	-830	

S. Structure-Activity relationships: substituent naming conventions

The combinations of substituents used allow the construction of Structure-Activity Relationships (SAR) that is applicable to most of the unsaturated compounds present in the troposphere. Table 29 lists the notational conventions used in the SARs in this work.

Table 29: SAR naming convention for carbonyl oxide substituents

Substituent label	Definition
R_1, R_2	These are the substituents implanted on the carbon in the carbonyl oxide moiety, where R_1 is always on the *syn*-side of the oxide O-atom, and R_2 on the *anti*-side, as indicated in the scheme on the right. These substituents can represent the following moieties: H-atoms, alkyl groups (any branching, any chain length), β-, γ- and other vinyl substituents, β-, γ- and other oxo-substituted chains, and generally substituted alkyl chains where the functional group is at least in γ-position, where it is currently assumed to assert only a minor influence. Some additional substitution patterns are discussed explicitly elsewhere in this supporting information. $(R_1)(R_2)COO$
R_3, R_4, R_5	Substituents implanted on unsaturated substituents, specifically vinyl- and oxo-groups (see scheme on the right). We always use the same naming for the site-specific and stereo-specific positions, i.e. R_3, R_4 and R_5 are always as indicated in the schemes on the right. These substituents can represent all of the moieties as for R_1 and R_2, though one should consider that no explicit data is available for multi-unsaturated CI (i.e. conjugated alkadiene or cumulene/ketene functionalities adjacent to the carbonyl oxide moiety).
R_6, R_7, …	These substituents can represent all the moieties defined for R_1 but are implanted in a position of the molecule that is not defined explicitly by R_1 through R_5.
R_a, R_b, R_c, R_d,...	These substituents allow for the same moieties as R_1, except for H-atoms. This is used to define the branching order of the bearing C-atom, i.e. $-CH_3$, $-CH_2R_a$, $-CHR_aR_b$, $-CR_aR_bR_c$ are primary, secondary, tertiary and quaternary carbon atoms with exactly 3, 2, 1, and 0 H-atoms, respectively.
R', R'', R'''	These substituents represent either an H-atom, or a substituent without (easily) mobile H-atoms on the connecting carbon, e.g. $-tC_4H_9$, $-C(R_a)=CR_4R_5$, a cyclic moiety where ring strain or geometric constraints prevents H-migration (e.g. nopinone oxide), etc. These labels are used to indicate compounds for which no H-migration path is accessible.
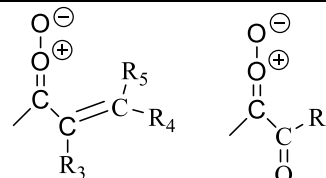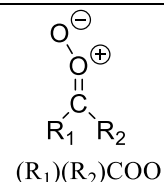
T. Structure-Activity Relationships (SARs) for SCI unimolecular reactions

Structure of the SAR tables as a function of the R$_1$ and R$_2$ substituents
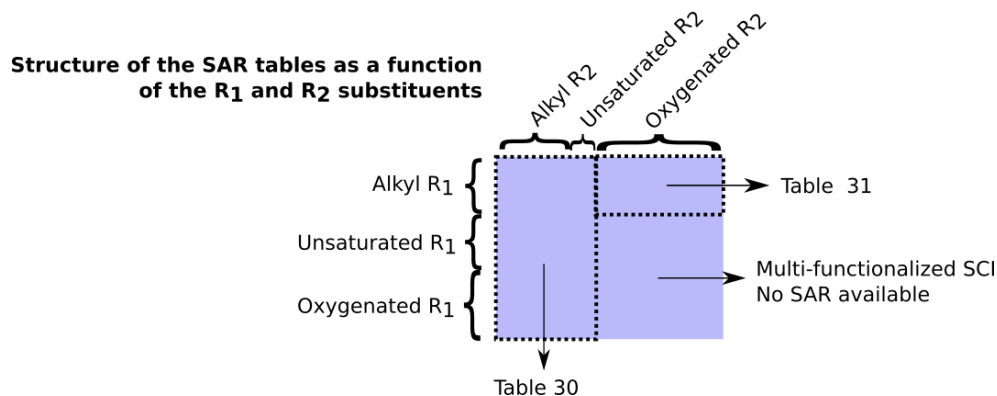
Table 30: Predicted total rate coefficients for unimolecular carbonyl oxide decay as a function of the two substituents R$_1$ and R$_2$. Indicated is the mode of reaction, the rate coefficient k (s^{-1}) at 298K, and the parameters of a Kooij equation fit $k(T) = A \times (T/K)^n \times \exp(-E_a/T)$ between 200 and 450 K (A in s^{-1}, E_a in K), and already account for all migratable H-atoms. The meaning of the SAR substituents is explained in section S. Note that the theoretical work here does not consider systematic variations for R$_a$/R$_b$/R$_c$/R$_3$/R$_4$/R$_5$/R', and the values listed are for substituents −H (when appropriate), −CH$_3$, −C$_2$H$_5$, or an average of the prediction for these substituents. Values in green are based directly on theoretical kinetic calculations, whereas values in orange are estimated values based on the reactivity trends for other substituents. The values are standardized in number of digits, see Vereecken et al.[8] for an uncertainty analysis.

	R$_2$= −CH$_3$	R$_2$= −CH$_2$R$_a$	R$_2$= −CHR$_a$R$_b$	R$_2$= −CR$_a$R$_b$R$_c$	R$_2$= −H	R$_2$ = vinyl
R$_1$= −CH$_3$	1,4-H-migration **k(298K)=478** A= 7.64×10^{-60} n= 23.59 E$_a$= -2367	1,4-H-migration **k(298K)=433** A= 8.63×10^{-61} n= 23.94 E$_a$= -2390	1,4-H-migration **k(298K)=611** A= 4.18×10^{-59} n= 23.38 E$_a$= -2276	1,4-H-migration **k(298K)=373** A= 9.26×10^{-61} n= 23.92 E$_a$= -2362	1,4-H-migration **k(298K)=136** A= 3.11×10^{-64} n= 24.95 E$_a$= -2685	1,4-H-migration **k(298K)=50** A= 4.36×10^{-67} n= 25.90 E$_a$= -2737
R$_1$= −CH$_2$R$_a$	1,4-H-migration **k(298K)=689** A= 5.91×10^{-58} n= 22.91 E$_a$= -2331	1,4-H-migration **k(298K)=534** A= 4.72×10^{-59} n= 23.29 E$_a$= -2358	1,4-H-migration **k(298K)=257** A= 4.83×10^{-61} n= 23.93 E$_a$= -2420	1,4-H-migration **k(298K)=12** A= 2.13×10^{-74} n= 28.47 E$_a$= -2964	1,4-H-migration **k(298K)=205** A= 2.41×10^{-62} n= 24.33 E$_a$= -2571	1,4-H-migration **k(298K)=30** A= 1.36×10^{-68} n= 26.38 E$_a$= -2809

R_1						
$R_1 = -CHR_aR_b$	1,4-H-migration **k(298K)=14** A= 4.45×10^{-76} n= 27.97 Ea= -2967	1,4-H-migration **k(298K)=13** A= 8.54×10^{-73} n= 27.89 Ea= -2858	1,4-H-migration **k(298K)=19** A= 1.62×10^{-70} n= 27.01 Ea= -2912	1,4-H-migration **k(298K)=1.1** A= 8.80×10^{-81} n= 30.47 Ea= -3249	1,4-H-migration **k(298K)=6.7** A= 1.52×10^{-75} n= 28.72 Ea= -3150	1,4-H-migration **k(298K)=11** A= 4.09×10^{-72} n= 27.42 Ea= -3149
$R_1 = -CR_aR_bR_c$	1,3-Cyclisation **k(298K)=0.17** A= 2.55×10^{10} n= 1.02 Ea= 9399	1,3-Cyclisation **k(298K)=0.15** A= 5.45×10^{11} n= 0.55 Ea= 9555	1,3-Cyclisation **k(298K)=1.1** A= 6.83×10^{10} n= 0.80 Ea= 8759	1,3-Cyclisation **k(298K)=0.075** A= 1.12×10^{11} n= 0.85 Ea= 9795	1,3-Cyclisation **k(298K)=1×10^{-2}** A= 2.58×10^{6} n= 2.32 Ea= 9710	1,3-Cyclisation **k(298K)=9.6×10^{-2}** A= 1.53×10^{8} n= 1.66 Ea= 9170
$R_1 = -H$	1,3-Cyclisation **k(298K)=53** A= 1.69×10^{9} n= 1.35 Ea= 7445	1,3-Cyclisation **k(298K)=74** A= 1.57×10^{10} n= 1.03 Ea= 7464	1,3-Cyclisation **k(298K)=102** A= 9.22×10^{9} n= 1.13 Ea= 7387	1,3-Cyclisation **k(298K)=111** A= 8.51×10^{9} n= 1.15 Ea= 7357	1,3-Cyclisation **k(298K)=0.3** A= 1.66×10^{1} n= 4.02 Ea= 8024	1,3-Cyclisation **k(298K)=22** A= 6.84×10^{10} n= 0.83 Ea= 7925
$R_1 = -CH_2-CR_3=CR_4R_5$	Allyl-1,4-Hmig. **k(298K)=7040** A= 2.97×10^{-45} n= 18.69 Ea= -1459	Allyl-1,4-Hmig. **k(298K)=7080** A= 6.14×10^{-45} n= 18.52 Ea= -1532	Allyl-1,4-Hmig. **k(298K)=7120** A= 1.27×10^{-44} n= 18.35 Ea= -1605	Allyl-1,4-Hmig. **k(298K)=247** A= 3.24×10^{-58} n= 23.01 Ea= -2023	Allyl-1,4-Hmig. **k(298K)=4180** A= 3.66×10^{-46} n= 18.87 Ea= -1630	Allyl-1,4-Hmig. **k(298K)=795** A= 2.16×10^{-50} n= 20.16 Ea= -1839
$R_1 = -CHR_a-CR_3=CR_4R_5$	Allyl-1,4-Hmig. **k(298K)=385** A= 7.22×10^{-57} n= 22.50 Ea= -2098	Allyl-1,4-Hmig. **k(298K)=388** A= 1.49×10^{-56} n= 22.33 Ea= -2171	Allyl-1,4-Hmig. **k(298K)=390** A= 3.09×10^{-56} n= 22.16 Ea= -2244	Allyl-1,4-Hmig. **k(298K)=13** A= 7.88×10^{-70} n= 26.82 Ea= -2662	Allyl-1,4-Hmig. **k(298K)=230** A= 8.89×10^{-58} n= 22.68 Ea= -2269	Allyl-1,4-Hmig. **k(298K)=43** A= 5.25×10^{-62} n= 23.97 Ea= -2478
$R_1 = -CR_aR_b-CR_3=CR_4R_5$	1,3-Cyclisation **k(298K)=0.23** A= 9.73×10^{10} n= 0.79 Ea= 9314	1,3-Cyclisation **k(298K)=0.20** A= 2.08×10^{12} n= 0.32 Ea= 9471	1,3-Cyclisation **k(298K)=1.5** A= 2.61×10^{11} n= 0.57 Ea= 8674	1,3-Cyclisation **k(298K)=0.10** A= 4.27×10^{11} n= 0.62 Ea= 9711	1,3-Cyclisation **k(298K)=0.013** A= 9.84×10^{6} n= 2.09 Ea= 9625	1,3-Cyclisation **k(298K)=0.13** A= 5.84×10^{8} n= 1.45 Ea= 9086
$R_1 = -(CR_3=CR_4CH_3)$	Allyl-1,6-Hmig. **k(298K)=2.5×10^{8}** A= 4.80×10^{-5} n= 5.44 Ea= 512	Allyl-1,6-Hmig. **k(298K)=3.4×10^{7}** A= 2.59×10^{-7} n= 6.11 Ea= 675	Allyl-1,6-Hmig. **k(298K)=3.4×10^{7}** A= 2.59×10^{-7} n= 6.11 Ea= 675	Allyl-1,6-Hmig. **k(298K)=3.4×10^{7}** A= 2.59×10^{-7} n= 6.11 Ea= 675	Allyl-1,6-Hmig. **k(298K)=4.8×10^{6}** A= 1.40×10^{-9} n= 6.77 Ea= 838	Allyl-1,6-Hmig. **k(298K)=1.7×10^{6}** A= 1.96×10^{-12} n= 7.72 Ea= 785
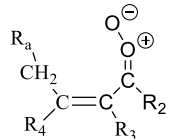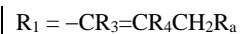
$R_1 = -CR_3=CR_4CH_2R_a$	Allyl-1,6-Hmig. $k(298K)=3.0\times10^8$ A= 5.39×10^{-4} n= 5.09 E_a= 591	Allyl-1,6-Hmig. $k(298K)=4.1\times10^7$ A= 2.90×10^{-6} n= 5.76 E_a= 754	Allyl-1,6-Hmig. $k(298K)=4.1\times10^7$ A= 2.90×10^{-6} n= 5.76 E_a= 754	Allyl-1,6-Hmig. $k(298K)=4.1\times10^7$ A= 2.90×10^{-6} n= 5.76 E_a= 754	Allyl-1,6-Hmig. $k(298K)=5.7\times10^6$ A= 1.57×10^{-8} n= 6.42 E_a= 917	Allyl-1,6-Hmig. $k(298K)=2.1\times10^6$ A= 2.20×10^{-11} n= 7.37 E_a= 864
$R_1 = -CR_3=CR_4CHR_aR_b$	Allyl-1,6-Hmig. $k(298K)=1.1\times10^8$ A= 5.21×10^{-5} n= 5.49 E_a= 884	Allyl-1,6-Hmig. $k(298K)=1.5\times10^7$ A= 2.81×10^{-7} n= 6.16 E_a= 1047	Allyl-1,6-Hmig. $k(298K)=1.5\times10^7$ A= 2.81×10^{-7} n= 6.16 E_a= 1047	Allyl-1,6-Hmig. $k(298K)=1.5\times10^7$ A= 2.81×10^{-7} n= 6.16 E_a= 1047	Allyl-1,6-Hmig. $k(298K)=2.0\times10^6$ A= 1.51×10^{-9} n= 6.83 E_a= 1210	Allyl-1,6-Hmig. $k(298K)=7.4\times10^5$ A= 2.13×10^{-12} n= 7.77 E_a= 1157
$R_1 = -CR_3=CR_4R'$	1,5-Cyclisation $k(298K)=4.5\times10^4$ A= 9.32×10^{10} n= 0.46 E_a= 5124	1,5-Cyclisation $k(298K)=1.2\times10^4$ A= 9.77×10^{10} n= 0.50 E_a= 5584	1,5-Cyclisation $k(298K)= 1.2\times10^4$ A= 1.68×10^{11} n= 0.44 E_a= 5668	1,5-Cyclisation $k(298K)=1.2\times10^4$ A= 1.28×10^{11} n= 0.44 E_a= 5625	1,5-Cyclisation $k(298K)=8.7\times10^3$ A= 7.01×10^{10} n= 0.44 E_a= 5485	1,5-Cyclisation $k(298K)=1.2\times10^4$ A= 1.28×10^{11} n= 0.44 E_a= 5625
$R_1 = -CHO$	1,3-Cyclisation $k(298K)= 7.1\times10^4$ A= 2.76×10^{10} n= 0.78 E_a= 5162	1,3-Cyclisation $k(298K)= 2.4\times10^4$ A= 7.73×10^{11} n= 0.36 E_a= 5756	1,3-Cyclisation $k(298K)= 4.8\times10^4$ A= 2.95×10^{10} n= 0.75 E_a= 5244	1,3-Cyclisation $k(298K)= 1.4\times10^4$ A= 1.29×10^{11} n= 0.57 E_a= 5755	1,3-Cyclisation $k(298K)= 144$ A= 2.49×10^6 n= 2.21 E_a= 6656	1,3-Cyclisation $k(298K)= 1.1\times10^4$ A= 5.22×10^{11} n= 0.25 E_a= 5712
$R_1 = -C(O)R_a$	1,3-Cyclisation $k(298K)= 1.6\times10^4$ A=3.95×10^9 n= 1.02 E_a= 5448	1,3-Cyclisation $k(298K)= 4.1\times10^3$ A= 1.38×10^{11} n= 0.58 E_a= 6141	1,3-Cyclisation $k(298K)= 8.3\times10^3$ A= 5.28×10^9 n= 0.97 E_a= 5629	1,3-Cyclisation $k(298K)= 2.3\times10^3$ A= 2.30×10^{10} n= 0.79 E_a= 6140	1,3-Cyclisation $k(298K)= 20$ A=5.55×10^5 n= 2.41 E_a= 7141	1,3-Cyclisation $k(298K)= 6.5\times10^3$ A= 1.43×10^{11} n= 0.39 E_a= 5701
$R_1 = -C(=O)OR'$	1,3-Cyclisation $k(298K)= 1.3\times10^3$ A= 1.85×10^8 n= 1.33 E_a= 5784	1,3-Cyclisation $k(298K)= 3.6\times10^2$ A= 6.49×10^9 n= 0.88 E_a= 6477	1,3-Cyclisation $k(298K)= 7.2\times10^2$ A= 2.48×10^8 n= 1.28 E_a= 5965	1,3-Cyclisation $k(298K)= 2.0\times10^2$ A= 1.08×10^9 n= 1.10 E_a= 6476	1,3-Cyclisation $k(298K)= 1.7$ A=2.61×10^4 n= 2.71 E_a= 7477	1,3-Cyclisation $k(298K)= 5.6\times10^2$ A= 6.70×10^9 n= 0.70 E_a= 6037
$R_1 = -ONO_2$	1,3-Cyclisation $k(298K)= 4.4\times10^6$ A= 8.19×10^{10} n= 0.66 E_a= 4047	1,3-Cyclisation $k(298K)= 6.0\times10^6$ A= 3.21×10^{12} n= 0.16 E_a= 4196	1,3-Cyclisation $k(298K)= 1.2\times10^7$ A= 1.22×10^{11} n= 0.55 E_a= 3684	1,3-Cyclisation $k(298K)= 3.4\times10^6$ A= 5.33×10^{11} n= 0.37 E_a= 4195	1,3-Cyclisation $k(298K)= 1.4\times10^5$ A=1.44×10^7 n= 1.93 E_a= 4650	1,3-Cyclisation $k(298K)= 1.0\times10^7$ A= 3.02×10^{12} n= -0.02 E_a= 3707
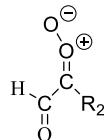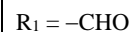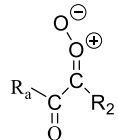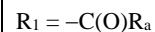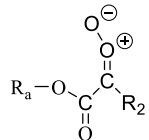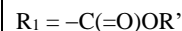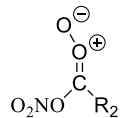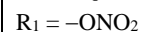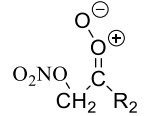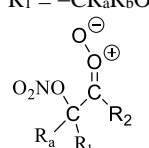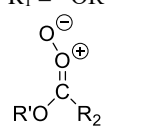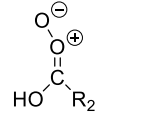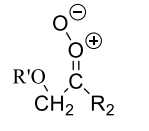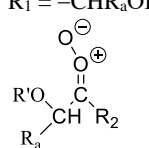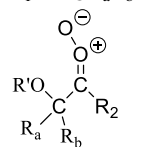
40
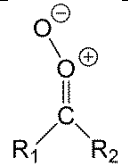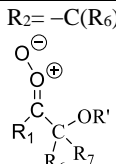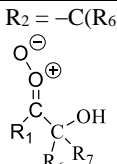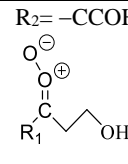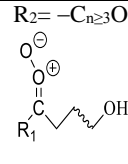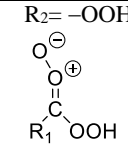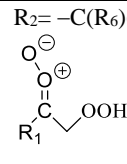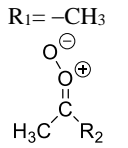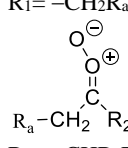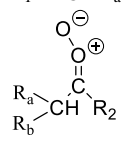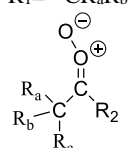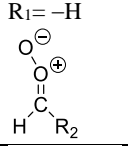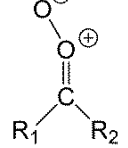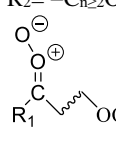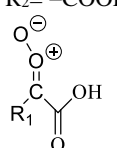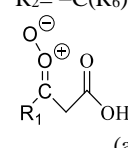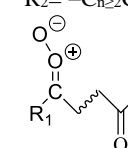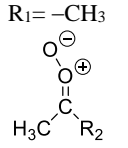
$R_1 = -CH_2ONO_2$	1,4-H-migration $k(298K)=2.2\times10^3$ A= 4.01×10^{-56} n= 22.41 E_a= -2271	1,4-H-migration $k(298K)=1.9\times10^3$ A= 1.04×10^{-56} n= 22.63 E_a= -2252	1,4-H-migration $k(298K)=1.9\times10^3$ A= 4.71×10^{-56} n= 22.36 E_a= -2253	1,4-H-migration $k(298K)=2.3\times10^2$ A= 1.77×10^{-64} n= 25.21 E_a= -2574	1,4-H-migration $k(298K)=7.5\times10^2$ A= 7.14×10^{-60} n= 23.59 E_a= -2518	1,4-H-migration $k(298K)=3.4\times10^2$ A= 9.20×10^{-62} n= 24.15 E_a= -2615
$R_1 = -CHR_aONO_2$	1,4-H-migration $k(298K)=47$ A= 6.42×10^{-71} n= 27.47 E_a= -2907	1,4-H-migration $k(298K)=45$ A= 1.87×10^{-70} n= 27.23 E_a= -2752	1,4-H-migration $k(298K)=141$ A= 1.58×10^{-65} n= 25.45 E_a= -2745	1,4-H-migration $k(298K)=21$ A= 7.31×10^{-71} n= 27.20 E_a= -2860	1,4-H-migration $k(298K)=25$ A= 4.52×10^{-73} n= 27.98 E_a= -3097	1,4-H-migration $k(298K)=122$ A= 2.76×10^{-65} n= 25.20 E_a= -2955
$R_1 = -CR_aR_bONO_2$	1,3-Cyclisation $k(298K)= 0.21$ A=1.64×10^7 n= 1.99 E_a= 8789	1,3-Cyclisation $k(298K)= 0.29$ A=6.42×10^8 n= 1.48 E_a= 8938	1,3-Cyclisation $k(298K)= 0.57$ A=2.45×10^7 n= 1.88 E_a= 8426	1,3-Cyclisation $k(298K)= 0.16$ A=1.07×10^8 n= 1.70 E_a= 8937	1,3-Cyclisation $k(298K)= 6.8\times10^{-3}$ A=2.88×10^3 n= 3.26 E_a= 9392	1,3-Cyclisation $k(298K)= 0.41$ A=7.27×10^8 n= 1.30 E_a= 8546
$R_1 = -OR'$	1,3-Cyclisation $k(298K)= 1.1\times10^5$ A=5.65×10^{10} n= 0.42 E_a= 4637	1,3-Cyclisation $k(298K)= 1.5\times10^5$ A= 2.21×10^{12} n= -0.08 E_a= 4785	1,3-Cyclisation $k(298K)= 2.9\times10^5$ A= 8.44×10^{10} n= 0.31 E_a= 4273	1,3-Cyclisation $k(298K)= 8.3\times10^4$ A= 3.68×10^{11} n= 0.13 E_a= 4784	1,3-Cyclisation $k(298K)= 2.6\times10^3$ A=4.74×10^9 n= 0.81 E_a= 5658	1,3-Cyclisation $k(298K)= 3.1\times10^5$ A= 2.50×10^{12} n= -0.27 E_a= 4393
$R_1 = -OH$	Unstable Converts to peracid	Unstable Converts to peracid	Unstable Converts to peracid	Unstable Converts to peracid	Unstable Converts to peracid	Unstable Converts to peracid
$R_1 = -CH_2OR'$	1,4-H-migration $k(298K)=280$ A= 4.45×10^{-66} n= 25.81 E_a= -2713	1,4-H-migration $k(298K)=237$ A= 1.15×10^{-66} n= 26.03 E_a= -2693	1,4-H-migration $k(298K)=239$ A= 5.24×10^{-66} n= 25.76 E_a= -2694	1,4-H-migration $k(298K)=28$ A= 1.97×10^{-74} n= 28.61 E_a= -3016	1,4-H-migration $k(298K)=95$ A= 7.94×10^{-70} n= 26.99 E_a= -2960	1,4-H-migration $k(298K)=42$ A= 1.02×10^{-71} n= 27.55 E_a= -3056
$R_1 = -CHR_aOR'$	1,4-H-migration $k(298K)=5.8$ A= 3.35×10^{-81} n= 30.87 E_a= -3349	1,4-H-migration $k(298K)=5.6$ A= 2.09×10^{-80} n= 30.63 E_a= -3194	1,4-H-migration $k(298K)=18$ A= 1.76×10^{-75} n= 28.85 E_a= -3187	1,4-H-migration $k(298K)=2.6$ A= 8.13×10^{-81} n= 30.60 E_a= -3301	1,4-H-migration $k(298K)=3.1$ A= 5.02×10^{-83} n= 31.38 E_a= -3538	1,4-H-migration $k(298K)=15$ A= 3.07×10^{-75} n= 28.60 E_a= -3397
$R_1 = -CR_aR_bOR'$	1,3-Cyclisation $k(298K)= 0.10$ A= 1.18×10^{11} n= 0.80 E_a= 9635	1,3-Cyclisation $k(298K)= 0.13$ A=6.42×10^8 n= 1.48 E_a= 8938	1,3-Cyclisation $k(298K)= 0.27$ A=2.45×10^7 n= 1.88 E_a= 8426	1,3-Cyclisation $k(298K)= 0.077$ A=1.07×10^8 n= 1.70 E_a= 8937	1,3-Cyclisation $k(298K)= 3.2\times10^{-3}$ A=2.88×10^3 n= 3.26 E_a= 9392	1,3-Cyclisation $k(298K)= 0.19$ A=7.27×10^8 n= 1.30 E_a= 8546
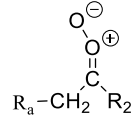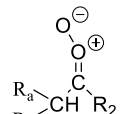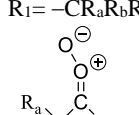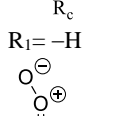
R_1						
$R_1 = -CH_2OH$	Intramol. insertion **k(298K)= 7.7×10²** A= 1.38×10¹¹ n= 0.31 Ea= 6186	Intramol. insertion **k(298K)= 5.4×10²** A= 4.91×10⁴ n= 2.51 Ea= 5608	Intramol. insertion **k(298K)= 5.4×10²** A= 4.91×10⁴ n= 2.51 Ea= 5608	Intramol. insertion **k(298K)= 5.4×10²** A= 4.91×10⁴ n= 2.51 Ea= 5608	Intramol. insertion **k(298K)= 1.9×10²** A= 7.87×10⁻⁵ n= 5.28 Ea= 4575	Intramol. insertion **k(298K)= 5.4×10²** A= 4.91×10⁴ n= 2.51 Ea= 5608
	1,4-H-migration **k(298K)=20** A= 9.76×10⁻⁷⁴ n= 28.23 Ea= -3070	1,4-H-migration **k(298K)=34** A= 1.40×10⁻⁷¹ n= 27.49 Ea= -3002	1,4-H-migration **k(298K)=34** A= 6.35×10⁻⁷¹ n= 27.23 Ea= -3003	1,4-H-migration **k(298K)=4.0** A= 2.39×10⁻⁷⁹ n= 30.07 Ea= -3325	1,4-H-migration **k(298K)=40** A= 5.39×10⁻⁷¹ n= 27.27 Ea= -3022	1,4-H-migration **k(298K)=13** A= 9.61×10⁻⁷⁵ n= 28.45 Ea= -3269
$R_1 = -CHR_aOH$	Intramol. insertion **k(298K)= 5.4×10²** A= 4.91×10⁴ n= 2.51 Ea= 5608	Intramol. insertion **k(298K)= 5.4×10²** A= 4.91×10⁴ n= 2.51 Ea= 5608	Intramol. insertion **k(298K)= 5.4×10²** A= 4.91×10⁴ n= 2.51 Ea= 5608	Intramol. insertion **k(298K)= 5.4×10²** A= 4.91×10⁴ n= 2.51 Ea= 5608	Intramol. insertion **k(298K)= 5.4×10²** A= 4.91×10⁴ n= 2.51 Ea= 5608	Intramol. insertion **k(298K)= 5.4×10²** A= 4.91×10⁴ n= 2.51 Ea= 5608
$R_1 = -CR_aR_bOH$	Intramol. insertion **k(298K)= 6.9×10²** A= 8.58×10¹⁰ n= 0.56 Ea= 6499	Intramol. insertion **k(298K)= 5.4×10²** A= 4.91×10⁴ n= 2.51 Ea= 5608	Intramol. insertion **k(298K)= 5.4×10²** A= 4.91×10⁴ n= 2.51 Ea= 5608	Intramol. insertion **k(298K)= 5.4×10²** A= 4.91×10⁴ n= 2.51 Ea= 5608	Intramol. insertion **k(298K)= 8.1×10²** A= 6.22×10⁰ n= 3.90 Ea= 5172	Intramol. insertion **k(298K)= 5.4×10²** A= 4.91×10⁴ n= 2.51 Ea= 5608
$R_1 = -CH_2C(R_6)(R_7)OH$	1,4-H-migration **k(298K)=105** A= 1.26×10⁻⁶⁴ n= 25.60 Ea= -2457	1,4-H-migration **k(298K)=89** A= 3.27×10⁻⁶⁶ n= 25.82 Ea= -2437	1,4-H-migration **k(298K)=90** A= 1.49×10⁻⁶⁵ n= 25.56 Ea= -2438	1,4-H-migration **k(298K)=11** A= 5.59×10⁻⁷⁴ n= 28.40 Ea= -2760	1,4-H-migration **k(298K)=36** A= 2.25×10⁻⁶⁹ n= 26.78 Ea= -2704	1,4-H-migration **k(298K)=16** A= 2.90×10⁻⁷¹ n= 27.35 Ea= -2801
	Intramol. insertion **k(298K)= 7.0** A= 4.49×10¹³ n= -0.91 Ea= 7251	Intramol. insertion **k(298K)= 7.0** A= 4.49×10¹³ n= -0.91 Ea= 7251	Intramol. insertion **k(298K)= 7.0** A= 4.49×10¹³ n= -0.91 Ea= 7251	Intramol. insertion **k(298K)= 7.0** A= 4.49×10¹³ n= -0.91 Ea= 7251	Intramol. insertion **k(298K)= 7.0** A= 4.49×10¹³ n= -0.91 Ea= 7251	Intramol. insertion **k(298K)= 7.0** A= 4.49×10¹³ n= -0.91 Ea= 7251
$R_1 = -CHR_aC(R_6)(R_7)OH$	1,4-H-migration **k(298K)=2.2** A= 9.50×10⁻⁸¹ n= 30.66 Ea= -3093	1,4-H-migration **k(298K)=2.1** A= 5.92×10⁻⁸⁰ n= 30.43 Ea= -2938	1,4-H-migration **k(298K)=6.6** A= 4.99×10⁻⁷⁵ n= 28.64 Ea= -2931	1,4-H-migration **k(298K)=1.0** A= 2.31×10⁻⁸⁰ n= 30.40 Ea= -3045	1,4-H-migration **k(298K)=1.2** A= 1.43×10⁻⁸² n= 31.18 Ea= -3282	1,4-H-migration **k(298K)=5.7** A= 8.72×10⁻⁷⁵ n= 28.39 Ea= -3141
	Intramol. insertion **k(298K)= 7.0** A= 4.49×10¹³ n= -0.91 Ea= 7251	Intramol. insertion **k(298K)= 7.0** A= 4.49×10¹³ n= -0.91 Ea= 7251	Intramol. insertion **k(298K)= 7.0** A= 4.49×10¹³ n= -0.91 Ea= 7251	Intramol. insertion **k(298K)= 7.0** A= 4.49×10¹³ n= -0.91 Ea= 7251	Intramol. insertion **k(298K)= 7.0** A= 4.49×10¹³ n= -0.91 Ea= 7251	Intramol. insertion **k(298K)= 7.0** A= 4.49×10¹³ n= -0.91 Ea= 7251
$R_1 = -CR_aR_bC(R_6)(R_7)OH$	Intramol. insertion **k(298K)= 7.0** A= 4.49×10¹³ n= -0.91 Ea= 7251	Intramol. insertion **k(298K)= 7.0** A= 4.49×10¹³ n= -0.91 Ea= 7251	Intramol. insertion **k(298K)= 7.0** A= 4.49×10¹³ n= -0.91 Ea= 7251	Intramol. insertion **k(298K)= 7.0** A= 4.49×10¹³ n= -0.91 Ea= 7251	Intramol. insertion **k(298K)= 7.0** A= 4.49×10¹³ n= -0.91 Ea= 7251	Intramol. insertion **k(298K)= 7.0** A= 4.49×10¹³ n= -0.91 Ea= 7251

R1 / structure	Column 1	Column 2	Column 3	Column 4	Column 5	Column 6
R1 = −C(R6)(R7)C(R8)(R9)−C(R10)(R11)OH	Intramol. insertion **k(298K)= 1.5×10^7** A= 1.01×10^15 n= -1.13 Ea= 3441	Intramol. insertion **k(298K)= 1.3×10^7** A= 6.58×10^16 n= -1.77 Ea= 3661	Intramol. insertion **k(298K)= 1.3×10^7** A= 6.58×10^16 n= -1.77 Ea= 3661	Intramol. insertion **k(298K)= 1.3×10^7** A= 6.58×10^16 n= -1.77 Ea= 3661	Intramol. insertion **k(298K)= 1.0×10^7** A= 4.30×10^18 n= -2.41 Ea= 3882	Intramol. insertion **k(298K)= 1.3×10^7** A= 6.58×10^16 n= -1.77 Ea= 3661
R1 = −C(R6)(R7)C(R8)(R9)−C(R10)(R11)C(R12)(R13)OH	Intramol. insertion **k(298K)= 1.7×10^6** A= 4.65×10^30 n= -7.03 Ea= 4843	Intramol. insertion **k(298K)= 1.7×10^6** A= 4.65×10^30 n= -7.03 Ea= 4843	Intramol. insertion **k(298K)= 1.7×10^6** A= 4.65×10^30 n= -7.03 Ea= 4843	Intramol. insertion **k(298K)= 1.7×10^6** A= 4.65×10^30 n= -7.03 Ea= 4843	Intramol. insertion **k(298K)= 1.7×10^6** A= 4.65×10^30 n= -7.03 Ea= 4843	Intramol. insertion **k(298K)= 1.7×10^6** A= 4.65×10^30 n= -7.03 Ea= 4843
R1 = −OOH	1,3-Cyclisation **k(298K)= 3.7×10^3** A= 5.97×10^10 n= 0.49 Ea= 5772	1,3-Cyclisation **k(298K)= 5.0×10^3** A= 2.34×10^12 n= -0.02 Ea= 5920	1,3-Cyclisation **k(298K)= 1.0×10^4** A= 8.92×10^10 n= 0.38 Ea= 5408	1,3-Cyclisation **k(298K)= 2.9×10^3** A= 3.89×10^11 n= 0.20 Ea= 5919	1,3-Cyclisation **k(298K)= 67** A= 1.86×10^9 n= 0.91 Ea= 6646	1,3-Cyclisation **k(298K)= 7.2×10^3** A= 2.64×10^12 n= -0.21 Ea= 5528
R1 = −CH2OOH	Intramol. insertion **k(298K)= 9.8×10^4** A= 2.45×10^3 n= 2.59 Ea= 3300	Intramol. insertion **k(298K)= 8.4×10^3** A= 4.14×10^6 n= 1.50 Ea= 4403	Intramol. insertion **k(298K)= 8.4×10^3** A= 4.14×10^6 n= 1.50 Ea= 4403	Intramol. insertion **k(298K)= 8.4×10^3** A= 4.14×10^6 n= 1.50 Ea= 4403	Intramol. insertion **k(298K)= 718** A= 6.99×10^9 n= 0.42 Ea= 5505	Intramol. insertion **k(298K)= 8.4×10^3** A= 4.14×10^6 n= 1.50 Ea= 4403
	1,4-H-migration **k(298K)= 663** A= 2.72×10^-57 n= 22.69 Ea= -2240	1,4-H-migration **k(298K)=564** A= 7.04×10^-58 n= 22.91 Ea= -2220	1,4-H-migration **k(298K)=568** A= 3.20×10^-57 n= 22.64 Ea= -2221	1,4-H-migration **k(298K)=68** A= 1.20×10^-65 n= 25.48 Ea= -2543	1,4-H-migration **k(298K)= 256** A= 8.64×10^-63 n= 24.51 Ea= -2629	1,4-H-migration **k(298K)=100** A= 6.25×10^-63 n= 24.43 Ea= -2583
R1 = −CHRaOOH	Intramol. insertion **k(298K)= 8.4×10^3** A= 4.14×10^6 n= 1.50 Ea= 4403	Intramol. insertion **k(298K)= 8.4×10^3** A= 4.14×10^6 n= 1.50 Ea= 4403	Intramol. insertion **k(298K)= 8.4×10^3** A= 4.14×10^6 n= 1.50 Ea= 4403	Intramol. insertion **k(298K)= 8.4×10^3** A= 4.14×10^6 n= 1.50 Ea= 4403	Intramol. insertion **k(298K)= 8.4×10^3** A= 4.14×10^6 n= 1.50 Ea= 4403	Intramol. insertion **k(298K)= 8.4×10^3** A= 4.14×10^6 n= 1.50 Ea= 4403
R1 = −CRaRbOOH	Intramol. insertion **k(298K)= 8.4×10^3** A= 4.14×10^6 n= 1.50 Ea= 4403	Intramol. insertion **k(298K)= 8.4×10^3** A= 4.14×10^6 n= 1.50 Ea= 4403	Intramol. insertion **k(298K)= 8.4×10^3** A= 4.14×10^6 n= 1.50 Ea= 4403	Intramol. insertion **k(298K)= 8.4×10^3** A= 4.14×10^6 n= 1.50 Ea= 4403	Intramol. insertion **k(298K)= 8.4×10^3** A= 4.14×10^6 n= 1.50 Ea= 4403	Intramol. insertion **k(298K)= 8.4×10^3** A= 4.14×10^6 n= 1.50 Ea= 4403
R1 = −C(R6)(R7)C(R8)(R9)OOH	Intramol. insertion **k(298K)= 1.6×10^7** A= 2.89×10^17 n= -1.96 Ea= 3708	Intramol. insertion **k(298K)= 1.6×10^7** A= 2.89×10^17 n= -1.96 Ea= 3708	Intramol. insertion **k(298K)= 1.6×10^7** A= 2.89×10^17 n= -1.96 Ea= 3708	Intramol. insertion **k(298K)= 1.6×10^7** A= 2.89×10^17 n= -1.96 Ea= 3708	Intramol. insertion **k(298K)= 1.6×10^7** A= 2.89×10^17 n= -1.96 Ea= 3708	Intramol. insertion **k(298K)= 1.6×10^7** A= 2.89×10^17 n= -1.96 Ea= 3708

$R_1 = -C(R_6)(R_7)C(R_8)(R_9)-C(R_{10})(R_{11})OOH$	Intramol. insertion **k(298K)= 1.7×10⁴** A= 1.16×10²¹ n= -3.12 Ea= 6253	Intramol. insertion **k(298K)= 1.7×10⁴** A= 1.16×10²¹ n= -3.12 Ea= 6253	Intramol. insertion **k(298K)= 1.7×10⁴** A= 1.16×10²¹ n= -3.12 Ea= 6253	Intramol. insertion **k(298K)= 1.7×10⁴** A= 1.16×10²¹ n= -3.12 Ea= 6253	Intramol. insertion **k(298K)= 1.7×10⁴** A= 1.16×10²¹ n= -3.12 Ea= 6253	Intramol. insertion **k(298K)= 1.7×10⁴** A= 1.16×10²¹ n= -3.12 Ea= 6253
$R_1 = -COOH$	Intramol. insertion **k(298K)= 9.0×10⁵** A= 9.81×10¹⁰ n= 0.79 Ea= 4790	Intramol. insertion **k(298K)= 9.0×10⁵** A= 9.81×10¹⁰ n= 0.79 Ea= 4790	Intramol. insertion **k(298K)= 9.0×10⁵** A= 9.81×10¹⁰ n= 0.79 Ea= 4790	Intramol. insertion **k(298K)= 9.0×10⁵** A= 9.81×10¹⁰ n= 0.79 Ea= 4790	Intramol. insertion **k(298K)= 9.0×10⁵** A= 9.81×10¹⁰ n= 0.79 Ea= 4790	Intramol. insertion **k(298K)= 9.0×10⁵** A= 9.81×10¹⁰ n= 0.79 Ea= 4790
$R_1 = -C(R_6)(R_7)COOH$	CO₂ + Alkene **k(298K)= 4.0×10¹⁰** A= 1.14×10¹¹ n= 0.54 Ea= 1232	CO₂ + Alkene **k(298K)= 4.0×10¹⁰** A= 1.14×10¹¹ n= 0.54 Ea= 1232	CO₂ + Alkene **k(298K)= 4.0×10¹⁰** A= 1.14×10¹¹ n= 0.54 Ea= 1232	CO₂ + Alkene **k(298K)= 4.0×10¹⁰** A= 1.14×10¹¹ n= 0.54 Ea= 1232	CO₂ + Alkene **k(298K)= 4.0×10¹⁰** A= 1.14×10¹¹ n= 0.54 Ea= 1232	CO₂ + Alkene **k(298K)= 4.0×10¹⁰** A= 1.14×10¹¹ n= 0.54 Ea= 1232
$R_1 = -C(R_6)(R_7)-C(R_8)(R_9)COOH$	SOZ formation **k(298K)= 8.9×10²** A= 5.32×10¹⁵ n= -1.70 Ea= 5877 Intramol. insertion **k(298K)= 5.0×10²** A= 1.69×10¹⁶ n= -1.68 Ea= 6435	SOZ formation **k(298K)= 8.9×10²** A= 5.32×10¹⁵ n= -1.70 Ea= 5877 Intramol. insertion **k(298K)= 5.0×10²** A= 1.69×10¹⁶ n= -1.68 Ea= 6435	SOZ formation **k(298K)= 8.9×10²** A= 5.32×10¹⁵ n= -1.70 Ea= 5877 Intramol. insertion **k(298K)= 5.0×10²** A= 1.69×10¹⁶ n= -1.68 Ea= 6435	SOZ formation **k(298K)= 8.9×10²** A= 5.32×10¹⁵ n= -1.70 Ea= 5877 Intramol. insertion **k(298K)= 5.0×10²** A= 1.69×10¹⁶ n= -1.68 Ea= 6435	SOZ formation **k(298K)= 8.9×10²** A= 5.32×10¹⁵ n= -1.70 Ea= 5877 Intramol. insertion **k(298K)= 5.0×10²** A= 1.69×10¹⁶ n= -1.68 Ea= 6435	SOZ formation **k(298K)= 8.9×10²** A= 5.32×10¹⁵ n= -1.70 Ea= 5877 Intramol. insertion **k(298K)= 5.0×10²** A= 1.69×10¹⁶ n= -1.68 Ea= 6435
$R_1 = -C(R_6)(R_7)C(R_8)(R_9)-C(R_{10})(R_{11})COOH$	SOZ formation **k(298K)= 8.2×10⁴** A= 6.15×10¹⁵ n= -2.28 Ea= 3596 Intramol. insertion **k(298K)= 1.2×10³** A= 4.71×10¹³ n= -1.19 Ea= 5241	SOZ formation **k(298K)= 8.2×10⁴** A= 6.15×10¹⁵ n= -2.28 Ea= 3596 Intramol. insertion **k(298K)= 1.2×10³** A= 4.71×10¹³ n= -1.19 Ea= 5241	SOZ formation **k(298K)= 8.2×10⁴** A= 6.15×10¹⁵ n= -2.28 Ea= 3596 Intramol. insertion **k(298K)= 1.2×10³** A= 4.71×10¹³ n= -1.19 Ea= 5241	SOZ formation **k(298K)= 8.2×10⁴** A= 6.15×10¹⁵ n= -2.28 Ea= 3596 Intramol. insertion **k(298K)= 1.2×10³** A= 4.71×10¹³ n= -1.19 Ea= 5241	SOZ formation **k(298K)= 8.2×10⁴** A= 6.15×10¹⁵ n= -2.28 Ea= 3596 Intramol. insertion **k(298K)= 1.2×10³** A= 4.71×10¹³ n= -1.19 Ea= 5241	SOZ formation **k(298K)= 8.2×10⁴** A= 6.15×10¹⁵ n= -2.28 Ea= 3596 Intramol. insertion **k(298K)= 1.2×10³** A= 4.71×10¹³ n= -1.19 Ea= 5241
$R_1 = -OOOH$	Unstable Converts to peracid + ¹O₂	Unstable Converts to peracid + ¹O₂	Unstable Converts to peracid + ¹O₂	Unstable Converts to peracid + ¹O₂	Unstable Converts to peracid + ¹O₂	Unstable Converts to peracid + ¹O₂

44

Table 31: Predicted total rate coefficients for unimolecular carbonyl oxide decay as a function of the two substituents R$_1$ and R$_2$. Indicated is the mode of reaction, the rate coefficient k (s^{-1}) at 298K, and the parameters of a Kooij equation fit $k(T) = A \times (T/K)^n \times \exp(-E_a/T)$ between 200 and 450 K (A in s^{-1}, E_a in K). The meaning of the SAR substituents is explained in section S. Note that the theoretical work here does not consider systematic variations for R$_a$/R$_b$/R$_c$/R$_3$/R$_4$/R$_5$/R', and the values listed are for substituents −H (when appropriate), −CH$_3$, −C$_2$H$_5$, or an average of the prediction for these substituents. Values in green are based directly on theoretical kinetic calculations, whereas values in orange are estimated values based on the reactivity trends for other substituents. The values are standardized in number of digits, see Vereecken et al.[8] for an uncertainty analysis.

R$_1$ = (carbonyl oxide)	R$_2$= α-C=O	R$_2$= α-ONO$_2$ (a)	R$_2$= α-ONO$_2$ (b)	R$_2$= −C(R$_6$)(R$_7$)ONO$_2$	R$_2$= −OR'	R$_2$= −OH
R$_1$= −CH$_3$	1,4-H-migration **k(298K)=3.6** A= 2.22×10^{-80} n= 30.26 E$_a$= -3670	1,3-Cyclisation **k(298K)=6.8×10^4** A= 2.84×10^{12} n= 0.09 E$_a$= 5388	1,4-H-migration **k(298K)=2.3×10^3** A= 7.77×10^{-51} n= 20.63 E$_a$= -1675	1,4-H-migration **k(298K)=477** A= 1.44×10^{-58} n= 23.12 E$_a$= -2282	1,3-Cyclisation **k(298K)=4.7×10^4** A= 5.31×10^{11} n= 0.47 E$_a$= 5646	1,3-Cyclisation **k(298K)=4.6×10^4** A= 8.54×10^{11} n= 0.37 E$_a$= 5618
R$_1$= −CH$_2$R$_a$	1,4-H-migration **k(298K)=1.8** A= 2.16×10^{-82} n= 30.89 E$_a$= -3783	1,3-Cyclisation **k(298K)=2.6×10^5** A= 3.23×10^{11} n= 0.44 E$_a$= 4932	1,4-H-migration **k(298K)=1.2×10^3** A= 7.56×10^{-53} n= 21.26 E$_a$= -1788	1,4-H-migration **k(298K)=246** A= 1.40×10^{-60} n= 23.75 E$_a$= -2395	1,3-Cyclisation **k(298K)=1.8×10^5** A= 6.04×10^{10} n= 0.82 E$_a$= 5190	1,3-Cyclisation **k(298K)=1.7×10^5** A= 9.71×10^{10} n= 0.72 E$_a$= 5163
R$_1$= −CHR$_a$R$_b$	1,4-H-migration **k(298K)=7.2×10^{-2}** A= 5.61×10^{-94} n= 34.72 E$_a$= -4282	1,3-Cyclisation **k(298K)=9.6×10^5** A= 1.83×10^{14} n= -0.48 E$_a$= 4871		1,4-H-migration **k(298K)=10** A= 3.65×10^{-72} n= 27.58 E$_a$= -2893	1,3-Cyclisation **k(298K)=6.6×10^5** A= 3.41×10^{13} n= -0.10 E$_a$= 5129	1,3-Cyclisation **k(298K)=6.4×10^5** A= 5.49×10^{13} n= -0.20 E$_a$= 5101
R$_1$= −CR$_a$R$_b$R$_c$	1,3-Cyclisation **k(298K)=1.4×10^{-4}** A= 6.31×10^7 n= 1.88 E$_a$= 11194	1,3-Cyclisation **k(298K)=2.7×10^6** A= 5.47×10^{13} n= -0.26 E$_a$= 4560		1,3-Cyclisation **k(298K)=0.55** A= 7.10×10^8 n= 1.40 E$_a$= 8635	1,3-Cyclisation **k(298K)=1.9×10^6** A= 1.02×10^{13} n= 0.12 E$_a$= 4818	1,3-Cyclisation **k(298K)=1.8×10^6** A= 1.64×10^{13} n= 0.01 E$_a$= 4791
R$_1$= −H	1,3-Cyclisation **k(298K)=0.031** A= 6.61×10^5 n= 2.51 E$_a$= 9286	1,3-Cyclisation **k(298K)=2.8×10^8** A= 6.54×10^{12} n= 0.08 E$_a$= 3130		1,3-Cyclisation **k(298K)=124** A= 7.44×10^6 n= 2.03 E$_a$= 6727	1,3-Cyclisation **k(298K)=7.1×10^7** A= 2.57×10^{12} n= 0.25 E$_a$= 3559	1,3-Cyclisation **k(298K)=6.1×10^7** A= 2.06×10^{12} n= 0.25 E$_a$= 3530

	R2= −C(R6)(R7)OR'	R2 = −C(R6)(R7)OH	R2= −CCOH	R2= −Cn≥3OH	R2= −OOH	R2= −C(R6)(R7)OOH
R_1= −CH$_3$	1,4-H-migration **k(298K)=109** A= 2.26×10^{-63} n= 24.68 E_a= -2483	1,4-H-migration **k(298K)=288** A= 8.11×10^{-61} n= 23.92 E_a= -2308	1,4-H-migration **k(298K)=462** A= 3.22×10^{-60} n= 23.75 E_a= -2343	Intramol. insertion **k(298K)=1.1×10^7** A= 2.54×10^{24} n= -4.84 E_a= 3685	1,3-Cyclisation **k(298K)=4.2×10^5** A= 4.82×10^{12} n= 0.02 E_a= 4871	1,4-H-migration **k(298K)=83** A= 8.73×10^{-63} n= 24.41 E_a= -2462
R_1= −CH$_2$R$_a$	1,4-H-migration **k(298K)=56** A= 2.20×10^{-65} n= 25.31 E_a= -2595	1,4-H-migration **k(298K)=149** A= 7.90×10^{-63} n= 24.55 E_a= -2421	1,4-H-migration **k(298K)=118** A= 7.86×10^{-65} n= 25.23 E_a= -2580	Intramol. insertion **k(298K)=1.1×10^7** A= 2.54×10^{24} n= -4.84 E_a= 3685	1,3-Cyclisation **k(298K)=1.6×10^6** A= 5.48×10^{11} n= 0.37 E_a= 4415	1,4-H-migration **k(298K)=43** A= 8.50×10^{-65} n= 25.04 E_a= -2574
R_1= −CHR$_a$R$_b$	1,4-H-migration **k(298K)=2.3** A= 5.73×10^{-77} n= 29.14 E_a= -3094	1,4-H-migration **k(298K)=6.1** A= 2.0×10^{-74} n= 28.38 E_a= -2919	1,4-H-migration **k(298K)=6.5** A= 1.07×10^{-74} n= 28.46 E_a= -3006	Intramol. insertion **k(298K)=1.1×10^7** A= 2.54×10^{24} n= -4.84 E_a= 3685	1,3-Cyclisation **k(298K)=6.0×10^6** A= 3.10×10^{14} n= -0.55 E_a= 4354	1,4-H-migration **k(298K)=1.7** A= 2.21×10^{-76} n= 28.87 E_a= -3073
R_1= −CR$_a$R$_b$R$_c$	1,3-Cyclisation **k(298K)=0.23** A= 1.24×10^{9} n= 1.26 E_a= 8811	1,3-Cyclisation **k(298K)=0.56** A= 7.29×10^{11} n= 0.41 E_a= 9016	1,3-Cyclisation **k(298K)=1.7** A= 9.89×10^{7} n= 1.25 E_a= 7438	Intramol. insertion **k(298K)=1.1×10^7** A= 2.54×10^{24} n= -4.84 E_a= 3685	1,3-Cyclisation **k(298K)=1.7×10^7** A= 9.28×10^{13} n= -0.34 E_a= 4043	1,3-Cyclisation **k(298K)=0.43** A= 3.11×10^{11} n= 0.45 E_a= 8907
R_1= −H	1,3-Cyclisation **k(298K)=53** A= 1.30×10^{7} n= 1.89 E_a= 6902	1,3-Cyclisation **k(298K)=77** A= 2.53×10^{9} n= 1.18 E_a= 7158	1,3-Cyclisation **k(298K)=390** A= 1.04×10^{6} n= 1.87 E_a= 5530	Intramol. insertion **k(298K)=4.6×10^8** A= 9.03×10^{30} n= -7.01 E_a= 3387	1,3-Cyclisation **k(298K)=1.7×10^8** A= 9.34×10^{8} n= 1.21 E_a= 2564	1,3-Cyclisation **k(298K)=97** A= 3.26×10^{9} n= 1.08 E_a= 6998

	R2= −Cn≥2OOH	R2= −COOH	R2= −C(R6)(R7)COOH		R2= −Cn≥2COOH	R2= −OOOH
			(a)	(b)		
R_1= −CH$_3$	Intramol. insertion **k(298K)=5.7×10^7** A= 3.47×10^{23} n= -4.41 E_a= 3335	1,4-H-migration **k(298K)=3.6** A= 2.22×10^{-80} n= 30.26 E_a= -3670	CO$_2$ + alkene **k(298K)=2.0** A= 3.59×10^{9} n= 0.48 E_a= 7162	1,4-H-migration **k(298K)=314** A= 1.60×10^{-62} n= 24.56 E_a= -2422	Intramol. insertion **k(298K)=5.3×10^4** A= 5.47×10^{12} n= -0.91 E_a= 3958	1,3-Cyclisation **k(298K)=3.8×10^5** A= 1.10×10^{13} n= -0.10 E_a= 4947

R_1						
$R_1= -CH_2R_a$	Intramol. insertion **k(298K)=5.7×10^7** A= 3.47×10^{23} n= -4.41 E_a= 3335	1,4-H-migration **k(298K)=1.8** A= 2.16×10^{-82} n= 30.89 E_a= -3783	CO_2 + alkene **k(298K)=2.0** A= 3.59×10^9 n= 0.48 E_a= 7162	1,4-H-migration **k(298K)=162** A= 1.56×10^{-64} n= 25.19 E_a= -2535	Intramol. insertion **k(298K)=5.3×10^4** A= 5.47×10^{12} n= -0.91 E_a= 3958	1,3-Cyclisation **k(298K)=1.5×10^6** A= 1.26×10^{12} n= 0.25 E_a= 4491
$R_1= -CHR_aR_b$	Intramol. insertion **k(298K)=5.7×10^7** A= 3.47×10^{23} n= -4.41 E_a= 3335	1,4-H-migration **k(298K)=7.2×10^{-2}** A= 5.61×10^{-94} n= 34.72 E_a= -4282	CO_2 + alkene **k(298K)=2.0** A= 3.59×10^9 n= 0.48 E_a= 7162	1,4-H-migration **k(298K)=6.6** A= 4.05×10^{-76} n= 29.02 E_a= -3033	Intramol. insertion **k(298K)=5.3×10^4** A= 5.47×10^{12} n= -0.91 E_a= 3958	1,3-Cyclisation **k(298K)=5.4×10^6** A= 7.10×10^{14} n= -0.67 E_a= 4430
$R_1= -CR_aR_bR_c$	Intramol. insertion **k(298K)=5.7×10^7** A= 3.47×10^{23} n= -4.41 E_a= 3335	1,3-Cyclisation **k(298K)=1.4×10^{-4}** A= 6.31×10^7 n= 1.88 E_a= 11194	CO_2 + alkene **k(298K)=2.0** A= 3.59×10^9 n= 0.48 E_a= 7162	1,3-Cyclisation **k(298K)=0.18** A= 1.25×10^9 n= 1.35 E_a= 9031	Intramol. insertion **k(298K)=5.3×10^4** A= 5.47×10^{12} n= -0.91 E_a= 3958	1,3-Cyclisation **k(298K)=1.5×10^7** A= 2.13×10^{14} n= -0.46 E_a= 4119
$R_1= -H$	Intramol. insertion **k(298K)=5.7×10^7** A= 3.47×10^{23} n= -4.41 E_a= 3335	1,3-Cyclisation **k(298K)=0.031** A= 6.61×10^5 n= 2.51 E_a= 9286	CO_2 + alkene **k(298K)=21** A= 6.40×10^{12} n= -0.53 E_a= 6970	1,3-Cyclisation **k(298K)=42** A= 1.31×10^7 n= 1.97 E_a= 7123	Intramol. insertion **k(298K)=5.3×10^4** A= 5.47×10^{12} n= -0.91 E_a= 3958	1,3-Cyclisation **k(298K)=2.7×10^8** A= 6.07×10^{11} n= 0.32 E_a= 2842

U. Structure-Activity Relationships (SARs) for SCI + H₂O reactions

Structure of the SAR tables as a function of the R₁ and R₂ substituents
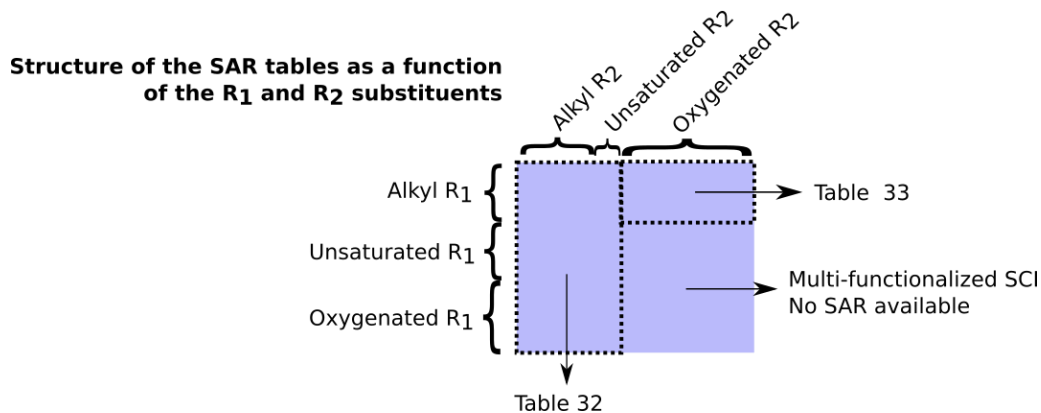
Table 32: Predicted total rate coefficients for the reaction of carbonyl oxide with H₂O monomers as a function of the two substituents R₁ and R₂, based on fitting theory-derived reaction trends to a set of literature data. The rate coefficient k (cm³ molecule⁻¹ s⁻¹) is given at 298 K, and the parameters of a Kooij equation fit $k(T) = A \times (T/K)^n \times \exp(-E_a/T)$ between 200 and 450 K (A in cm³ molecule⁻¹ s⁻¹, E_a in K). The definition of $R_a/R_b/R_c/R_3/R_4/R_5/R'$ is given in Table 29. Values in green are based directly on experimental and/or theoretical kinetic calculations, values in orange are values estimated by applying (averaged) reaction trends for other substituents.

	$R_2 = -CH_3$	$R_2 = -CH_2R_a$	$R_2 = -CHR_aR_b$	$R_2 = -CR_aR_bR_c$	$R_2 = -H$	$R_2 = $ vinyl
$R_1 = -CH_3$	k=7.5×10⁻¹⁸ A= 3.87×10⁻²⁰ n= 1.91 Ea= 1677	k=9.1×10⁻¹⁸ A= 1.41×10⁻²⁰ n= 2.03 Ea= 1524	k=4.3×10⁻¹⁸ A= 2.06×10⁻¹⁹ n= 1.60 Ea= 1813	k=1.5×10⁻¹⁷ A= 1.64×10⁻¹⁹ n= 1.64 Ea= 1441	k=6.7×10⁻¹⁹ A= 2.19×10⁻¹⁹ n= 1.68 Ea= 2513	k=8.1×10⁻²⁰ A= 7.07×10⁻¹⁹ n= 1.46 Ea= 3132
$R_1 = -CH_2R_a$	k=1.5×10⁻¹⁷ A= 4.19×10⁻²⁰ n= 1.78 Ea= 1265	k=1.8×10⁻¹⁷ A= 3.24×10⁻²⁰ n= 1.74 Ea= 1057	k=3.3×10⁻¹⁸ A= 8.90×10⁻²⁰ n= 1.59 Ea= 1631	k=2.9×10⁻¹⁷ A= 1.78×10⁻¹⁹ n= 1.50 Ea= 1029	k=1.5×10⁻¹⁸ A= 1.23×10⁻¹⁸ n= 1.39 Ea= 2300	k=1.9×10⁻¹⁹ A= 3.33×10⁻¹⁷ n= 0.82 Ea= 2932
$R_1 = -CHR_aR_b$	k=9.8×10⁻¹⁸ A= 1.39×10⁻²⁰ n= 1.74 Ea= 998	k=2.0×10⁻¹⁷ A= 1.21×10⁻¹⁸ n= 1.08 Ea= 1000	k=1.0×10⁻¹⁷ A= 1.61×10⁻²⁰ n= 1.63 Ea= 842	k=1.9×10⁻¹⁷ A= 5.89×10⁻²⁰ n= 1.46 Ea= 762	k=9.2×10⁻¹⁸ A= 5.76×10⁻¹⁸ n= 1.11 Ea= 1740	k=1.1×10⁻¹⁸ A= 6.69×10⁻²⁰ n= 1.52 Ea= 1734

R1	Col 1	Col 2	Col 3	Col 4	Col 5	Col 6
$R_1 = -CR_aR_bR_c$	$k=1.0\times10^{-17}$ $A=1.38\times10^{-20}$ $n=1.89$ $E_a=1234$	$k=8.2\times10^{-17}$ $A=6.04\times10^{-20}$ $n=1.58$ $E_a=1215$	$k=8.3\times10^{-18}$ $A=9.18\times10^{-20}$ $n=1.59$ $E_a=1358$	$k=5.2\times10^{-17}$ $A=5.40\times10^{-19}$ $n=1.33$ $E_a=902$	$k=1.0\times10^{-18}$ $A=2.40\times10^{-19}$ $n=1.57$ $E_a=2241$	$k=1.3\times10^{-19}$ $A=1.05\times10^{-19}$ $n=1.59$ $E_a=2622$
$R_1 = -H$	$k=2.3\times10^{-14}$ $A=4.32\times10^{-18}$ $n=1.27$ $E_a=-405$	$k=1.6\times10^{-14}$ $A=9.64\times10^{-18}$ $n=0.92$ $E_a=-652$	$k=3.5\times10^{-14}$ $A=6.69\times10^{-18}$ $n=1.16$ $E_a=-581$	$k=4.5\times10^{-14}$ $A=1.83\times10^{-17}$ $n=0.99$ $E_a=-641$	$k=8.7\times10^{-16}$ $A=8.13\times10^{-18}$ $n=1.23$ $E_a=698$	$k=1.4\times10^{-16}$ $A=2.93\times10^{-19}$ $n=1.66$ $E_a=973$
$R_1 = -CH_2-CR_3=CR_4R_5$	$k=7.8\times10^{-18}$ $A=3.44\times10^{-22}$ $n=2.50$ $E_a=1246$	$k=9.2\times10^{-18}$ $A=5.34\times10^{-21}$ $n=2.07$ $E_a=1287$	$k=5.4\times10^{-18}$ $A=1.85\times10^{-24}$ $n=3.14$ $E_a=890$	$k=1.5\times10^{-17}$ $A=2.92\times10^{-20}$ $n=1.83$ $E_a=1259$	$k=1.4\times10^{-18}$ $A=5.03\times10^{-20}$ $n=1.84$ $E_a=2120$	$k=1.9\times10^{-19}$ $A=2.20\times10^{-20}$ $n=1.85$ $E_a=2500$
$R_1 = -CHR_a-CR_3=CR_4R_5$	$k=4.9\times10^{-18}$ $A=2.29\times10^{-21}$ $n=2.07$ $E_a=1228$	$k=1.0\times10^{-17}$ $A=1.99\times10^{-19}$ $n=1.41$ $E_a=1230$	$k=1.7\times10^{-17}$ $A=3.33\times10^{-25}$ $n=3.17$ $E_a=101$	$k=9.5\times10^{-18}$ $A=9.69\times10^{-21}$ $n=1.79$ $E_a=992$	$k=4.8\times10^{-18}$ $A=1.55\times10^{-20}$ $n=1.88$ $E_a=1484$	$k=1.2\times10^{-18}$ $A=1.67\times10^{-21}$ $n=2.15$ $E_a=1687$
$R_1 = -CR_aR_b-CR_3=CR_4R_5$	$k=5.2\times10^{-18}$ $A=2.27\times10^{-21}$ $n=2.22$ $E_a=1464$	$k=4.1\times10^{-18}$ $A=9.94\times10^{-21}$ $n=1.91$ $E_a=1445$	$k=1.4\times10^{-17}$ $A=1.91\times10^{-24}$ $n=3.14$ $E_a=617$	$k=2.6\times10^{-17}$ $A=8.89\times10^{-20}$ $n=1.66$ $E_a=1132$	$k=1.4\times10^{-18}$ $A=7.07\times10^{-19}$ $n=1.39$ $E_a=2150$	$k=1.3\times10^{-19}$ $A=6.94\times10^{-23}$ $n=2.62$ $E_a=2189$
$R_1 = -CR_3=CR_4CH_3$	$k=3.9\times10^{-18}$ $A=2.65\times10^{-22}$ $n=2.34$ $E_a=1117$	$k=4.8\times10^{-18}$ $A=2.05\times10^{-22}$ $n=2.30$ $E_a=909$	$k=4.0\times10^{-18}$ $A=3.06\times10^{-22}$ $n=2.23$ $E_a=961$	$k=7.7\times10^{-18}$ $A=1.12\times10^{-21}$ $n=2.07$ $E_a=881$	$k=4.9\times10^{-21}$ $A=1.06\times10^{-18}$ $n=1.44$ $E_a=4044$	$k=6.5\times10^{-22}$ $A=4.65\times10^{-19}$ $n=1.45$ $E_a=4424$
$R_1 = -CR_3=CR_4CH_2R_a$	$k=3.9\times10^{-18}$ $A=2.65\times10^{-22}$ $n=2.34$ $E_a=1117$	$k=4.8\times10^{-18}$ $A=2.05\times10^{-22}$ $n=2.30$ $E_a=909$	$k=4.0\times10^{-18}$ $A=3.06\times10^{-22}$ $n=2.23$ $E_a=961$	$k=7.7\times10^{-18}$ $A=1.12\times10^{-21}$ $n=2.07$ $E_a=881$	$k=4.9\times10^{-21}$ $A=1.06\times10^{-18}$ $n=1.44$ $E_a=4044$	$k=6.5\times10^{-22}$ $A=4.65\times10^{-19}$ $n=1.45$ $E_a=4424$
$R_1 = -CR_3=CR_4CHR_aR_b$	$k=3.9\times10^{-18}$ $A=2.65\times10^{-22}$ $n=2.34$ $E_a=1117$	$k=4.8\times10^{-18}$ $A=2.05\times10^{-22}$ $n=2.30$ $E_a=909$	$k=4.0\times10^{-18}$ $A=3.06\times10^{-22}$ $n=2.23$ $E_a=961$	$k=7.7\times10^{-18}$ $A=1.12\times10^{-21}$ $n=2.07$ $E_a=881$	$k=4.9\times10^{-21}$ $A=1.06\times10^{-18}$ $n=1.44$ $E_a=4044$	$k=6.5\times10^{-22}$ $A=4.65\times10^{-19}$ $n=1.45$ $E_a=4424$
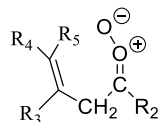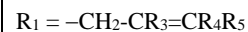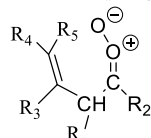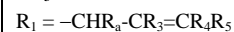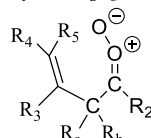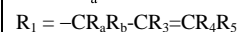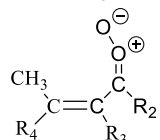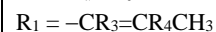
R_1	Col 1	Col 2	Col 3	Col 4	Col 5	Col 6
$R_1 = -CR_3=CR_4R'$	k=1.8×10^{-18} A= 2.21×10^{-21} n= 2.27 E_a= 1858	k=2.4×10^{-18} A= 1.12×10^{-23} n= 2.99 E_a= 1423	k=1.8×10^{-18} A= 2.55×10^{-21} n= 2.16 E_a= 1702	k=3.5×10^{-18} A= 9.36×10^{-21} n= 1.99 E_a= 1622	k=1.4×10^{-19} A= 3.20×10^{-20} n= 1.92 E_a= 2819	k=1.9×10^{-20} A= 1.40×10^{-20} n= 1.93 E_a= 3200
$R_1 = -CH=O$	k=1.4×10^{-14} A= 7.81×10^{-20} n= 1.68 E_a= -757	k=1.7×10^{-14} A= 6.04×10^{-20} n= 1.64 E_a= -966	k=1.4×10^{-14} A= 9.03×10^{-20} n= 1.57 E_a= -913	k=2.8×10^{-14} A= 3.31×10^{-19} n= 1.41 E_a= -993	k=7.7×10^{-16} A= 3.04×10^{-19} n= 1.59 E_a= 370	k=1.0×10^{-16} A= 1.33×10^{-19} n= 1.61 E_a= 750
$R_1 = -C(=O)R_a$	k=5.5×10^{-14} A= 2.18×10^{-19} n= 1.43 E_a= -1268	k=6.7×10^{-14} A= 1.68×10^{-19} n= 1.39 E_a= -1477	k=5.6×10^{-14} A= 2.52×10^{-19} n= 1.32 E_a= -1425	k=1.1×10^{-13} A= 9.23×10^{-19} n= 1.16 E_a= -1504	k=3.0×10^{-15} A= 8.48×10^{-19} n= 1.35 E_a= -141	k=3.9×10^{-16} A= 3.71×10^{-19} n= 1.36 E_a= 239
$R_1 = -C(=O)OR'$	k=1.7×10^{-15} A= 5.44×10^{-20} n= 1.58 E_a= -406	k=2.1×10^{-15} A= 4.21×10^{-20} n= 1.54 E_a= -615	k=1.8×10^{-15} A= 6.29×10^{-20} n= 1.47 E_a= -562	k=3.4×10^{-15} A= 2.30×10^{-19} n= 1.31 E_a= -642	k=1.7×10^{-15} A= 5.44×10^{-20} n= 1.58 E_a= -406	k=1.2×10^{-17} A= 9.27×10^{-20} n= 1.51 E_a= 1101
$R_1 = -C(R_6)(R_7)ONO_2$	k=3.4×10^{-18} A= 1.40×10^{-21} n= 2.46 E_a= 1848	k=4.2×10^{-18} A= 1.08×10^{-21} n= 2.42 E_a= 1640	k=3.5×10^{-18} A= 1.62×10^{-21} n= 2.34 E_a= 1692	k=6.7×10^{-18} A= 5.93×10^{-21} n= 2.18 E_a= 1612	k=2.8×10^{-19} A= 7.08×10^{-32} n= 5.90 E_a= 1372	k=2.8×10^{-20} A= 1.56×10^{-21} n= 2.43 E_a= 3264
$R_1 = -OR'$	k=2.4×10^{-15} A= 1.45×10^{-19} n= 1.43 E_a= -471	k=3.0×10^{-15} A= 1.12×10^{-19} n= 1.39 E_a= -679	k=2.5×10^{-15} A= 1.67×10^{-19} n= 1.32 E_a= -627	k=4.8×10^{-15} A= 6.14×10^{-19} n= 1.16 E_a= -707	k=4.3×10^{-16} A= 3.13×10^{-19} n= 1.43 E_a= 272	k=5.6×10^{-17} A= 1.37×10^{-19} n= 1.44 E_a= 652
$R_1 = -OH$	Unstable	Unstable	Unstable	Unstable	Unstable	Unstable
$R_1 = -C(R_6)(R_7)OR'$	k=1.2×10^{-17} A= 2.72×10^{-18} n= 1.35 E_a= 1852	k=1.4×10^{-17} A= 2.10×10^{-18} n= 1.31 E_a= 1644	k=1.2×10^{-17} A= 3.14×10^{-18} n= 1.23 E_a= 1696	k=2.3×10^{-17} A= 1.15×10^{-17} n= 1.07 E_a= 1616	k=9.5×10^{-19} A= 1.38×10^{-28} n= 4.79 E_a= 1376	k=9.5×10^{-20} A= 3.03×10^{-18} n= 1.32 E_a= 3269
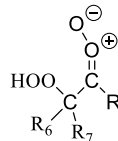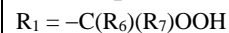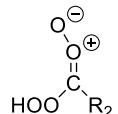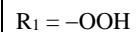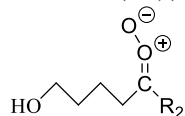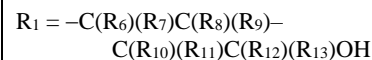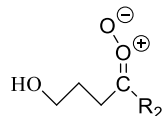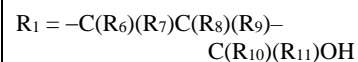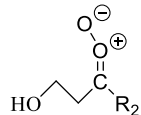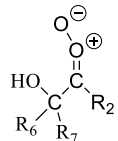
$R_1 = -C(R_6)(R_7)OH$					
Addition **k=1.4×10⁻¹⁷** A= 1.36×10⁻²¹ n= 2.22 Ea= 1016	Addition **k=1.7×10⁻¹⁷** A= 1.05×10⁻²¹ n= 2.18 Ea= 808	Addition **k=1.5×10⁻¹⁷** A= 1.57×10⁻²¹ n= 2.11 Ea= 860	Addition **k=2.8×10⁻¹⁷** A= 5.74×10⁻²¹ n= 1.95 Ea= 780	Addition **k=7.8×10⁻¹⁸** A= 1.03×10⁻¹⁸ n= 1.30 Ea= 1610	Addition **k=1.0×10⁻¹⁸** A= 4.52×10⁻¹⁹ n= 1.32 Ea= 1990
Ringcl. Catal. **k=3.6×10⁻¹⁷** A= 1.52×10⁻⁴⁸ n= 11.21 Ea= -2500	Ringcl. Catal. **k=4.5×10⁻¹⁷** A= 1.18×10⁻⁴⁸ n= 11.17 Ea= -2709	Ringcl. Catal. **k=3.7×10⁻¹⁷** A= 1.76×10⁻⁴⁸ n= 11.09 Ea= -2656	Ringcl. Catal. **k=7.1×10⁻¹⁷** A= 6.46×10⁻⁴⁸ n= 10.93 Ea= -2736	Ringcl. Catal. **k=2.1×10⁻¹⁷** A= 8.35×10⁻³³ n= 5.91 Ea= -535	Ringcl. Catal. **k=2.8×10⁻¹⁸** A= 3.65×10⁻³³ n= 5.92 Ea= -155

$R_1 = -C(R_6)(R_7)C(R_8)(R_9)OH$					
Addition **k=5.3×10⁻¹⁶** A= 1.77×10⁻¹⁵ n= -0.44 Ea= -387	Addition **k=4.2×10⁻¹⁶** A= 7.77×10⁻¹⁵ n= -0.75 Ea= -406	Addition **k=4.2×10⁻¹⁶** A= 1.18×10⁻¹⁴ n= -0.74 Ea= -263	Addition **k=2.7×10⁻¹⁵** A= 6.95×10⁻¹⁴ n= -1.00 Ea= -719	Addition **k=5.1×10⁻¹⁷** A= 3.08×10⁻¹⁴ n= -0.76 Ea= 620	Addition **k=6.8×10⁻¹⁸** A= 1.35×10⁻¹⁴ n= -0.74 Ea= 1000
Ringcl. Catal. **k=5.6×10⁻¹⁶** A= 2.99×10⁻¹⁵ n= -0.38 Ea= -151	Ringcl. Catal. **k=4.4×10⁻¹⁶** A= 1.31×10⁻¹⁴ n= -0.70 Ea= -170	Ringcl. Catal. **k=4.5×10⁻¹⁶** A= 1.99×10⁻¹⁴ n= -0.68 Ea= -27	Ringcl. Catal. **k=2.8×10⁻¹⁵** A= 1.17×10⁻¹³ n= -0.94 Ea= -483	Ringcl. Catal. **k=5.4×10⁻¹⁷** A= 5.20×10⁻¹⁴ n= -0.70 Ea= 856	Ringcl. Catal. **k=7.1×10⁻¹⁸** A= 2.28×10⁻¹⁴ n= -0.69 Ea= 1236

$R_1 = -C(R_6)(R_7)C(R_8)(R_9)-C(R_{10})(R_{11})OH$					
Ringcl. Catal. **(k ~ 5×10⁻¹¹)**	Ringcl. Catal. **(k ~ 5×10⁻¹¹)**	Ringcl. Catal. **(k ~ 5×10⁻¹¹)**	Ringcl. Catal. **(k ~ 5×10⁻¹¹)**	Ringcl. Catal. **(k ~ 5×10⁻¹¹)**	Ringcl. Catal. **(k ~ 5×10⁻¹¹)**

$R_1 = -C(R_6)(R_7)C(R_8)(R_9)-C(R_{10})(R_{11})C(R_{12})(R_{13})OH$					
Ringcl. Catal. **(k ~ 5×10⁻¹¹)**	Ringcl. Catal. **(k ~ 5×10⁻¹¹)**	Ringcl. Catal. **(k ~ 5×10⁻¹¹)**	Ringcl. Catal. **(k ~ 5×10⁻¹¹)**	Ringcl. Catal. **(k ~ 5×10⁻¹¹)**	Ringcl. Catal. **(k ~ 5×10⁻¹¹)**

$R_1 = -OOH$					
No data	No data	No data	No data	No data	No data

$R_1 = -C(R_6)(R_7)OOH$					
Ringcl. Catal. **k=1.7×10⁻¹⁴** A= 7.63×10⁻²⁵ n= 3.08 Ea= -1865	Ringcl. Catal. **k=2.1×10⁻¹⁴** A= 5.90×10⁻²⁵ n= 3.04 Ea= -2073	Ringcl. Catal. **k=1.7×10⁻¹⁴** A= 8.82×10⁻²⁵ n= 2.97 Ea= -2021	Ringcl. Catal. **k=3.3×10⁻¹⁴** A= 3.23×10⁻²⁴ n= 2.81 Ea= -2101	Ringcl. Catal. **k=1.4×10⁻¹⁵** A= 1.50×10⁻¹⁷ n= 0.59 Ea= -352	Ringcl. Catal. **k=1.8×10⁻¹⁶** A= 6.55×10⁻¹⁸ n= 0.60 Ea= 28
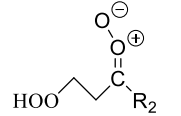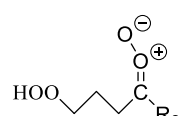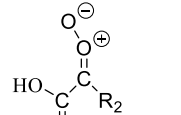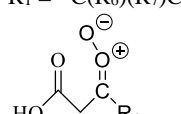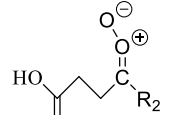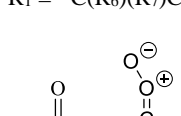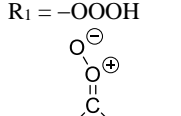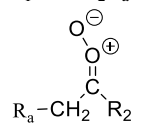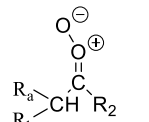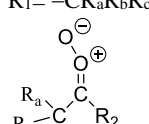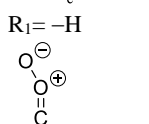
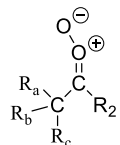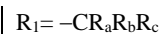| R_1 structure						
$R_1 = -C(R_6)(R_7)C(R_8)(R_9)OOH$	Ringcl. Catal. (k ~ 5×10^{-11})	Ringcl. Catal. (k ~ 5×10^{-11})	Ringcl. Catal. (k ~ 5×10^{-11})	Ringcl. Catal. (k ~ 5×10^{-11})	Ringcl. Catal. (k ~ 5×10^{-11})	Ringcl. Catal. (k ~ 5×10^{-11})
$R_1 = -C(R_6)(R_7)C(R_8)(R_9)-C(R_{10})(R_{11})OOH$	Ringcl. Catal. (k ~ 5×10^{-11})	Ringcl. Catal. (k ~ 5×10^{-11})	Ringcl. Catal. (k ~ 5×10^{-11})	Ringcl. Catal. (k ~ 5×10^{-11})	Ringcl. Catal. k=3.6×10^{-12} A= 3.11×10^{-9} n= -2.12 E_a= -1582	Ringcl. Catal. k=4.8×10^{-13} A= 1.36×10^{-9} n= -2.10 E_a= -1202
$R_1 = -COOH$	Ringcl. Catal. k=2.8×10^{-13} A= 5.74×10^{-34} n= 6.54 E_a= -3086	Ringcl. Catal. k=2.2×10^{-13} A= 2.51×10^{-33} n= 6.23 E_a= -3105	Ringcl. Catal. k=2.2×10^{-13} A= 3.83×10^{-33} n= 6.24 E_a= -2961	Ringcl. Catal. k=1.4×10^{-12} A= 2.25×10^{-32} n= 5.99 E_a= -3418	Ringcl. Catal. k=2.7×10^{-14} A= 9.99×10^{-33} n= 6.22 E_a= -2078	Ringcl. Catal. k=3.6×10^{-15} A= 4.37×10^{-33} n= 6.24 E_a= -1698
$R_1 = -C(R_6)(R_7)COOH$	CO_2+alkene Catal. k=3.0×10^{-13} A= 4.64×10^{-33} n= 6.18 E_a= -3094	CO_2+alkene Catal. k=2.4×10^{-13} A= 2.03×10^{-32} n= 5.87 E_a= -3114	CO_2+alkene Catal. k=2.4×10^{-13} A= 3.09×10^{-32} n= 5.88 E_a= -2970	CO_2+alkene Catal. k=1.5×10^{-12} A= 1.82×10^{-31} n= 5.63 E_a= -3426	CO_2+alkene Catal. k=2.9×10^{-14} A= 8.08×10^{-32} n= 5.86 E_a= -2087	CO_2+alkene Catal. k=3.8×10^{-15} A= 3.53×10^{-32} n= 5.88 E_a= -1707
$R_1 = -C(R_6)(R_7)C(R_8)(R_9)COOH$	Ringcl. Catal. k=4.8×10^{-13} A= 4.59×10^{-21} n= 1.61 E_a= -2764	Ringcl. Catal. k=3.8×10^{-13} A= 2.01×10^{-20} n= 1.30 E_a= -2783	Ringcl. Catal. k=3.8×10^{-13} A= 3.06×10^{-20} n= 1.31 E_a= -2639	Ringcl. Catal. k=2.4×10^{-12} A= 1.80×10^{-19} n= 1.06 E_a= -3096	Ringcl. Catal. k=4.6×10^{-14} A= 7.98×10^{-20} n= 1.29 E_a= -1756	Ringcl. Catal. k=6.1×10^{-15} A= 3.49×10^{-20} n= 1.31 E_a= -1376
$R_1 = -C(R_6)(R_7)C(R_8)(R_9)-C(R_{10})(R_{11})COOH$	Ringcl. Catal. k=6.2×10^{-12} A= 5.54×10^{-19} n= 0.42 E_a= -4129	Ringcl. Catal. k=4.9×10^{-12} A= 2.43×10^{-18} n= 0.10 E_a= -4148	Ringcl. Catal. k=5.0×10^{-12} A= 3.69×10^{-18} n= 0.12 E_a= -4005	Ringcl. Catal. k=3.1×10^{-11} A= 2.17×10^{-17} n= -0.14 E_a= -4461	Ringcl. Catal. k=6.0×10^{-13} A= 9.63×10^{-18} n= 0.10 E_a= -3122	Ringcl. Catal. k=8.0×10^{-14} A= 4.22×10^{-18} n= 0.11 E_a= -2742
$R_1 = -OOOH$	No data	No data	No data	No data	No data	No data

Table 33: Predicted total rate coefficients for the reaction of carbonyl oxide with H_2O monomers as a function of the two substituents R_1 and R_2, based on fitting theory-derived reaction trends to a set of literature data. The rate coefficient k (cm^3 molecule^{-1} s^{-1}) is given at 298 K, and the parameters of a Kooij equation fit $k(T) = A \times (T/K)^n \times \exp(-E_a/T)$ between 200 and 450 K (A in cm^3 molecule^{-1} s^{-1}, E_a in K). The definition of $R_a/R_b/R_c/R_3/R_4/R_5/R'$ is given in Table 29. Values in green are based directly on experimental and/or theoretical kinetic calculations, values in orange are values estimated by applying (averaged) reaction trends for other substituents.

	$R_2=$ α-C=O	$R_2=$ α-ONO$_2$	$R_2=$ −C(R$_6$)(R$_7$)ONO$_2$	$R_2=$ −OR'	$R_2=$ −OH	$R_2=$ −C(R$_6$)(R$_7$)OR'
$R_1=$ −CH$_3$	k=7.8×10^{-21} A= 3.90×10^{-20} n= 1.97 E$_a$= 3825	No data	k=7.3×10^{-18} A= 3.64×10^{-21} n= 2.21 E$_a$= 1478	k=3.7×10^{-15} A= 6.80×10^{-22} n= 2.42 E$_a$= -512	No data	k=9.2×10^{-18} A= 2.12×10^{-19} n= 1.56 E$_a$= 1533
$R_1=$ −CH$_2$R$_a$	k=1.2×10^{-20} A= 5.37×10^{-20} n= 1.83 E$_a$= 3556	No data	k=1.1 ×10^{-17} A= 5.02×10^{-21} n= 2.06 E$_a$= 1209	k=5.6×10^{-15} A= 9.36×10^{-22} n= 2.28 E$_a$= -781	No data	k=1.4×10^{-17} A= 2.92×10^{-19} n= 1.42 E$_a$= 1264
$R_1=$ −CHR$_a$R$_b$	k=1.3×10^{-20} A= 2.16×10^{-19} n= 1.41 E$_a$= 3223	No data	k=1.2×10^{-17} A= 2.02×10^{-20} n= 1.64 E$_a$= 876	k=6.3×10^{-15} A= 3.77×10^{-21} n= 1.86 E$_a$= -1114	No data	k=1.6×10^{-17} A= 1.18×10^{-18} n= 1.00 E$_a$= 931
$R_1=$ −CR$_a$R$_b$R$_c$	k=1.2×10^{-20} A= 4.27×10^{-20} n= 1.87 E$_a$= 3553	No data	k=1.1×10^{-17} A= 3.98×10^{-21} n= 2.10 E$_a$= 1206	k=5.6×10^{-15} A= 7.43×10^{-22} n= 2.32 E$_a$= -784	No data	k=1.4×10^{-17} A= 2.32×10^{-19} n= 1.46 E$_a$= 1261
$R_1=$ −H	k=5.0×10^{-18} A= 1.59×10^{-18} n= 1.53 E$_a$= 2258	No data	k=2.0×10^{-14} A= 3.57×10^{-19} n= 1.54 E$_a$= -639	k=3.0×10^{-12} A= 2.01×10^{-19} n= 1.68 E$_a$= -2078	No data	k=2.5×10^{-14} A= 2.08×10^{-17} n= 0.90 E$_a$= -584

(structure: R$_1$, R$_2$ carbonyl oxide)	R$_2$ = −C(R$_6$)(R$_7$)OH	R$_2$= −CCOH	R$_2$= −C$_{n\geq3}$OH	R$_2$= −OOH	R$_2$= −C(R$_6$)(R$_7$)OOH (a)	(b)
R$_1$= −CH$_3$	Addition **k=6.6×10^{-17}** A= 3.74×10^{-19} n= 1.45 E$_a$= 914	Addition **k=2.3×10^{-16}** A= 4.55×10^{-31} n= 5.12 E$_a$= -1396	Ringcl. Catal. (k ~ 5×10^{-11})	No data	Addition **k=1.2×10^{-16}** A= 2.43×10^{-41} n= 8.53 E$_a$= -2460	Ringcl. Catal. **k=2.1×10^{-16}** A= 8.77×10^{-27} n= 3.33 E$_a$= -1475
R$_1$= −CH$_2$R$_a$	Addition **k=9.8×10^{-17}** A= 5.14×10^{-19} n= 1.30 E$_a$= 645	Addition **k=5.5×10^{-16}** A= 2.86×10^{-30} n= 4.66 E$_a$= -1895	Ringcl. Catal. (k ~ 5×10^{-11})	No data	Addition **k=1.8×10^{-16}** A= 3.34×10^{-41} n= 8.39 E$_a$= -2729	Ringcl. Catal. **k=3.2×10^{-16}** A= 1.21×10^{-26} n= 3.18 E$_a$= -1744
R$_1$= −CHR$_a$R$_b$	Addition **k=1.1×10^{-16}** A= 2.07×10^{-18} n= 0.88 E$_a$= 313	Addition **k=1.1×10^{-15}** A= 2.93×10^{-30} n= 4.63 E$_a$= -2147	Ringcl. Catal. (k ~ 5×10^{-11})	No data	Addition **k=2.1×10^{-16}** A= 1.35×10^{-40} n= 7.97 E$_a$= -3061	Ringcl. Catal. **k=3.6×10^{-16}** A= 4.87×10^{-26} n= 2.76 E$_a$= -2077
R$_1$= −CR$_a$R$_b$R$_c$	Addition **k=9.9×10^{-17}** A= 4.08×10^{-19} n= 1.34 E$_a$= 643	Addition **k=7.4×10^{-16}** A= 1.31×10^{-30} n= 4.80 E$_a$= -1969	Ringcl. Catal. (k ~ 5×10^{-11})	No data	Addition **k=1.8×10^{-16}** A= 2.65×10^{-41} n= 8.43 E$_a$= -2731	Ringcl. Catal. **k=3.2×10^{-16}** A= 9.59×10^{-27} n= 3.22 E$_a$= -1746
R$_1$= −H	Addition **k=1.1×10^{-13}** A= 2.19×10^{-19} n= 1.49 E$_a$= -1387	Addition **k=6.4×10^{-13}** A= 4.45×10^{-29} n= 4.46 E$_a$= -3513	Ringcl. Catal. (k ~ 5×10^{-11})	No data	Addition **k=4.3×10^{-13}** A= 1.32×10^{-26} n= 3.88 E$_a$= -2693	Ringcl. Catal. **k=9.3×10^{-15}** A= 1.70×10^{-15} n= -0.45 E$_a$= -1273

(structure: R$_1$, R$_2$ carbonyl oxide)	R$_2$= −C$_{n\geq2}$OOH	R$_2$= −COOH	R$_2$= −C(R$_6$)(R$_7$)COOH	−C$_{n\geq2}$COOH	R$_2$= −OOOH
R$_1$= −CH$_3$	Ringcl. Catal. (k ~ 5×10^{-11})	No data	CO$_2$+alkene Catal. **k=3.6×10^{-16}** A= 1.37×10^{-26} n= 3.66 E$_a$= -938	Ringcl. Catal. (k ~ 5×10^{-11})	No data

$R_1 = -CH_2R_a$	Ringcl. Catal. $(k \sim 5\times10^{-11})$	No data	CO$_2$+alkene Catal. $k=8.6\times10^{-16}$ $A= 8.58\times10^{-26}$ $n= 3.20$ $E_a= -1437$	Ringcl. Catal. $(k \sim 5\times10^{-11})$	No data
$R_1 = -CHR_aR_b$	Ringcl. Catal. $(k \sim 5\times10^{-11})$	No data	CO$_2$+alkene Catal. $k=1.8\times10^{-15}$ $A= 8.80\times10^{-26}$ $n= 3.17$ $E_a= -1689$	Ringcl. Catal. $(k \sim 5\times10^{-11})$	No data
$R_1 = -CR_aR_bR_c$	Ringcl. Catal. $(k \sim 5\times10^{-11})$	No data	CO$_2$+alkene Catal. $k=1.2\times10^{-15}$ $A= 3.94\times10^{-26}$ $n= 3.34$ $E_a= -1511$	Ringcl. Catal. $(k \sim 5\times10^{-11})$	No data
$R_1 = -H$	Ringcl. Catal. $(k \sim 5\times10^{-11})$	No data	CO$_2$+alkene Catal. $k=1.0\times10^{-12}$ $A= 1.34\times10^{-24}$ $n= 3.00$ $E_a= -3055$	Ringcl. Catal. $(k \sim 5\times10^{-11})$	No data

V. Structure-Activity Relationships (SARs) for SCI + (H₂O)₂ reactions

Structure of the SAR tables as a function of the R_1 and R_2 substituents
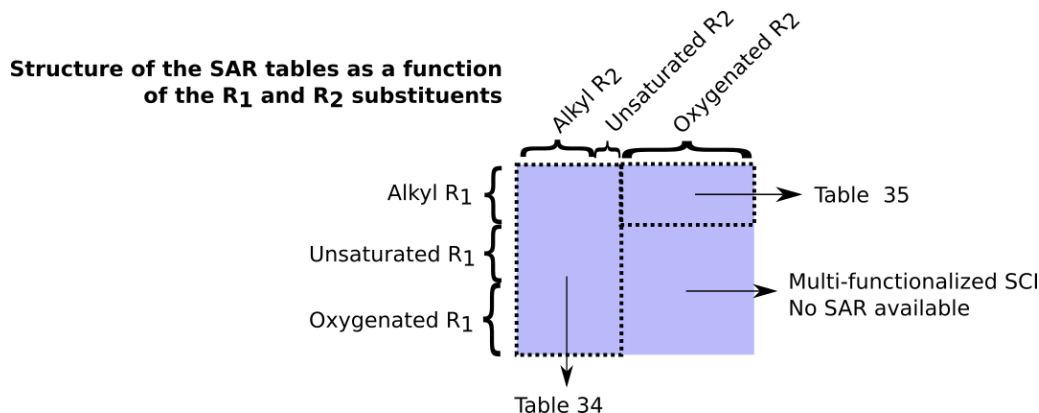
Table 34: Predicted total rate coefficients for the reaction of carbonyl oxide with (H₂O)₂ as a function of the two substituents R_1 and R_2, based on fitting theory-derived reaction trends to a set of literature data. The rate coefficient k (cm³ molecule⁻¹ s⁻¹) is given at 298K, and the parameters of a Kooij equation fit $k(T) = A \times (T/K)^n \times \exp(-E_a/T)$ between 200 and 450 K (A in cm³ molecule⁻¹ s⁻¹, E_a in K). The definition of $R_a/R_b/R_c/R_3/R_4/R_5/R'$ is given in Table 29. Values in green are based directly on experimental and/or theoretical kinetic calculations, values in orange are values estimated by applying (averaged) reaction trends for other substituents.

	$R_2 = -CH_3$	$R_2 = -CH_2R_a$	$R_2 = -CHR_aR_b$	$R_2 = -CR_aR_bR_c$	$R_2 = -H$	$R_2 = $ vinyl
$R_1 = -CH_3$	$k=1.8 \times 10^{-14}$ $A=3.90 \times 10^{-20}$ $n=1.91$ $E_a=-643$	$k=2.1 \times 10^{-14}$ $A=1.41 \times 10^{-20}$ $n=2.03$ $E_a=-786$	$k=1.1 \times 10^{-14}$ $A=2.05 \times 10^{-19}$ $n=1.60$ $E_a=-512$	$k=3.2 \times 10^{-14}$ $A=1.70 \times 10^{-19}$ $n=1.63$ $E_a=-849$	$k=2.1 \times 10^{-15}$ $A=2.27 \times 10^{-19}$ $n=1.67$ $E_a=121$	$k=3.1 \times 10^{-16}$ $A=7.63 \times 10^{-19}$ $n=1.45$ $E_a=675$
$R_1 = -CH_2R_a$	$k=3.2 \times 10^{-14}$ $A=4.27 \times 10^{-20}$ $n=1.77$ $E_a=-1022$	$k=3.8 \times 10^{-14}$ $A=3.39 \times 10^{-20}$ $n=1.73$ $E_a=-1213$	$k=7.6 \times 10^{-15}$ $A=8.75 \times 10^{-20}$ $n=1.60$ $E_a=-682$	$k=5.7 \times 10^{-13}$ $A=1.86 \times 10^{-19}$ $n=1.50$ $E_a=-1227$	$k=4.3 \times 10^{-15}$ $A=1.26 \times 10^{-18}$ $n=1.39$ $E_a=-68$	$k=6.5 \times 10^{-16}$ $A=3.52 \times 10^{-17}$ $n=0.81$ $E_a=510$
$R_1 = -CHR_aR_b$	$k=1.9 \times 10^{-14}$ $A=1.39 \times 10^{-20}$ $n=1.74$ $E_a=-1261$	$k=3.8 \times 10^{-14}$ $A=1.23 \times 10^{-18}$ $n=1.08$ $E_a=-1249$	$k=1.8 \times 10^{-14}$ $A=1.60 \times 10^{-20}$ $n=1.63$ $E_a=-1396$	$k=3.4 \times 10^{-14}$ $A=6.04 \times 10^{-20}$ $n=1.46$ $E_a=-1466$	$k=2.1 \times 10^{-14}$ $A=5.93 \times 10^{-18}$ $n=1.10$ $E_a=-568$	$k=2.8 \times 10^{-15}$ $A=6.86 \times 10^{-20}$ $n=1.51$ $E_a=-590$

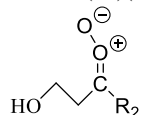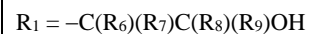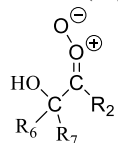| R_1						
$R_1= -CR_aR_bR_c$	$k=2.2\times10^{-14}$ $A=1.37\times10^{-20}$ $n=1.89$ $E_a=-1046$	$k=1.7\times10^{-14}$ $A=6.11\times10^{-20}$ $n=1.58$ $E_a=-1063$	$k=1.8\times10^{-14}$ $A=9.11\times10^{-20}$ $n=1.59$ $E_a=-922$	$k=9.4\times10^{-14}$ $A=5.51\times10^{-19}$ $n=1.33$ $E_a=-1329$	$k=2.8\times10^{-15}$ $A=2.42\times10^{-19}$ $n=1.57$ $E_a=-124$	$k=4.4\times10^{-16}$ $A=3.40\times10^{-21}$ $n=2.23$ $E_a=985$
$R_1= -H$	$k=2.7\times10^{-11}$ $A=4.17\times10^{-18}$ $n=1.27$ $E_a=-2510$	$k=1.7\times10^{-11}$ $A=9.97\times10^{-18}$ $n=0.91$ $E_a=-2739$	$k=3.8\times10^{-11}$ $A=6.79\times10^{-18}$ $n=1.16$ $E_a=-2659$	$k=4.7\times10^{-11}$ $A=1.81\times10^{-17}$ $n=0.99$ $E_a=-2715$	$k=1.4\times10^{-12}$ $A=7.95\times10^{-18}$ $n=1.24$ $E_a=-1510$	$k=2.7\times10^{-13}$ $A=3.24\times10^{-19}$ $n=1.65$ $E_a=-1271$
$R_1 = -CH_2-CR_3=CR_4R_5$	$k=1.7\times10^{-14}$ $A=3.54\times10^{-22}$ $n=2.49$ $E_a=-1043$	$k=1.9\times10^{-14}$ $A=5.68\times10^{-21}$ $n=2.06$ $E_a=-984$	$k=1.1\times10^{-14}$ $A=1.88\times10^{-24}$ $n=3.13$ $E_a=-1376$	$k=2.9\times10^{-13}$ $A=3.11\times10^{-20}$ $n=1.82$ $E_a=-998$	$k=3.9\times10^{-15}$ $A=5.17\times10^{-20}$ $n=1.83$ $E_a=-234$	$k=6.0\times10^{-16}$ $A=2.37\times10^{-20}$ $n=1.84$ $E_a=103$
$R_1 = -CHR_a-CR_3=CR_4R_5$	$k=9.6\times10^{-15}$ $A=2.33\times10^{-21}$ $n=2.07$ $E_a=-1032$	$k=1.9\times10^{-14}$ $A=2.06\times10^{-19}$ $n=1.41$ $E_a=-1020$	$k=2.6\times10^{-14}$ $A=3.44\times10^{-25}$ $n=3.16$ $E_a=-2090$	$k=1.7\times10^{-14}$ $A=1.01\times10^{-20}$ $n=1.79$ $E_a=-1237$	$k=1.1\times10^{-14}$ $A=1.55\times10^{-20}$ $n=1.88$ $E_a=-819$	$k=3.0\times10^{-15}$ $A=1.83\times10^{-21}$ $n=2.14$ $E_a=-637$
$R_1 = -CR_aR_b-CR_3=CR_4R_5$	$k=1.1\times10^{-14}$ $A=2.30\times10^{-21}$ $n=2.22$ $E_a=-817$	$k=8.6\times10^{-15}$ $A=1.02\times10^{-20}$ $n=1.90$ $E_a=-834$	$k=2.5\times10^{-14}$ $A=1.96\times10^{-24}$ $n=3.13$ $E_a=-1616$	$k=4.7\times10^{-14}$ $A=9.23\times10^{-20}$ $n=1.66$ $E_a=-1100$	$k=3.7\times10^{-15}$ $A=7.24\times10^{-19}$ $n=1.38$ $E_a=-200$	$k=4.0\times10^{-16}$ $A=7.46\times10^{-23}$ $n=2.60$ $E_a=-193$
$R_1 = -CR_3=CR_4CH_3$	$k=8.9\times10^{-15}$ $A=3.02\times10^{-22}$ $n=2.32$ $E_a=-1182$	$k=1.0\times10^{-14}$ $A=2.40\times10^{-22}$ $n=2.28$ $E_a=-1373$	$k=8.5\times10^{-15}$ $A=3.48\times10^{-22}$ $n=2.21$ $E_a=-1317$	$k=1.6\times10^{-14}$ $A=1.31\times10^{-21}$ $n=2.05$ $E_a=-1387$	$k=2.5\times10^{-17}$ $A=1.12\times10^{-18}$ $n=1.43$ $E_a=1505$	$k=3.8\times10^{-18}$ $A=5.12\times10^{-19}$ $n=1.44$ $E_a=1843$
$R_1 = -CR_3=CR_4CH_2R_a$	$k=8.9\times10^{-15}$ $A=3.02\times10^{-22}$ $n=2.32$ $E_a=-1182$	$k=1.0\times10^{-14}$ $A=2.40\times10^{-22}$ $n=2.28$ $E_a=-1373$	$k=8.5\times10^{-15}$ $A=3.48\times10^{-22}$ $n=2.21$ $E_a=-1317$	$k=1.6\times10^{-14}$ $A=1.31\times10^{-21}$ $n=2.05$ $E_a=-1387$	$k=2.5\times10^{-17}$ $A=1.12\times10^{-18}$ $n=1.43$ $E_a=1505$	$k=3.8\times10^{-18}$ $A=5.12\times10^{-19}$ $n=1.44$ $E_a=1843$
$R_1 = -CR_3=CR_4CHR_aR_b$	$k=8.9\times10^{-15}$ $A=3.02\times10^{-22}$ $n=2.32$ $E_a=-1182$	$k=1.0\times10^{-14}$ $A=2.40\times10^{-22}$ $n=2.28$ $E_a=-1373$	$k=8.5\times10^{-15}$ $A=3.48\times10^{-22}$ $n=2.21$ $E_a=-1317$	$k=1.6\times10^{-14}$ $A=1.31\times10^{-21}$ $n=2.05$ $E_a=-1387$	$k=2.5\times10^{-17}$ $A=1.12\times10^{-18}$ $n=1.43$ $E_a=1505$	$k=3.8\times10^{-18}$ $A=5.12\times10^{-19}$ $n=1.44$ $E_a=1843$
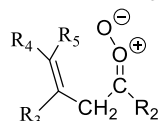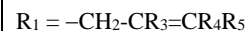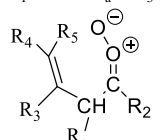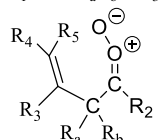
$R_1 = -CR_3=CR_4R'$	$k=4.8\times10^{-15}$ A= 2.25×10^{-21} n= 2.27 E_a= -493	$k=5.9\times10^{-15}$ A= 1.17×10^{-23} n= 2.99 E_a= -898	$k=4.6\times10^{-15}$ A= 260×10^{-21} n= 2.15 E_a= -628	$k=8.5\times10^{-15}$ A= 9.79×10^{-21} n= 1.99 E_a= -698	$k=5.0\times10^{-16}$ A= 3.33×10^{-20} n= 1.91 E_a= 384	$k=7.7\times10^{-17}$ A= 1.52×10^{-20} n= 1.92 E_a= 722
$R_1 = -CHO$	$k=1.5\times10^{-11}$ A= 8.07×10^{-20} n= 1.67 E_a= -2828	$k=1.7\times10^{-11}$ A= 6.40×10^{-20} n= 1.63 E_a= -3019	$k=1.4\times10^{-11}$ A= 9.30×10^{-20} n= 1.56 E_a= -2963	$k=2.6\times10^{-11}$ A= 3.51×10^{-19} n= 1.40 E_a= -3033	$k=1.1\times10^{-12}$ A= 3.04×10^{-19} n= 1.59 E_a= -1804	$k=1.7\times10^{-13}$ A= 1.39×10^{-19} n= 1.60 E_a= -1467
$R_1 = -C(O)R_a$	$k=4.7\times10^{-11}$ A= 2.26×10^{-19} n= 1.43 E_a= -3279	$k=5.5\times10^{-11}$ A= 1.80×10^{-19} n= 1.38 E_a= -3471	$k=4.5\times10^{-11}$ A= 2.61×10^{-19} n= 1.32 E_a= -3414	$k=8.3\times10^{-11}$ A= 9.83×10^{-19} n= 1.15 E_a= -3485	$k=3.6\times10^{-12}$ A= 8.53×10^{-19} n= 1.35 E_a= -2256	$k=5.5\times10^{-13}$ A= 3.91×10^{-19} n= 1.35 E_a= -1918
$R_1 = -C(=O)OR'$	$k=2.0\times10^{-12}$ A= 5.17×10^{-20} n= 1.59 E_a= -2508	$k=2.3\times10^{-12}$ A= 4.10×10^{-20} n= 1.54 E_a= -2700	$k=1.9\times10^{-12}$ A= 5.96×10^{-20} n= 1.47 E_a= -2643	$k=3.5\times10^{-12}$ A= 2.25×10^{-19} n= 1.31 E_a= -2714	$k=1.5\times10^{-13}$ A= 1.95×10^{-19} n= 1.51 E_a= -1485	$k=2.3\times10^{-14}$ A= 8.94×10^{-20} n= 1.51 E_a= -1147
$R_1 = -C(R_6)(R_7)ONO_2$	$k=8.8\times10^{-15}$ A= 1.43×10^{-21} n= 2.45 E_a= -492	$k=1.0\times10^{-14}$ A= 1.14×10^{-21} n= 2.41 E_a= -683	$k=8.4\times10^{-15}$ A= 1.65×10^{-21} n= 2.34 E_a= -627	$k=1.6\times10^{-14}$ A= 6.22×10^{-21} n= 2.18 E_a= -697	$k=1.2\times10^{-15}$ A= 2.01×10^{-20} n= 2.17 E_a= 393	$k=1.2\times10^{-16}$ A= 1.76×10^{-21} n= 2.41 E_a= 787
$R_1 = -OR'$	$k=3.0\times10^{-12}$ A= 1.46×10^{-19} n= 1.43 E_a= -2589	$k=3.5\times10^{-12}$ A= 1.16×10^{-19} n= 1.38 E_a= -2780	$k=2.8\times10^{-12}$ A= 1.68×10^{-19} n= 1.32 E_a= -2724	$k=5.3\times10^{-12}$ A= 6.34×10^{-19} n= 1.15 E_a= -2794	$k=6.4\times10^{-13}$ A= 3.17×10^{-19} n= 1.43 E_a= -1906	$k=9.8\times10^{-14}$ A= 1.45×10^{-19} n= 1.43 E_a= -1569
$R_1 = -OH$	Unstable	Unstable	Unstable	Unstable	Unstable	Unstable
$R_1 = -C(R_6)(R_7)OR'$	$k=2.7\times10^{-14}$ A= 2.78×10^{-18} n= 1.34 E_a= -460	$k=3.2\times10^{-14}$ A= 2.21×10^{-18} n= 1.30 E_a= -651	$k=2.6\times10^{-14}$ A= $3.20\times10^{-18/}$ n= 1.23 E_a= -595	$k=4.9\times10^{-14}$ A= 1.21×10^{-17} n= 1.06 E_a= -665	$k=3.8\times10^{-15}$ A= 3.91×10^{-17} n= 1.05 E_a= 425	$k=3.6\times10^{-16}$ A= 3.43×10^{-18} n= 1.30 E_a= 819
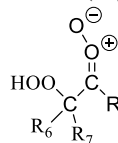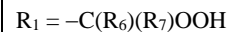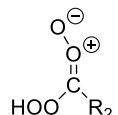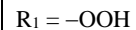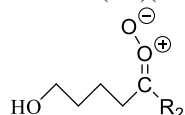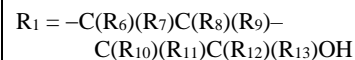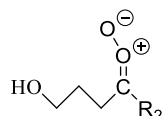
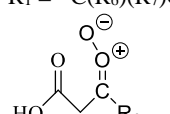| Structure	Col 1	Col 2	Col 3	Col 4	Col 5	Col 6
$R_1 = -C(R_6)(R_7)OH$	Addition $k=3.0\times10^{-14}$ $A=1.46\times10^{-21}$ $n=2.21$ $E_a=-1260$	Addition $k=3.5\times10^{-14}$ $A=1.16\times10^{-21}$ $n=2.17$ $E_a=-1451$	Addition $k=2.8\times10^{-14}$ $A=1.68\times10^{-21}$ $n=2.10$ $E_a=-1395$	Addition $k=5.3\times10^{-14}$ $A=6.34\times10^{-21}$ $n=1.93$ $E_a=-1465$	Addition $k=1.7\times10^{-14}$ $A=1.06\times10^{-18}$ $n=1.30$ $E_a=-686$	Addition $k=2.7\times10^{-15}$ $A=4.84\times10^{-19}$ $n=1.31$ $E_a=-349$
	Ringcl. Catal. $k=8.1\times10^{-14}$ $A=1.69\times10^{-46}$ $n=10.53$ $E_a=-4553$	Ringcl. Catal. $k=9.5\times10^{-14}$ $A=1.35\times10^{-46}$ $n=10.48$ $E_a=-4745$	Ringcl. Catal. $k=7.8\times10^{-14}$ $A=1.95\times10^{-46}$ $n=10.41$ $E_a=-4688$	Ringcl. Catal. $k=1.4\times10^{-13}$ $A=7.37\times10^{-46}$ $n=10.25$ $E_a=-4759$	Ringcl. Catal. $k=4.7\times10^{-14}$ $A=3.53\times10^{-32}$ $n=5.70$ $E_a=-2755$	Ringcl. Catal. $k=7.2\times10^{-15}$ $A=1.62\times10^{-32}$ $n=5.71$ $E_a=-2418$
$R_1 = -C(R_6)(R_7)C(R_8)(R_9)OH$	Addition $k=6.1\times10^{-13}$ $A=1.72\times10^{-15}$ $n=-0.44$ $E_a=-2488$	Addition $k=4.8\times10^{-13}$ $A=7.69\times10^{-15}$ $n=-0.75$ $E_a=-2504$	Addition $k=4.9\times10^{-13}$ $A=1.15\times10^{-14}$ $n=-0.73$ $E_a=-2364$	Addition $k=2.6\times10^{-12}$ $A=6.93\times10^{-14}$ $n=-1.00$ $E_a=-2771$	Addition $k=7.9\times10^{-14}$ $A=3.04\times10^{-14}$ $n=-0.76$ $E_a=-1565$	Addition $k=1.2\times10^{-14}$ $A=1.39\times10^{-14}$ $n=-0.75$ $E_a=-1228$
	Ringcl. Catal. $k=6.7\times10^{-13}$ $A=2.90\times10^{-15}$ $n=-0.38$ $E_a=-2263$	Ringcl. Catal. $k=5.2\times10^{-13}$ $A=1.29\times10^{-14}$ $n=-0.69$ $E_a=-2280$	Ringcl. Catal. $k=5.3\times10^{-13}$ $A=1.92\times10^{-14}$ $n=-0.68$ $E_a=-2140$	Ringcl. Catal. $k=2.8\times10^{-12}$ $A=1.17\times10^{-13}$ $n=-0.94$ $E_a=-2547$	Ringcl. Catal. $k=8.6\times10^{-14}$ $A=5.11\times10^{-14}$ $n=-0.70$ $E_a=-1341$	Ringcl. Catal. $k=1.3\times10^{-14}$ $A=2.34\times10^{-14}$ $n=-0.69$ $E_a=-1004$
$R_1 = -C(R_6)(R_7)C(R_8)(R_9)-C(R_{10})(R_{11})OH$	Ringcl. Catal. $(k \sim 5\times10^{-11})$	Ringcl. Catal. $(k \sim 5\times10^{-11})$	Ringcl. Catal. $(k \sim 5\times10^{-11})$	Ringcl. Catal. $(k \sim 5\times10^{-11})$	Ringcl. Catal. $(k \sim 5\times10^{-11})$	Ringcl. Catal. $(k \sim 5\times10^{-11})$
$R_1 = -C(R_6)(R_7)C(R_8)(R_9)-C(R_{10})(R_{11})C(R_{12})(R_{13})OH$	Ringcl. Catal. $(k \sim 5\times10^{-11})$	Ringcl. Catal. $(k \sim 5\times10^{-11})$	Ringcl. Catal. $(k \sim 5\times10^{-11})$	Ringcl. Catal. $(k \sim 5\times10^{-11})$	Ringcl. Catal. $(k \sim 5\times10^{-11})$	Ringcl. Catal. $(k \sim 5\times10^{-11})$
$R_1 = -OOH$	No data	No data	No data	No data	No data	No data
$R_1 = -C(R_6)(R_7)OOH$	Ringcl. Catal. $k=1.8\times10^{-11}$ $A=9.59\times10^{-25}$ $n=3.05$ $E_a=-3923$	Ringcl. Catal. $k=2.1\times10^{-11}$ $A=7.61\times10^{-25}$ $n=3.00$ $E_a=-4115$	Ringcl. Catal. $k=1.7\times10^{-11}$ $A=1.11\times10^{-24}$ $n=2.94$ $E_a=-4058$	Ringcl. Catal. $k=3.1\times10^{-11}$ $A=4.17\times10^{-24}$ $n=2.77$ $E_a=-4129$	Ringcl. Catal. $k=1.7\times10^{-12}$ $A=1.59\times10^{-17}$ $n=0.58$ $E_a=-2474$	Ringcl. Catal. $k=2.7\times10^{-13}$ $A=7.29\times10^{-18}$ $n=0.59$ $E_a=-2137$
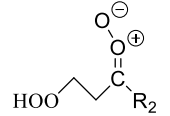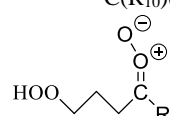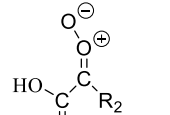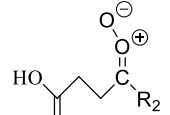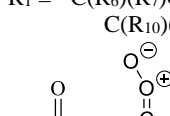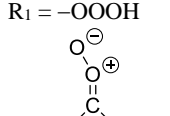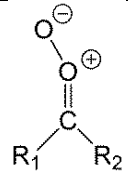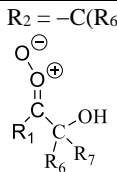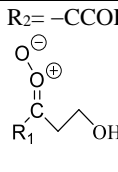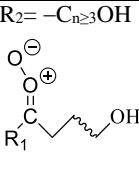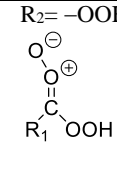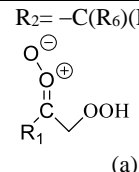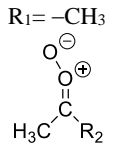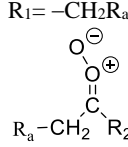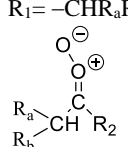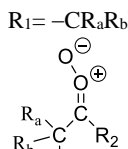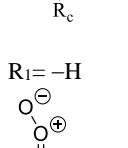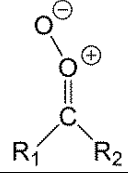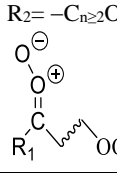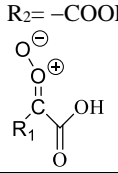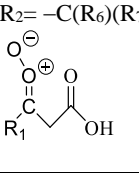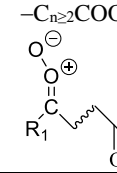
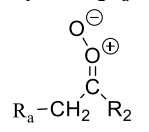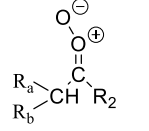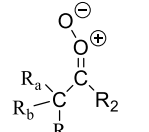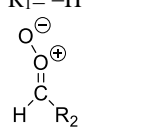| Structure / R_1	Col 1	Col 2	Col 3	Col 4	Col 5	Col 6
$R_1 = -C(R_6)(R_7)C(R_8)(R_9)OOH$	Ringcl. Catal. ($k \sim 5\times10^{-11}$)	Ringcl. Catal. ($k \sim 5\times10^{-11}$)	Ringcl. Catal. ($k \sim 5\times10^{-11}$)	Ringcl. Catal. ($k \sim 5\times10^{-11}$)	Ringcl. Catal. ($k \sim 5\times10^{-11}$)	Ringcl. Catal. ($k \sim 5\times10^{-11}$)
$R_1 = -C(R_6)(R_7)C(R_8)(R_9)-$ $C(R_{10})(R_{11})OOH$	Ringcl. Catal. ($k \sim 5\times10^{-11}$)	Ringcl. Catal. ($k \sim 5\times10^{-11}$)	Ringcl. Catal. ($k \sim 5\times10^{-11}$)	Ringcl. Catal. ($k \sim 5\times10^{-11}$)	Ringcl. Catal. ($k \sim 5\times10^{-11}$)	Ringcl. Catal. ($k \sim 5\times10^{-11}$)
$R_1 = -COOH$	Ringcl. Catal. ($k \sim 5\times10^{-11}$)	Ringcl. Catal. ($k \sim 5\times10^{-11}$)	Ringcl. Catal. ($k \sim 5\times10^{-11}$)	Ringcl. Catal. ($k \sim 5\times10^{-11}$)	Ringcl. Catal. ($k \sim 5\times10^{-11}$)	Ringcl. Catal. $k=5.3\times10^{-12}$ A= 1.95×10^{-32} n= 6.02 E_a= -3796
$R_1 = -C(R_6)(R_7)COOH$	CO_2+alkene Catal. ($k \sim 5\times10^{-11}$)	CO_2+alkene Catal. ($k \sim 5\times10^{-11}$)	CO_2+alkene Catal. ($k \sim 5\times10^{-11}$)	CO_2+alkene Catal. ($k \sim 5\times10^{-11}$)	CO_2+alkene Catal. ($k \sim 5\times10^{-11}$)	CO_2+alkene Catal. ($k \sim 5\times10^{-11}$)
$R_1 = -C(R_6)(R_7)C(R_8)(R_9)COOH$	Ringcl. Catal. ($k \sim 5\times10^{-11}$)	Ringcl. Catal. ($k \sim 5\times10^{-11}$)	Ringcl. Catal. ($k \sim 5\times10^{-11}$)	Ringcl. Catal. ($k \sim 5\times10^{-11}$)	Ringcl. Catal. ($k \sim 5\times10^{-11}$)	Ringcl. Catal. $k=6.4\times10^{-12}$ A= 3.63×10^{-20} n= 1.30 E_a= -3445
$R_1 = -C(R_6)(R_7)C(R_8)(R_9)-$ $C(R_{10})(R_{11})COOH$	Ringcl. Catal. ($k \sim 5\times10^{-11}$)	Ringcl. Catal. ($k \sim 5\times10^{-11}$)	Ringcl. Catal. ($k \sim 5\times10^{-11}$)	Ringcl. Catal. ($k \sim 5\times10^{-11}$)	Ringcl. Catal. ($k \sim 5\times10^{-11}$)	Ringcl. Catal. ($k \sim 5\times10^{-11}$)
$R_1 = -OOOH$	No data	No data	No data	No data	No data	No data

Table 35: Predicted total rate coefficients for the reaction of carbonyl oxide with $(H_2O)_2$ as a function of the two substituents R_1 and R_2, based on fitting theory-derived reaction trends to a set of literature data. The rate coefficient k (cm^3 molecule^{-1} s^{-1}) is given at 298K, and the parameters of a Kooij equation fit $k(T) = A \times (T/K)^n \times \exp(-E_a/T)$ between 200 and 450 K (A in cm^3 molecule^{-1} s^{-1}, E_a in K). The definition of $R_a/R_b/R_c/R_3/R_4/R_5/R'$ is given in Table 29. Values in green are based directly on experimental and/or theoretical kinetic calculations, values in orange are values estimated by applying (averaged) reaction trends for other substituents.

	$R_2= \alpha\text{-}C=O$	$R_2= \alpha\text{-}ONO_2$	$R_2= -C(R_6)(R_7)ONO_2$	$R_2= -OR'$	$R_2= -OH$	$R_2= -C(R_6)(R_7)OR'$
$R_1= -CH_3$	k=3.7×10⁻¹⁷ A= 3.97×10⁻²⁰ n= 1.97 Ea= 1301	No data	k=1.6×10⁻¹⁴ A= 3.57×10⁻²¹ n= 2.21 Ea= -819	k=5.0×10⁻¹² A= 7.34×10⁻²² n= 2.41 Ea= -2651	No data	k=2.0×10⁻¹⁴ A= 2.17×10⁻¹⁹ n= 1.56 Ea= -759
$R_1= -CH_2R_a$	k=5.2×10⁻¹⁷ A= 5.47×10⁻²⁰ n= 1.82 Ea= 1055	No data	k=2.3×10⁻¹⁴ A= 4.91×10⁻²¹ n= 2.07 Ea= -1064	k=6.9×10⁻¹² A= 1.01×10⁻²¹ n= 2.27 Ea= -2896	No data	k=2.8×10⁻¹⁴ A= 2.99×10⁻¹⁹ n= 1.42 Ea= -1004
$R_1= -CHR_aR_b$	k=5.1×10⁻¹⁷ A= 2.22×10⁻¹⁹ n= 1.40 Ea= 760	No data	k=2.2×10⁻¹⁴ A= 1.99×10⁻²⁰ n= 1.65 Ea= -1359	k=6.9×10⁻¹² A= 4.10×10⁻²¹ n= 1.85 Ea= -3191	No data	k=2.8×10⁻¹⁴ A= 1.21×10⁻¹⁸ n= 1.00 Ea= -1299
$R_1= -CR_aR_bR_c$	k=5.1×10⁻¹⁷ A= 4.24×10⁻²⁰ n= 1.87 Ea= 1056	No data	k=2.2×10⁻¹⁴ A= 3.81×10⁻²¹ n= 2.11 Ea= -1063	k=6.8×10⁻¹² A= 7.83×10⁻²² n= 2.31 Ea= -2895	No data	k=2.8×10⁻¹⁴ A= 2.31×10⁻¹⁹ n= 1.46 Ea= -1003
$R_1= -H$	k=1.4×10⁻¹⁴ A= 1.56×10⁻¹⁸ n= 1.53 Ea= -100	No data	k=2.1×10⁻¹¹ A= 3.46×10⁻¹⁹ n= 1.55 Ea= -2718	Addition (k ~ 5×10⁻¹¹)	No data	k=2.6×10⁻¹¹ A= 2.10×10⁻¹⁷ n= 0.90 Ea= -2658

(structure, R1)	R2 = −C(R6)(R7)OH	R2 = −CCOH	R2 = −Cn≥3OH	R2 = −OOH	R2 = −C(R6)(R7)OOH (a)	(b)
R1 = −CH3	Addition $k=1.2\times10^{-13}$ $A=3.77\times10^{-19}$ $n=1.44$ $E_a=-1318$	Addition $k=3.7\times10^{-13}$ $A=3.06\times10^{-31}$ $n=5.18$ $E_a=-3612$	Ringcl. Catal. ($k \sim 5\times10^{-11}$)	No data	Addition $k=3.1\times10^{-13}$ $A=1.63\times10^{-40}$ $n=8.26$ $E_a=-4575$	Ringcl. Catal. $k=2.9\times10^{-13}$ $A=1.54\times10^{-26}$ $n=3.25$ $E_a=-3597$
R1 = −CH2Ra	Addition $k=1.6\times10^{-13}$ $A=5.20\times10^{-19}$ $n=1.30$ $E_a=-1564$	Addition $k=7.5\times10^{-13}$ $A=1.97\times10^{-30}$ $n=4.71$ $E_a=-4065$	Ringcl. Catal. ($k \sim 5\times10^{-11}$)	No data	Addition $k=2.8\times10^{-13}$ $A=2.24\times10^{-40}$ $n=8.11$ $E_a=-4820$	Ringcl. Catal. $k=4.0\times10^{-13}$ $A=2.13\times10^{-26}$ $n=3.10$ $E_a=-3842$
R1 = −CHRaRb	Addition $k=1.6\times10^{-13}$ $A=2.11\times10^{-18}$ $n=0.88$ $E_a=-1859$	Addition $k=1.4\times10^{-12}$ $A=2.00\times10^{-30}$ $n=4.69$ $E_a=-4285$	Ringcl. Catal. ($k \sim 5\times10^{-11}$)	No data	Addition $k=2.8\times10^{-13}$ $A=9.10\times10^{-40}$ $n=7.69$ $E_a=-5115$	Ringcl. Catal. $k=4.0\times10^{-13}$ $A=8.63\times10^{-26}$ $n=2.68$ $E_a=-4137$
R1 = −CRaRbRc	Addition $k=1.6\times10^{-13}$ $A=4.03\times10^{-19}$ $n=1.34$ $E_a=-1563$	Addition $k=9.6\times10^{-13}$ $A=9.00\times10^{-31}$ $n=4.86$ $E_a=-4126$	Ringcl. Catal. ($k \sim 5\times10^{-11}$)	No data	Addition $k=2.8\times10^{-13}$ $A=1.74\times10^{-40}$ $n=8.16$ $E_a=-4819$	Ringcl. Catal. $k=4.0\times10^{-13}$ $A=1.65\times10^{-26}$ $n=3.15$ $E_a=-3841$
R1 = −H	Addition $k=9.9\times10^{-11}$ $A=2.21\times10^{-19}$ $n=1.49$ $E_a=-3400$	Addition ($k \sim 5\times10^{-11}$)	Ringcl. Catal. ($k \sim 5\times10^{-11}$)	No data	Addition ($k \sim 5\times10^{-11}$)	Ringcl. Catal. $k=8.5\times10^{-12}$ $A=1.75\times10^{-15}$ $n=-0.46$ $E_a=-3304$

(structure, R1)	R2 = −Cn≥2OOH	R2 = −COOH	R2 = −C(R6)(R7)COOH	−Cn≥2COOH	R2 = −OOOH
R1 = −CH3	Ringcl. Catal. ($k \sim 5\times10^{-11}$)	No data	CO2+alkene Catal. $k=5.4\times10^{-13}$ $A=8.20\times10^{-27}$ $n=3.73$ $E_a=-3139$	Ringcl. Catal. ($k \sim 5\times10^{-11}$)	No data

Structure					
$R_1= -CH_2R_a$	Ringcl. Catal. ($k \sim 5 \times 10^{-11}$)	No data	CO$_2$+alkene Catal. $k=1.1 \times 10^{-12}$ A= 5.29×10^{-26} n= 3.26 E$_a$= -3592	Ringcl. Catal. ($k \sim 5 \times 10^{-11}$)	No data
$R_1= -CHR_aR_b$	Ringcl. Catal. ($k \sim 5 \times 10^{-11}$)	No data	CO$_2$+alkene Catal. $k=2.0 \times 10^{-12}$ A= 5.36×10^{-26} n= 3.24 E$_a$= -3812	Ringcl. Catal. ($k \sim 5 \times 10^{-11}$)	No data
$R_1= -CR_aR_bR_c$	Ringcl. Catal. ($k \sim 5 \times 10^{-11}$)	No data	CO$_2$+alkene Catal. $k=1.4 \times 10^{-12}$ A= 2.41×10^{-26} n= 3.41 E$_a$= -3653	Ringcl. Catal. ($k \sim 5 \times 10^{-11}$)	No data
$R_1= -H$	Ringcl. Catal. ($k \sim 5 \times 10^{-11}$)	No data	CO$_2$+alkene Catal. ($k \sim 5 \times 10^{-11}$)	Ringcl. Catal. ($k \sim 5 \times 10^{-11}$)	No data

W. Counterexamples of SAR extrapolation to multi-functionalized SCI

In this section we attempt to apply the SAR for unimolecular reaction to a set of multi-functionalized species and compare them to the results of explicit theoretical calculations. The current recommendation is to apply the SAR several times, each time while considering only one of the functionalities, replacing the others with a (set of) alkyl group(s), and use the resulting rates to determine the dominant (set of) reactions. This approach is expected to work when the functionalities have no or only weak interactions. The multi-functionalized SCI chosen in this section are selected to highlight potential problems in applying the SAR, using substitution patterns that interact in specific ways.

1. OH substituents in β-unsaturated SCI

We have examined 4 *syn*-β-unsaturated hydroxylated SCI, for which we expect up to 3 important reaction classes: 1,5-ring closure on the double bond, insertion in the OH group, and allyl-1,6-H-migration for *Z*-substituted double bonds. These reactions are usually fast and have comparable rates, such that we can probe the relative contribution of the various channels. The impact of the substituents is expected to be correlated, as H-bonding between the OH-group and carbonyl oxide moiety is likely to impact the approach of the COO group onto the double bond, while the change in bond length and rigid bond angles of the double bond is likely to impact the cyclisation process of the insertion reaction.

The theoretical rate predictions are listed in Table 36 (omitting minor other channels listed elsewhere), where we also include the SAR rate predictions at 298 K for analogous compounds where either the OH or C=C moiety is substituted with an alkyl equivalent. Following the procedure for SAR extrapolation, we then assign the reaction rates from the SAR to the individual channels of the target bi-functionalized SCI.

Table 36: Analysis of the reaction rates of bi-substituted SCI, showing the dominant reaction classes, *a priori* predictions of the rate coefficients, SAR predictions for analogous SCI, and application of the SAR predictions to the various pathways in the bi-substituted SCI.

SCI	Reaction class	Calculated k(298 K) / s^{-1}	SAR extrapolation / s^{-1}
Z-(C(=CH$_2$)CH$_2$OH)CHOO	1,5-ring closure	1.6×10^2	8.7×10^3
	insertion in OH	3.7×10^{-3}	
Z-(C(=CH$_2$)CH$_2$CH$_2$OH)CHOO	1,5-ring closure	8.5×10^2	
	insertion in OH	6.3×10^4	1.0×10^7
Z-(Z-CH=CHCH$_2$OH)CHOO	1,5-ring closure	9.2×10^5	
	allyl-1,6-H-migration	8.7×10^6	5.7×10^6
	insertion in OH	5.7×10^5	1.0×10^7
Z-(Z-CH=CHCH$_2$CH$_2$OH)CHOO	1,5-ring closure	1.6×10^5	
	allyl-1,6-H-migration	1.3×10^8	5.7×10^6
	insertion in OH	1.4×10^6	1.7×10^6
Comparison SCI	**SAR reaction class**	**SAR k(298 K) / s^{-1}**	
Z-(C(=CH$_2$)CH$_2$CH$_3$)CHOO	1,5-ring closure	8.7×10^3	
Z-(C(CH$_3$)$_2$CH$_2$OH)CHOO	insertion in OH	7.0×10^0	
Z-(C(=CH$_2$)CH$_2$CH$_2$CH$_3$)CHOO	1,5-ring closure	8.7×10^3	
Z-(C(CH$_3$)$_2$CH$_2$CH$_2$OH)CHOO	insertion in OH	1.0×10^7	
Z-(CH=CHCH$_2$CH$_3$)CHOO	allyl-1,6-H-migration	5.7×10^6	
Z-(CH$_2$CH$_2$CH$_2$OH)CHOO	insertion in OH	1.0×10^7	
Z-(CH=CHCH$_2$CH$_2$CH$_3$)CHOO	allyl-1,6-H-migration	5.7×10^6	
Z-(CH$_2$CH$_2$CH$_2$CH$_2$OH)CHOO	insertion in OH	1.7×10^6	

For the first two compounds in Table 36, with a C(=CH$_2$)(CH$_2$)$_n$OH *syn*-substituent, we notice a clear impact of the bi-substitution, where the SAR rates for 1,5-ring closure do not account for the H-bonding by the OH group, and the insertion in the OH bond is affected by the different bond angle around the double bonded carbon in the formed ring. The SAR rates and theory-predicted rates differ by over an order of magnitude, but in both cases the correct dominant channel is identified, and the reaction rates are sufficiently fast to prevent bimolecular reactions.

For the last two compounds in Table 36, with a CH=CH-(CH$_2$)$_n$OH *syn*-substituent, we find similar differences between the extrapolated SAR rates and theory-predicted rates. Furthermore, as the SAR only lists the dominant channels, we do not have information on the 1,5-ring closure provided by the SAR, though technically we could have used the rate of ring closure of the SAR category for Z-(CH=CH$_2$)CHOO. The SAR extrapolation correctly finds that SCI losses are fast and that no bimolecular reactions are competitive, but neither the absolute rates nor the relative rates of the channels are particularly accurate.

2. Combining two oxygenated substituents

For an OOH- and OH-bi-substituted SCI we typically expect insertion reactions to be dominant. As discussed elsewhere, the rate of insertion is affected by H-bonding with the carbonyl oxide moiety, where different distances of the O$_n$H group yield rates that do not follow a monotonous increase or decrease with distance. For example (section N), we found that insertion in the OH bond of a Z-(CH$_2$CH$_2$OH)CHOO SCI was slower than insertion with a shorter or longer intervening number of carbons, precisely due to the interaction between OH and the carbonyl oxide moiety. For the first compound in Table 37, two O$_n$–H bonds are accessible for insertion, at identical distance from the outer oxide O-atom. The two –O$_n$H groups can form several H-bonds between themselves and with the oxide moiety, where H-bonding changes when transitioning from the reactant to either of the insertion TS. Extrapolating the SAR does correctly predict that insertion in the OOH bond is dominant with a rate near 10^5 s^{-1}, but significantly underestimates the 10% contribution of insertion into the OH bond. The H-bonding afforded by the OOH group negates the slowdown of insertion into an OH group at this distance, enhancing the rate of the insertion reaction compared to the mono-substituted SCI; this is not accounted for in the SAR. At the same time, H-bonding seems to negatively affect the rate of the 1,4-H-migration.

The second SCI in Table 37 similarly probes the impact of the interaction between H-bond donors and acceptors, as well as changing the bond lengths and angles by introducing a double-bonded carbon in the insertion TS ring. The theoretical predictions find that insertion in the OH group is greatly enhanced by the neighboring carbonyl group, while the SAR extrapolation would instead suggest that insertion and 1,3-ring closure have similar contributions to the loss rate. The total loss rate by the SAR extrapolation is also significantly lower than the *a priori* prediction, incorrectly allowing bimolecular reactions from becoming competitive under some atmospheric conditions.

Table 37: Analysis of the reaction rates of bi-substituted SCI, showing the dominant reaction classes, *a priori* predictions of the rate coefficients, SAR predictions for analogous SCI, and application of the SAR predictions to the various pathways in the bi-substituted SCI.

SCI	Reaction class	Calculated k(298 K) / s^{-1}	SAR extrapolation / s^{-1}
Z-(CH(OOH)CH$_2$OH)(CH$_3$)COO	insertion in OOH	8.5×10^4	9.8×10^4
	insertion in OH	4.7×10^3	7.0×10^0
	1,4-H-shift	1.2×10^1	6.6×10^2
Z-(C(=O)CH$_2$OH)CHOO	insertion in OH	8.7×10^3	7.0×10^0
	1,3-ring closure	1.6×10^0	2.0×10^1
Comparison SCI	**SAR reaction class**	**SAR k(298 K) / s^{-1}**	
Z-(CH(OOH)CH$_2$CH$_3$)(CH$_3$)COO	insertion in OOH	9.8×10^4	
	1,4-H-migration	6.6×10^2	
Z-(CH$_2$CH$_2$OH)(CH$_3$)COO	insertion in OH	7.0×10^0	
Z-(C(=O)CH$_2$CH$_3$)CHOO	1,3-ring closure	2.0×10^1	
Z-(C(CH$_3$)$_2$CH$_2$OH)CHOO	insertion in OH	7.0×10^0	

3. SCI with two oxygenated α-substituents

Non-alkyl α-substituents tend to have a large impact on the reactivity of the SCI, and two α-substituents are expected to have very specific interactions both with each other and the carbonyl oxide moiety. It is thus not expected that the SAR is able to correctly predict such compounds, as they each should be considered a separate reaction class. To illustrate this, we have examined the rates of $(OCH_3)_2COO$, $(CHO)_2COO$, and Z-$(OCH_3)(OH)COO$ (see Table 38). For two of the SCI, the only existing reaction channel is 1,3-ring closure, while $(CHO)_2COO$ can undergo either 1,3-ring closure or acyl-1,4-H-migration, where the former is expected to be the fastest channel. To apply the SAR, we would consider variations with either of the two substituents replaced with an alkyl group, for which we also tabulate the rate coefficients at 298 K.

Table 38: Analysis of the reaction rates of bi-substituted SCI, showing the dominant reaction classes, *a priori* predictions of the rate coefficients, and SAR predictions for mono-substituted SCI with similar substituents.

SCI	Reaction class	Calculated k(298 K) / s^{-1}
$(OCH_3)_2COO$	1,3-ring closure	1.7×10^7
$(CHO)_2COO$	1,3-ring closure	4.2×10^1
	acyl-1,4-H-migration	4.3×10^0
Z-$(OCH_3)(OH)COO$	1,3-ring closure	2.1×10^9
Comparison SCI	**SAR reaction class**	**SAR k(298 K) / s^{-1}**
Z-$(OCH_3)(CH_3)COO$	1,3-ring closure	1.1×10^5
E-$(CH_3)(OCH_3)COO$	1,3-ring closure	4.7×10^4
Z-$(CHO)(CH_3)COO$	1,3-ring closure	7.1×10^4
E-$(CH_3)(CHO)COO$	(1,4-H-migration)	
E-$(CH_3)(OH)COO$	1,3-ring closure	4.6×10^4

Estimating the $(CHO)_2COO$ rate against the SAR prediction for E-$(CH_3)(CHO)COO$ does not work, as for the latter 1,4-H-migration is dominant. The procedure for multi-functionalized SCI would correctly determine that 1,3-ring closure is the dominant path, but none of the mono-functionalized SCI have a SAR rate coefficient within an order of magnitude of the calculated rate for the bi-substituted SCI. For $(OCH_3)_2COO$ and Z-$(OCH_3)(OH)COO$, the procedure would correctly conclude that the unimolecular loss is dominant in all atmospheric conditions, even if the SAR-predicted rate would be too low. For $(CHO)_2COO$, however, the *a priori* rate is significantly slower than any of the SAR predictions, and bimolecular reactions with water or other co-reactants could start to contribute, contrary to what the SAR extrapolation procedure suggests.

For such bi-α-substituted SCI, we feel that SAR extrapolations are unlikely to work in general, and explicit calculations or experiments seem to be the only recourse. Rather than applying a SAR, then, one would use tabulated rate coefficient values and reaction classes.

X. Raw quantum chemical data

Selected quantum chemical data is available on all SCI, transition states and products discussed in this work. This includes geometries, moments of inertia for molecular rotation, vibrational wavenumbers, zero point energies, potential energies at various levels of theory, and T1 diagnostics.

The data is hosted in the Data repository of Forschungszentrum Jülich GmbH, and can be cited under DOI 10.26165/JUELICH-DATA/MCZDGS, and accessed as https://doi.org/10.26165/JUELICH-DATA/MCZDGS .

Y. References

1   L. Vereecken and J. S. Francisco, Theoretical studies of atmospheric reaction mechanisms in the troposphere, *Chem. Soc. Rev.*, 2012, **41**, 6259–6293.
2   L. Vereecken, D. R. Glowacki and M. J. Pilling, Theoretical Chemical Kinetics in Tropospheric Chemistry: Methodologies and Applications, *Chem. Rev.*, 2015, **115**, 4063–4114.
3   T. Berndt, R. Kaethner, J. Voigtländer, F. Stratmann, M. Pfeifle, P. Reichle, M. Sipilä, M. Kulmala and M. Olzmann, Kinetics of the unimolecular reaction of CH_2OO and the bimolecular reactions with the water monomer, acetaldehyde and acetone at atmospheric conditions, *Phys. Chem. Chem. Phys.*, 2015, **17**, 19862–19873.
4   B. Long, J. L. Bao and D. G. Truhlar, Atmospheric Chemistry of Criegee Intermediates. Unimolecular Reactions and Reactions with Water, *J. Am. Chem. Soc.*, 2016, **138**, 14409–14422.
5   T. L. Nguyen, H. Lee, D. A. Matthews, M. C. McCarthy and J. F. Stanton, Stabilization of the Simplest Criegee Intermediate from the Reaction between Ozone and Ethylene: A High Level Quantum Chemical and Kinetic Analysis of Ozonolysis, *J. Phys. Chem. A*, 2015, **119**, 5524–5533.
6   R. Chhantyal-Pun, O. Welz, J. D. Savee, A. J. Eskola, E. P. F. Lee, L. Blacker, H. R. Hill, M. Ashcroft, M. A. H. H. Khan, G. C. Lloyd-Jones, L. A. Evans, B. Rotavera, H. Huang, D. L. Osborn, D. K. W. Mok, J. M. Dyke, D. E. Shallcross, C. J. Percival, A. J. Orr-Ewing and C. A. Taatjes, Direct Measurements of Unimolecular and Bimolecular Reaction Kinetics of the Criegee Intermediate $(CH_3)_2COO$, *J. Phys. Chem. A*, 2017, **121**, 4–15.
7   M. J. Newland, A. R. Rickard, M. S. Alam, L. Vereecken, A. Muñoz, M. Ródenas and W. J. Bloss, Kinetics of stabilised Criegee intermediates derived from alkene ozonolysis: reactions with SO_2, H_2O and decomposition under boundary layer conditions, *Phys. Chem. Chem. Phys.*, 2015, **17**, 4076–4088.
8   L. Vereecken, A. Novelli and D. Taraborrelli, Unimolecular decay strongly limits concentration of Criegee intermediates in the atmosphere, *Phys. Chem. Chem. Phys.*, 2017, **19**, 31599–31612.
9   D. Stone, K. Au, S. Sime, D. J. Medeiros, M. Blitz, P. W. Seakins, Z. Decker and L. Sheps, Unimolecular decomposition kinetics of the stabilised Criegee intermediates CH_2OO and CD_2OO, *Phys. Chem. Chem. Phys.*, 2018, **20**, 24940–24954.
10 J. Peltola, P. Seal, A. Inkila and A. Eskola, Time-resolved, broadband UV-absorption spectrometry measurements of Criegee intermediate kinetics using a new photolytic precursor: unimolecular decomposition of CH_2OO and its reaction with formic acid, *Phys. Chem. Chem. Phys.*, 2020, **22**, 11797–11808.
11 Y. Fang, F. Liu, V. P. Barber, S. J. Klippenstein, A. B. McCoy and M. I. Lester, Communication: Real time observation of unimolecular decay of Criegee intermediates to OH radical products, *J. Chem. Phys.*, 2016, **144**, 061102.
12 Y. Fang, F. Liu, V. P. Barber, S. J. Klippenstein, A. B. McCoy and M. I. Lester, Deep tunneling in the unimolecular decay of CH_3CHOO Criegee intermediates to OH radical products, *J. Chem. Phys.*, 2016, **145**, 234308.
13 J. D. Fenske, A. S. Hasson, A. W. Ho and S. E. Paulson, Measurement of Absolute Unimolecular and Bimolecular Rate Constants for CH_3CHOO Generated by the trans-2-Butene Reaction with Ozone in the Gas Phase, *J. Phys. Chem. A*, 2000, **104**, 9921–9932.
14 A. Novelli, L. Vereecken, J. Lelieveld and H. Harder, Direct observation of OH formation from stabilised Criegee intermediates, *Phys. Chem. Chem. Phys.*, 2014, **16**, 19941–19951.
15 Y. Fang, F. Liu, S. J. Klippenstein and M. I. Lester, Direct observation of unimolecular decay of CH_3CH_2CHOO Criegee intermediates to OH radical products, *J. Chem. Phys.*, 2016, **145**, 044312.
16 Y. Fang, V. P. Barber, S. J. Klippenstein, A. B. Mccoy and M. I. Lester, Tunneling effects in the unimolecular decay of $(CH_3)_2COO$ Criegee intermediates to OH radical products, *J. Chem. Phys.*, 2017, **146**, 134307.
17 M. C. Smith, W. Chao, K. Takahashi, K. A. Boering and J. J.-M. Lin, Unimolecular Decomposition Rate of the Criegee Intermediate $(CH_3)_2COO$ Measured Directly with UV Absorption Spectroscopy, *J. Phys. Chem. A*, 2016, **120**, 4789–4798.
18 T. Berndt, T. Jokinen, M. Sipilä, R. L. Mauldin, H. Herrmann, F. Stratmann, H. Junninen and M. Kulmala, H_2SO_4 formation from the gas-phase reaction of stabilized Criegee Intermediates with SO_2: Influence of water vapour content and temperature, *Atmos. Environ.*, 2014, **89**, 603–612.

19 B. Long, J. L. Bao and D. G. Truhlar, Unimolecular reaction of acetone oxide and its reaction with water in the atmosphere, *Proc. Natl. Acad. Sci.*, 2018, 201804453.

20 P. Deng, L. Wang and L. Wang, Mechanism of Gas-Phase Ozonolysis of β-Myrcene in the Atmosphere, *J. Phys. Chem. A*, 2018, **122**, 3013–3020.

21 V. P. Barber, S. Pandit, A. M. Green, N. Trongsiriwat, P. J. Walsh, S. J. Klippenstein and M. I. Lester, Four Carbon Criegee Intermediate from Isoprene Ozonolysis: Methyl Vinyl Ketone Oxide Synthesis, Infrared Spectrum, and OH Production, *J. Am. Chem. Soc.*, 2018, **140**, 10866–10880.

22 Y.-H. Lin, C.-H. Yang, K. Takahashi and J. J.-M. Lin, Kinetics of Unimolecular Decay of Methyl Vinyl Ketone Oxide, an Isoprene-Derived Criegee Intermediate, under Atmospherically Relevant Conditions, *J. Phys. Chem. A*, 2020, **124**, 9375–9381.

23 B. Long, J. L. Bao and D. G. Truhlar, Rapid unimolecular reaction of stabilized Criegee intermediates and implications for atmospheric chemistry, *Nat. Commun.*, 2019, **10**, 2003.

24 B. Chuong, J. Zhang and N. M. Donahue, Cycloalkene Ozonolysis: Collisionally Mediated Mechanistic Branching, *J. Am. Chem. Soc.*, 2004, **126**, 12363–12373.

25 K. T. Kuwata, B. J. Kujala, Z. W. Morrow and E. Tonc, Quantum chemical and RRKM/master equation studies of cyclopropene ozonolysis, *Comput. Theor. Chem.*, 2011, **965**, 305–312.

26 R. Winterhalter, F. Herrmann, B. Kanawati, T. L. Nguyen, J. Peeters, L. Vereecken and G. K. Moortgat, The gas-phase ozonolysis of β-caryophyllene ($C_{15}H_{24}$). Part I: an experimental study, *Phys. Chem. Chem. Phys.*, 2009, **11**, 4152–4172.

27 F. A. Mackenzie-Rae, A. Karton and S. M. Saunders, Computational investigation into the gas-phase ozonolysis of the conjugated monoterpene α-phellandrene, *Phys. Chem. Chem. Phys.*, 2016, **18**, 27991–28002.

28 O. Welz, J. D. Savee, D. L. Osborn, S. S. Vasu, C. J. Percival, D. E. Shallcross and C. A. Taatjes, Direct Kinetic Measurements of Criegee Intermediate (CH_2OO) Formed by Reaction of CH_2I with O_2, *Science*, 2012, **335**, 204–207.

29 K. E. Leather, A. Bacak, R. Wamsley, A. T. Archibald, A. Husk, D. E. Shallcross and C. J. Percival, Temperature and pressure dependence of the rate coefficient for the reaction between ClO and CH_3O_2 in the gas-phase, *Phys. Chem. Chem. Phys.*, 2012, **14**, 3425–3434.

30 B. Ouyang, M. W. McLeod, R. L. Jones and W. J. Bloss, NO_3 radical production from the reaction between the Criegee intermediate CH_2OO and NO_2, *Phys. Chem. Chem. Phys.*, 2013, **15**, 17070–17075.

31 D. Stone, M. Blitz, L. Daubney, N. U. M. Howes and P. Seakins, Kinetics of CH_2OO reactions with SO_2, NO_2, NO, H_2O and CH_3CHO as a function of pressure, *Phys. Chem. Chem. Phys.*, 2014, **16**, 1139–1149.

32 J. M. Anglada, J. González and M. Torrent-Sucarrat, Effects of the substituents on the reactivity of carbonyl oxides. A theoretical study on the reaction of substituted carbonyl oxides with water, *Phys. Chem. Chem. Phys.*, 2011, **13**, 13034–13045.

33 J. M. Anglada, P. Aplincourt, J. M. Bofill and D. Cremer, Atmospheric Formation of OH Radicals and H_2O_2 from Alkene Ozonolysis under Humid Conditions, *ChemPhysChem*, 2002, **3**, 215–221.

34 A. B. Ryzhkov and P. A. Ariya, A theoretical study of the reactions of parent and substituted Criegee intermediates with water and the water dimer, *Phys. Chem. Chem. Phys.*, 2004, **6**, 5042–5050.

35 L.-C. Lin, H.-T. Chang, C.-H. Chang, W. Chao, M. C. Smith, C.-H. Chang, J. J.-M. Lin and K. Takahashi, Competition between H_2O and $(H_2O)_2$ reactions with CH_2OO/CH_3CHOO, *Phys. Chem. Chem. Phys.*, 2016, **18**, 4557–4568.

36 J. M. Anglada and A. Solé, Impact of water dimer on the atmospheric reactivity of carbonyl oxides., *Phys. Chem. Chem. Phys.*, 2016, **18**, 17698–17712.

37 L. Chen, W. Wang, W. Wang, Y. Liu, F. Liu, N. Liu and B. Wang, Water-catalyzed decomposition of the simplest Criegee intermediate CH_2OO, *Theor. Chem. Acc.*, 2016, **135**, 131.

38 R. L. Caravan, M. F. Vansco, K. Au, M. A. H. Khan, Y.-L. Li, F. A. F. Winiberg, K. Zuraski, Y.-H. Lin, W. Chao, N. Trongsiriwat, P. J. Walsh, D. L. Osborn, C. J. Percival, J. J.-M. Lin, D. E. Shallcross, L. Sheps, S. J. Klippenstein, C. A. Taatjes and M. I. Lester, Direct kinetic measurements and theoretical predictions of an isoprene-derived Criegee intermediate, *Proc. Natl. Acad. Sci.*, 2020, 201916711.

39 C. Yin and K. Takahashi, Effect of unsaturated substituents in the reaction of Criegee intermediates with water vapor, *Phys. Chem. Chem. Phys.*, 2018, **20**, 20217–20227.

40 C. A. Taatjes, O. Welz, A. J. Eskola, J. D. Savee, A. M. Scheer, D. E. Shallcross, B. Rotavera, E. P. F. Lee, J. M. Dyke, D. K. W. Mok, D. L. Osborn and C. J. Percival, Direct Measurements of Conformer-Dependent Reactivity of the Criegee Intermediate CH_3CHOO, *Science*, 2013, **340**, 177–180.

41 L. Sheps, A. M. Scully and K. Au, UV absorption probing of the conformer-dependent reactivity of a Criegee intermediate CH_3CHOO, *Phys. Chem. Chem. Phys.*, 2014, **16**, 26701–26706.

42 K. T. Kuwata, M. R. Hermes, M. J. Carlson and C. K. Zogg, Computational Studies of the Isomerization and Hydration Reactions of Acetaldehyde Oxide and Methyl Vinyl Carbonyl Oxide, *J. Phys. Chem. A*, 2010, **114**, 9192–9204.

43 L. Jiang, R. Lan, Y.-S. Xu, W.-J. Zhang and W. Yang, Reaction of Stabilized Criegee Intermediates from Ozonolysis of Limonene with Water: Ab Initio and DFT Study, *Int. J. Mol. Sci.*, 2013, **14**, 5784–5805.

44 H.-L. Huang, W. Chao and J. J.-M. Lin, Kinetics of a Criegee intermediate that would survive high humidity and may oxidize atmospheric SO$_2$, *Proc. Natl. Acad. Sci.*, 2015, 201513149.

45 X.-X. Lin, Y.-R. Liu, T. Huang, K.-M. Xu, Y. Zhang, S. Jiang, Y.-B. Gai, W.-J. Zhang and W. Huang, Theoretical studies of the hydration reactions of stabilized Criegee intermediates from the ozonolysis of β-pinene, *RSC Adv.*, 2014, **4**, 28490–28498.

46 P. Aplincourt and J. M. Anglada, Theoretical Studies on Isoprene Ozonolysis under Tropospheric Conditions. 1. Reaction of Substituted Carbonyl Oxides with Water, *J. Phys. Chem. A*, 2003, **107**, 5798–5811.

47 Y.-H. Lin, C. Yin, K. Takahashi and J. J.-M. Lin, Surprisingly long lifetime of methacrolein oxide, an isoprene derived Criegee intermediate, under humid conditions, *Commun. Chem.*, 2021, **4**, 12.

48 H. J. Tobias and P. J. Ziemann, Kinetics of the Gas-Phase Reactions of Alcohols, Aldehydes, Carboxylic Acids, and Water with the C13 Stabilized Criegee Intermediate Formed from Ozonolysis of 1-Tetradecene, *J. Phys. Chem. A*, 2001, **105**, 6129–6135.

49 W. Chao, J.-T. Hsieh, C.-H. Chang and J. J.-M. Lin, Direct kinetic measurement of the reaction of the simplest Criegee intermediate with water vapor, *Science*, 2015, **347**, 751–754.

50 T. R. Lewis, M. A. Blitz, D. E. Heard and P. W. Seakins, Direct evidence for a substantive reaction between the Criegee intermediate, CH$_2$OO, and the water vapour dimer, *Phys. Chem. Chem. Phys.*, 2015, **17**, 4859–4863.

51 M. C. Smith, C.-H. Chang, W. Chao, L.-C. Lin, K. Takahashi, K. A. Boering and J. J.-M. Lin, Strong Negative Temperature Dependence of the Simplest Criegee Intermediate CH$_2$OO Reaction with Water Dimer, *J. Phys. Chem. Lett.*, 2015, **6**, 2708–2713.

52 A. B. Ryzhkov and P. A. Ariya, The importance of water clusters (H$_2$O)$_n$ (n=2,…,4) in the reaction of Criegee intermediate with water in the atmosphere, *Chem. Phys. Lett.*, 2006, **419**, 479–485.

53 D. Cremer, J. Gauss, E. Kraka, J. F. Stanton and R. J. Bartlett, A CCSD (T) investigation of carbonyl oxide and dioxirane. Equilibrium geometries, dipole moments, infrared spectra, heats of formation and isomerization energies, *Chem. Phys. Lett.*, 1993, **209**, 547–556.

54 J. M. Anglada, J. M. Bofill, S. Olivella and A. Solé, Unimolecular Isomerizations and Oxygen Atom Loss in Formaldehyde and Acetaldehyde Carbonyl Oxides. A Theoretical Investigation, *J. Am. Chem. Soc.*, 1996, **118**, 4636–4647.

55 M. T. Nguyen, T. L. Nguyen, V. T. Ngan and H. M. T. Nguyen, Heats of formation of the Criegee formaldehyde oxide and dioxirane, *Chem. Phys. Lett.*, 2007, **448**, 183–188.

56 J. H. Lehman, H. Li, J. M. Beames and M. I. Lester, Ultraviolet photodissociation dynamics of the simplest Criegee intermediate CH$_2$OO, *J. Chem. Phys.*, 2013, **139**, 141103.

57 A. Karton, M. Kettner and D. A. Wild, Sneaking up on the Criegee intermediate from below: Predicted photoelectron spectrum of the CH$_2$OO$^-$ anion and W3-F12 electron affinity of CH$_2$OO, *Chem. Phys. Lett.*, 2013, **585**, 15–20.

58 T.-N. Nguyen, R. Putikam and M. C. Lin, A novel and facile decay path of Criegee intermediates by intramolecular insertion reactions via roaming transition states, *J. Chem. Phys.*, 2015, **142**, 124312.

59 R. Dawes, B. Jiang and H. Guo, UV Absorption Spectrum and Photodissociation Channels of the Simplest Criegee Intermediate (CH$_2$OO), *J. Am. Chem. Soc.*, 2015, **137**, 50–53.

60 H. Li, Y. Fang, J. M. Beames and M. I. Lester, Velocity map imaging of O-atom products from UV photodissociation of the CH$_2$OO Criegee intermediate, *J. Chem. Phys.*, 2015, **142**, 214312.

61 R. Gutbrod, R. N. Schindler, E. Kraka and D. Cremer, Formation of OH radicals in the gas phase ozonolysis of alkenes: the unexpected role of carbonyl oxides, *Chem. Phys. Lett.*, 1996, **252**, 221–229.

62 P. Aplincourt and M. F. Ruiz-López, Theoretical Study of Formic Acid Anhydride Formation from Carbonyl Oxide in the Atmosphere, *J. Phys. Chem. A*, 2000, **104**, 380–388.

63 J. H. Kroll, S. R. Sahay, J. G. Anderson, K. L. Demerjian and N. M. Donahue, Mechanism of HOx Formation in the Gas-Phase Ozone-Alkene Reaction. 2. Prompt versus Thermal Dissociation of Carbonyl Oxides to Form OH, *J. Phys. Chem. A*, 2001, **105**, 4446–4457.

64 C. Selçuki and V. Aviyente, Electrostatic solvent effects on the conversion of substituted carbonyl oxides to dioxiranes, *J. Mol. Model.*, 2001, **7**, 70–79.

65 D. Zhang and R. Zhang, Mechanism of OH Formation from Ozonolysis of Isoprene: A Quantum-Chemical Study, *J. Am. Chem. Soc.*, 2002, **124**, 2692–2703.

66 D. Zhang, W. Lei and R. Zhang, Mechanism of OH formation from ozonolysis of isoprene: kinetics and product yields, *Chem. Phys. Lett.*, 2002, **358**, 171–179.

67 R. D. Bach, J. L. Andres, A. L. Owensby, H. B. Schlegel and J. J. W. McDouall, Electronic structure and reactivity of dioxirane and carbonyl oxide, *J. Am. Chem. Soc.*, 1992, **114**, 7207–7217.

68 M. Olzmann, E. Kraka, D. Cremer, R. Gutbrod and S. Andersson, Energetics, Kinetics, and Product Distributions of the Reactions of Ozone with Ethene and 2,3-Dimethyl-2-butene, *J. Phys. Chem. A*, 1997, **101**, 9421–9429.

69 J. Kalinowski, M. Räsänen, P. Heinonen, I. Kilpeläinen and R. B. Gerber, Isomerization and Decomposition of a Criegee Intermediate in the Ozonolysis of Alkenes: Dynamics Using a Multireference Potential, *Angew. Chem. Int. Ed.*, 2014, **53**, 265–268.

70 B.-Z. Chen, J. M. Anglada, M.-B. Huang and F. Kong, The Reaction of $CH_2(X^3B_1)$ with $O_2(X^3S_g^-)$: A Theoretical CASSCF/CASPT2 Investigation, *J. Phys. Chem. A*, 2002, **106**, 1877–1884.

71 J. Li, S. Carter, J. M. Bowman, R. Dawes, D. Xie and H. Guo, High-Level, First-Principles, Full-Dimensional Quantum Calculation of the Ro-vibrational Spectrum of the Simplest Criegee Intermediate (CH_2OO), *J. Phys. Chem. Lett.*, 2014, **5**, 2364–2369.

72 D. Cremer, T. Schmidt, J. Gauss and T. P. Radhakrishnan, Formation of Dioxirane from Carbonyl Oxide, *Angew. Chem.-Int. Ed. Engl.*, 1988, **27**, 427–428.

73 R. Chhantyal-Pun, A. Davey, D. E. Shallcross, C. J. Percival and A. J. Orr-Ewing, A kinetic study of the CH_2OO Criegee intermediate self-reaction, reaction with SO_2 and unimolecular reaction using cavity ring-down spectroscopy, *Phys. Chem. Chem. Phys.*, 2015, **17**, 3617–3626.

74 D.-C. Fang and X.-Y. Fu, CASSCF and CAS+1+2 Studies on the Potential Energy Surface and the Rate Constants for the Reactions between CH_2 and O_2, *J. Phys. Chem. A*, 2002, **106**, 2988–2993.

75 T. L. Nguyen, M. C. McCarthy and J. F. Stanton, Relatively Selective Production of the Simplest Criegee Intermediate in a CH_4/O_2 Electric Discharge: Kinetic Analysis of a Plausible Mechanism, *J. Phys. Chem. A*, 2014, **119**, 7197–7204.

76 C. Yin and K. Takahashi, How does substitution affect the unimolecular reaction rates of Criegee intermediates?, *Phys. Chem. Chem. Phys.*, 2017, **19**, 12075–12084.

77 L. A. Hull, Mindo-3 Calculations on Stability of Criegee Carbonyl Oxides, *J. Org. Chem.*, 1978, **43**, 2780–2785.

78 D. Cremer, Theoretical Determination of Molecular-Structure and Conformation. 6. Criegee Intermediate - Evidence for a Stabilization of Its Syn Form by Alkyl Substituents, *J. Am. Chem. Soc.*, 1979, **101**, 7199–7205.

79 R. Gutbrod, E. Kraka, R. N. Schindler and D. Cremer, Kinetic and Theoretical Investigation of the Gas-Phase Ozonolysis of Isoprene: Carbonyl Oxides as an Important Source for OH Radicals in the Atmosphere, *J. Am. Chem. Soc.*, 1997, **119**, 7330–7342.

80 T. L. Nguyen, R. Winterhalter, G. Moortgat, B. Kanawati, J. Peeters and L. Vereecken, The gas-phase ozonolysis of β-caryophyllene ($C_{15}H_{24}$). Part II: A theoretical study, *Phys. Chem. Chem. Phys.*, 2009, **11**, 4173–4183.

81 K. T. Kuwata, L. Luu, A. B. Weberg, K. Huang, A. J. Parsons, L. A. Peebles, N. B. Rackstraw and M. J. Kim, Quantum Chemical and Statistical Rate Theory Studies of the Vinyl Hydroperoxides Formed in *trans*-2-Butene and 2,3-Dimethyl-2-butene Ozonolysis, *J. Phys. Chem. A*, 2018, **122**, 2485–2502.

82 K. T. Kuwata, K. L. Templeton and A. S. Hasson, Computational Studies of the Chemistry of Syn Acetaldehyde Oxide, *J. Phys. Chem. A*, 2003, **107**, 11525–11532.

83 D. Zhang and R. Zhang, Ozonolysis of α-pinene and β-pinene: Kinetics and mechanism, *J. Chem. Phys.*, 2005, **122**, 114308.

84 F. Liu, J. M. Beames, A. S. Petit, A. B. McCoy and M. I. Lester, Infrared-driven unimolecular reaction of CH_3CHOO Criegee intermediates to OH radical products, *Science*, 2014, **345**, 1596–1598.

85 F. Liu, J. M. Beames, A. M. Green and M. I. Lester, UV Spectroscopic Characterization of Dimethyl- and Ethyl-Substituted Carbonyl Oxides, *J. Phys. Chem. A*, 2014, **118**, 2298–2306.

86 F. Liu, Y. Fang, M. Kumar, W. H. Thompson and M. I. Lester, Direct observation of vinyl hydroperoxide, *Phys. Chem. Chem. Phys.*, 2015, **17**, 20490–20494.

87 T. Leonardo, L. Baptista, E. C. da Silva and G. Arbilla, Carbonyl Oxides Reactions from Geraniol-trans-(3,7-dimethylocta-2,6-dien-1-ol), 6-Methyl-5-hepten-2-one, and 6-Hydroxy-4-methyl-4-hexenal Ozonolysis: Kinetics and Mechanisms, *J. Phys. Chem. A*, 2011, **115**, 7709–7721.

88 T. Berndt, T. Jokinen, R. L. Mauldin, T. Petäjä, H. Herrmann, H. Junninen, P. Paasonen, D. R. Worsnop and M. Sipilä, Gas-Phase Ozonolysis of Selected Olefins: The Yield of Stabilized Criegee Intermediate and the Reactivity toward SO_2, *J. Phys. Chem. Lett.*, 2012, **3**, 2892–2896.

89 O. Horie, P. Neeb and G. K. Moortgat, The reactions of the Criegee intermediate CH$_3$CHOO in the gas-phase ozonolysis of 2-butene isomers, *Int. J. Chem. Kinet.*, 1997, **29**, 461–468.

90 O. Horie, C. Schafer and G. K. Moortgat, High reactivity of hexafluoro acetone toward Criegee intermediates in the gas-phase ozonolysis of simple alkenes, *Int. J. Chem. Kinet.*, 1999, **31**, 261–269.

91 N. M. Kidwell, H. Li, X. Wang, J. M. Bowman and M. I. Lester, Unimolecular dissociation dynamics of vibrationally activated CH$_3$CHOO Criegee intermediates to OH radical products, *Nat. Chem.*, 2016, **8**, 509–514.

92 T. L. Nguyen, L. McCaslin, M. C. McCarthy and J. F. Stanton, Communication: Thermal unimolecular decomposition of syn-CH$_3$CHOO: A kinetic study, *J. Chem. Phys.*, 2016, **145**, 131102.

93 A. M. Green, V. P. Barber, Y. Fang, S. J. Klippenstein and M. I. Lester, Selective deuteration illuminates the importance of tunneling in the unimolecular decay of Criegee intermediates to hydroxyl radical products, *Proc. Natl. Acad. Sci.*, 2017, **114**, 12372–12377.

94 T. A. H. Burd, X. Shan and D. C. Clary, Catalysis and tunnelling in the unimolecular decay of Criegee intermediates, *Phys. Chem. Chem. Phys.*, 2018, **20**, 25224–25234.

95 K. T. Kuwata, L. C. Valin and A. D. Converse, Quantum Chemical and Master Equation Studies of the Methyl Vinyl Carbonyl Oxides Formed in Isoprene Ozonolysis, *J. Phys. Chem. A*, 2005, **109**, 10710–10725.

96 J. M. Bowman, X. Wang and Z. Homayoon, Ab initio computational spectroscopy and vibrational dynamics of polyatomic molecules: Applications to syn and anti-CH$_3$CHOO and NO$_3$, *J. Mol. Spectrosc.*, 2015, **311**, 2–11.

97 T. Sun, Y. Wang, C. Zhang, X. Sun and W. Wang, The chemical mechanism of the limonene ozonolysis reaction in the SOA formation: A quantum chemistry and direct dynamic study, *Atmos. Environ.*, 2011, **45**, 1725–1731.

98 F. Liu, J. M. Beames and M. I. Lester, Direct production of OH radicals upon CH overtone activation of (CH$_3$)$_2$COO Criegee intermediates, *J. Chem. Phys.*, 2014, **141**, 234312.

99 H. Li, N. M. Kidwell, X. Wang, J. M. Bowman and M. I. Lester, Velocity map imaging of OH radical products from IR activated (CH$_3$)$_2$COO Criegee intermediates, *J. Chem. Phys.*, 2016, **145**, 104307.

100 G. T. Drozd, T. Kurtén, N. M. Donahue and M. I. Lester, Unimolecular Decay of the Dimethyl Substituted Criegee Intermediate in Alkene Ozonolysis: Decay Timescales and the Importance of Tunneling, *J. Phys. Chem. A*, 2017, **121**, 6036–6045.

101 J. M. Anglada and J. M. Bofill, Electronic Structure and Unimolecular Reactions of Cyclopropenone Carbonyl Oxide. A Theoretical Study, *J. Org. Chem.*, 1997, **62**, 2720–2726.

102 T. L. Nguyen, J. Peeters and L. Vereecken, Theoretical study of the gas-phase ozonolysis of β-pinene (C$_{10}$H$_{16}$), *Phys. Chem. Chem. Phys.*, 2009, **11**, 5643–5656.

103 L. Wang and L. Wang, Mechanism of gas-phase ozonolysis of sabinene in the atmosphere, *Phys. Chem. Chem. Phys.*, 2017, **19**, 24209–24218.

104 K. T. Kuwata and L. C. Valin, Quantum chemical and RRKM/master equation studies of isoprene ozonolysis: Methacrolein and methacrolein oxide, *Chem. Phys. Lett.*, 2008, **451**, 186–191.

105 D. Cremer, R. Crehuet and J. Anglada, The Ozonolysis of Acetylene: A Quantum Chemical Investigation, *J. Am. Chem. Soc.*, 2001, **123**, 6127–6141.

106 C. Selçuki and V. Aviyente, How does the OH group affect the conversion of carbonyl oxide to dioxirane?, *J. Mol. Struct. THEOCHEM*, 2000, **530**, 97–107.

107 X. Lei, W. Wang, J. Gao, S. Wang and W. Wang, Atmospheric Chemistry of Enols: The Formation Mechanisms of Formic and Peroxyformic Acids in Ozonolysis of Vinyl Alcohol, *J. Phys. Chem. A*, 2020, **124**, 4271–4279.

108 I. Ljubić and A. Sabljić, Theoretical Study of the Mechanism and Kinetics of Gas-Phase Ozone Additions to Ethene, Fluoroethene, and Chloroethene: A Multireference Approach, *J. Phys. Chem. A*, 2002, **106**, 4745–4757.

109 I. Ljubić and A. Sabljić, Fluorocarbonyl oxide: CASSCF/CASPT2 study of structure, cis effect and unimolecular decomposition paths, *Chem. Phys.*, 2005, **309**, 157–165.

110 S. Keßel, D. Cabrera-Perez, A. Horowitz, P. R. Veres, R. Sander, D. Taraborrelli, M. Tucceri, J. N. Crowley, A. Pozzer, C. Stönner, L. Vereecken, J. Lelieveld and J. Williams, Atmospheric chemistry, sources and sinks of carbon suboxide, C$_3$O$_2$, *Atmospheric Chem. Phys.*, 2017, **17**, 8789–8804.

111 M. E. Squillacote and F. T. Liang, Conformational thermodynamic and kinetic parameters of methyl-substituted 1,3-butadienes, *J. Org. Chem.*, 2005, **70**, 6564–6573.

112 Z. C. J. Decker, K. Au, L. Vereecken and L. Sheps, Direct Experimental Probing and Theoretical Analysis of the Reaction between the Simplest Criegee Intermediate CH$_2$OO and Isoprene, *Phys. Chem. Chem. Phys.*, 2017, **19**, 8541–8551.

113 C. Fittschen, The reaction of peroxy radicals with OH radicals, *Chem. Phys. Lett.*, 2019, **725**, 102–108.

114 E. Assaf, L. Sheps, L. K. Whalley, D. E. Heard, A. Tomas, C. Schoemaecker and C. Fittschen, The Reaction between CH_3O_2 and OH Radicals: Product Yields and Atmospheric Implications, *Environ. Sci. Technol.*, 2017, **51**, 2170–2177.

115 E. Assaf, B. Song, A. Tomas, C. Schoemaecker and C. Fittschen, Rate Constant of the Reaction between CH_3O_2 Radicals and OH Radicals Revisited, *J. Phys. Chem. A*, 2016, **120**, 8923–8932.

116 E. Assaf, C. Schoemaecker, L. Vereecken and C. Fittschen, Experimental and theoretical investigation of the reaction of RO_2 radicals with OH radicals: Dependence of the HO_2 yield on the size of the alkyl group, *Int. J. Chem. Kinet.*, 2018, **50**, 670–680.

117 A. Bossolasco, E. P. Farago, C. Schoemaecker and C. Fittschen, Rate constant of the reaction between CH_3O_2 and OH radicals, *Chem. Phys. Lett.*, 2014, **593**, 7–13.

118 R. L. Caravan, M. A. H. Khan, J. Zádor, L. Sheps, I. O. Antonov, B. Rotavera, K. Ramasesha, K. Au, M.-W. Chen, D. Rösch, D. L. Osborn, C. Fittschen, C. Schoemaecker, M. Duncianu, A. Grira, S. Dusanter, A. Tomas, C. J. Percival, D. E. Shallcross and C. A. Taatjes, The reaction of hydroxyl and methylperoxy radicals is not a major source of atmospheric methanol, *Nat. Commun.*, 2018, **9**, 4343.

119 J.-F. Müller, Z. Liu, V. S. Nguyen, T. Stavrakou, J. N. Harvey and J. Peeters, The reaction of methyl peroxy and hydroxyl radicals as a major source of atmospheric methanol, *Nat. Commun.*, 2016, **7**, 13213.

120 M. F. Vansco, R. L. Caravan, K. L. Zuraski, F. A. F. Winiberg, K. Au, N. Trongsiriwat, P. J. Walsh, D. L. Osborn, C. J. Percival, M. A. H. Khan, D. E. Shallcross, C. A. Taatjes and M. I. Lester, Experimental Evidence of Dioxole Unimolecular Decay Pathway for Isoprene-Derived Criegee Intermediates, *J. Phys. Chem. A*, 2020, **124**, 3542–3554.

121 L. Vereecken, The Reaction of Criegee Intermediates with Acids and Enols, *Phys. Chem. Chem. Phys.*, 2017, **19**, 28630–28640.

122 N. M. Donahue, G. T. Drozd, S. A. Epstein, A. A. Presto and J. H. Kroll, Adventures in ozoneland: down the rabbit-hole, *Phys. Chem. Chem. Phys.*, 2011, **13**, 10848–10857.

123 S. Enami and A. J. Colussi, Reactions of Criegee Intermediates with Alcohols at Air-Aqueous Interfaces, *J. Phys. Chem. A*, 2017, **121**, 5175–5182.

124 M. R. McGillen, B. F. E. Curchod, R. Chhantyal-Pun, J. M. Beames, N. Watson, M. A. H. H. Khan, L. McMahon, D. E. Shallcross and A. J. Orr-Ewing, Criegee Intermediate–Alcohol Reactions, A Potential Source of Functionalized Hydroperoxides in the Atmosphere, *ACS Earth Space Chem.*, 2017, **1**, 664–672.

125 S. V. Tadayon, E. S. Foreman and C. Murray, Kinetics of the Reactions between the Criegee Intermediate CH_2OO and Alcohols, *J. Phys. Chem. A*, 2018, **122**, 258–268.

126 N. A. I. Watson, J. A. Black, T. M. Stonelake, P. J. Knowles and J. M. Beames, An Extended Computational Study of Criegee Intermediate-Alcohol Reactions, *J. Phys. Chem. A*, 2019, **123**, 218–229.

127 P. J. Ziemann, Formation of Alkoxyhydroperoxy Aldehydes and Cyclic Peroxyhemiacetals from Reactions of Cyclic Alkenes with O_3 in the Presence of Alcohols, *J. Phys. Chem. A*, 2003, **107**, 2048–2060.

128 S. Wolff, A. Boddenberg, J. Thamm, W. V. Turner and S. Gab, Gas-phase ozonolysis of ethene in the presence of carbonyl-oxide scavengers, *Atmos. Environ.*, 1997, **31**, 2965–2969.

129 P. Neeb, O. Horie and G. K. Moortgat, Gas-phase ozonolysis of ethene in the presence of hydroxylic compounds, *Int. J. Chem. Kinet.*, 1996, **28**, 721–730.

130 L. Vereecken, A. R. Rickard, M. J. Newland and W. J. Bloss, Theoretical study of the reactions of Criegee intermediates with ozone, alkylhydroperoxides, and carbon monoxide, *Phys. Chem. Chem. Phys.*, 2015, **17**, 23847–23858.

131 Y. Sakamoto, S. Inomata and J. Hirokawa, Oligomerization Reaction of the Criegee Intermediate Leads to Secondary Organic Aerosol Formation in Ethylene Ozonolysis, *J. Phys. Chem. A*, 2013, **117**, 12912–12921.

132 A. C. Rousso, N. Hansen, A. W. Jasper and Y. Ju, Identification of the Criegee intermediate reaction network in ethylene ozonolysis: impact on energy conversion strategies and atmospheric chemistry, *Phys. Chem. Chem. Phys.*, 2019, **21**, 7341–7357.

133 M. Chen, S. Tong, Z. Wang, W. Li, Y. Xu, S. Wang and M. Ge, Reaction mechanism and kinetics of Criegee intermediate and hydroperoxymethyl formate, *J. Environ. Sci.*, 2021, **105**, 128–137.

134 C. Cabezas and Y. Endo, Observation of hydroperoxyethyl formate from the reaction between the methyl Criegee intermediate and formic acid, *Phys. Chem. Chem. Phys.*, 2020, **22**, 446–454.

135 R. Chhantyal-Pun, B. Rotavera, M. R. McGillen, M. A. H. H. Khan, A. J. Eskola, R. L. Caravan, L. Blacker, D. P. Tew, D. L. Osborn, C. J. Percival, C. A. Taatjes, D. E. Shallcross and A. J. Orr-Ewing, Criegee Intermediate Reactions with Carboxylic Acids: A Potential Source of Secondary Organic Aerosol in the Atmosphere, *ACS Earth Space Chem.*, 2018, **2**, 833–842.

136 E. S. Foreman, K. M. Kapnas and C. Murray, Reactions between Criegee Intermediates and the Inorganic Acids HCl and HNO$_3$: Kinetics and Atmospheric Implications, *Angew. Chem. Int. Ed.*, 2016, **55**, 10419–10422.

137 M. Kumar, D. H. Busch, B. Subramaniam and W. Thompson, Barrierless Tautomerization of Criegee Intermediates via Acid Catalysis, *Phys Chem Chem Phys*, 2014, **16**, 22968–22973.

138 M. Kumar, J. Zhong, X. C. Zeng and J. S. Francisco, Reaction of Criegee Intermediate with Nitric Acid at the Air-Water Interface, *J. Am. Chem. Soc.*, 2018, **140**, 4913–4921.

139 M. Monge-Palacios, M. P. Rissanen, Z. Wang and S. M. Sarathy, Theoretical Kinetic Study of the Formic Acid Catalyzed Criegee Intermediate Isomerization: Multistructural Anharmonicity and Atmospheric Implications, *Phys. Chem. Chem. Phys.*, 2018, **20**, 10806–10814.

140 M. Sipilä, T. Jokinen, T. Berndt, S. Richters, R. Makkonen, N. M. Donahue, R. L. Mauldin, T. Kurtén, P. Paasonen, N. Sarnela, M. Ehn, H. Junninen, M. P. Rissanen, J. Thornton, F. Stratmann, H. Herrmann, D. R. Worsnop, M. Kulmala, V.-M. Kerminen and T. Petäjä, Reactivity of stabilized Criegee intermediates (sCIs) from isoprene and monoterpene ozonolysis toward SO$_2$ and organic acids, *Atmospheric Chem. Phys.*, 2014, **14**, 12143–12153.

141 C. A. Taatjes, R. L. Caravan, F. A. F. Winiberg, K. Zuraski, K. Au, L. Sheps, D. L. Osborn, L. Vereecken and C. J. Percival, Insertion products in the reaction of carbonyl oxide Criegee intermediates with acids: Chloro(hydroperoxy)methane formation from reaction of CH$_2$OO with HCl and DCl, *Mol. Phys.*, 2021, **119**, e1975199.

142 O. Welz, A. J. Eskola, L. Sheps, B. Rotavera, J. D. Savee, A. M. Scheer, D. L. Osborn, D. Lowe, A. Murray Booth, P. Xiao, M. Anwar H. Khan, C. J. Percival, D. E. Shallcross and C. A. Taatjes, Rate Coefficients of C1 and C2 Criegee Intermediate Reactions with Formic and Acetic Acid Near the Collision Limit: Direct Kinetics Measurements and Atmospheric Implications, *Angew. Chem.*, 2014, **126**, 4635–4638.

143 W.-C. Liang, P.-L. Luo and Y.-P. Lee, Infrared characterization of the products and the rate coefficient of the reaction between Criegee intermediate CH$_2$OO and HCl, *Phys. Chem. Chem. Phys.*, 2021, **23**, 11082–11090.

144 C.-A. Chung, J. W. Su and Y.-P. Lee, Detailed mechanism and kinetics of the reaction of Criegee intermediate CH$_2$OO with HCOOH investigated via infrared identification of conformers of hydroperoxymethyl formate and formic acid anhydride, *Phys. Chem. Chem. Phys.*, 2019, **21**, 21445–21455.

145 S. Liu, X. Zhou, Y. Chen, Y. Liu, S. Yu, K. Takahashi, H. Ding, Z. Ding, X. Yang and W. Dong, Experimental and Computational Studies of Criegee Intermediate syn-CH$_3$CHOO Reaction with Hydrogen Chloride, *J. Phys. Chem. A*, 2021, **125**, 8587–8594.

146 M. F. Vansco, K. Zuraski, F. A. F. Winiberg, K. Au, N. Trongsiriwat, P. J. Walsh, D. L. Osborn, C. J. Percival, S. J. Klippenstein, C. A. Taatjes, M. I. Lester and R. L. Caravan, Functionalized Hydroperoxide Formation from the Reaction of Methacrolein-Oxide, an Isoprene-Derived Criegee Intermediate, with Formic Acid: Experiment and Theory, *Molecules*, 2021, **26**, 3058.

147 C. Cabezas and Y. Endo, The Criegee intermediate-formic acid reaction explored by rotational spectroscopy, *Phys. Chem. Chem. Phys.*, 2019, **21**, 18059–18064.

148 C. A. Taatjes, M. A. H. Khan, A. J. Eskola, C. J. Percival, D. L. Osborn, T. J. Wallington and D. E. Shallcross, Reaction of Perfluorooctanoic Acid with Criegee Intermediates and Implications for the Atmospheric Fate of Perfluorocarboxylic Acids, *Environ. Sci. Technol.*, 2019, **53**, 1245–1251.

149 L. Vereecken, T. L. Nguyen, I. Hermans and J. Peeters, Computational study of the stability of α-hydroperoxyl- or α-alkylperoxyl substituted alkyl radicals, *Chem. Phys. Lett.*, 2004, **393**, 432–436.

150 O. M. Anglada, R. Crehuet and J. S. Francisco, The Stability of α-Hydroperoxyalkyl Radicals, *Chem.- Eur. J.*, 2016, **22**, 18092–18100.

151 L. Vereecken, in *Advances in Atmospheric Chemistry: Volume 2: Organic Oxidation and Multiphase Chemistry*, eds. J. R. Barker, A. L. Steiner and T. J. Wallington, World Scientific Publishing Co. Pte. Ltd., Singapore, 1st edn., 2019, pp. 377–527.